An investigation of *Epstein-Barr Virus (EBV)* latency type and *MYC* gene aberrations in plasmablastic lymphoma diagnosed at Groote Schuur Hospital, Cape Town, South Africa.

Raymond Frank Kriel

Supervisors:

Dr Amsha Ramburan and Emeritus Professor Dhiren Govender

Presented for the degree of

Master of Science in Medicine

Anatomical Pathology

Division of Anatomical Pathology

Department of Pathology

Faculty of Health Sciences

University of Cape Town

April 2020

DECLARATION

I, Raymond Frank Kriel, hereby declare that the work on which this dissertation/thesis is based is my original work (except where acknowledgements indicate otherwise) and that neither the whole work nor any part of it has been, is being, or is to be submitted for another degree in this or any other university.

I empower the university to reproduce for the purpose of research either the whole or any portion of the contents in any manner whatsoever.

Signature: Signed by candidate

Date: ……24/04/2020…….

ACKNOWLEDGMENTS

Without my creator, I would not have had the strength or ability to complete this project.

I would like to thank my supervisors, Dr Amsha Ramburan and Emeritus Professor Dhiren Govender; your patience, support and confidence in me was crucial to the completion of this project.

Dr Ramburan, your patience and guidance during my *MYC* FISH assay, my write-up, countless corrections and frustrations, will never be forgotten. Thank you for sharing your time, wealth of knowledge, and entertaining my many questions, thoughts and crazy ideas.

I would especially like to thank Emeritus Professor Dhiren Govender for giving me the wonderful opportunity to do this project and educating me on the pathology of plasmablastic lymphomas, and lymphomas in general.

Thank you to Dr Darshnee Chetty for your much-appreciated encouragement, advice, and kind words during the tough times.

I would also like to thank Mrs Subash Govender for constant encouragement and showing me the "tricks of the trade" when it comes to manual immunohistochemistry. Also, a word of thanks to Ms Nafiesa Allie from the GSH NHLS D7 laboratories, for help with the automated immunohistochemistry set up on our analyser. Thanks also to Mrs Thelma Galsworthy for taking care of the administration of slide and block archives. I would also like to thank the NHLS trust for the funding of this project.

Lastly, I would like to thank my ever supportive, understanding, and encouraging wife Belinda and my children Christine and Matthew. Without your support and understanding and putting up with busy grumpy dad and husband, I would not have been able to complete my masters project and make you all proud.

TABLE OF CONTENTS

FIGURES

TABLES

LIST OF ABBREVIATIONS

Abbreviation	Name
AID	Activation induced cytidine deaminase
AIDS	Acquired Immune Deficiency Syndrome
Ala	Alanine
ALK	Anaplastic lymphoma kinase
ATP	Adenosine triphosphate
AVG	Average
BAP	Break apart probe
BART	*Bam*HI fragment A rightward transcript
BCL2	B-cell lymphoma 2
BCL6	B-cell lymphoma 6
BCR	B-cell receptor
BL	Burkitt lymphoma
BLIMP1	B lymphocyte induced maturation protein
BRLF1 or Rta	*Epstein-Barr virus* replication and transcription activator
BZLF1 or Zta or Zebra	*Bam*HI Z *Epstein-Barr virus* replication activator
CCND1	Cyclin D1
CD4	Cluster of differentiation 4
CD8	Cluster of differentiation 8
CD10	Cluster of differentiation 10
CD19	Cluster of differentiation 19
CD20	Cluster of differentiation 20
CD21	Cluster of differentiation 21
CD30	Cluster of differentiation 30
CD38	Cluster of differentiation 38
CD40	Cluster of differentiation 40
CD45	Cluster of differentiation 45
CD56	Cluster of differentiation 56
CD79a	Cluster of differentiation 79a
CD138	Cluster of differentiation 138
cHART	Combined antiretroviral therapy
CHBAH	Chris Hani Baragwanath Academic Hospital
CR2	Complement receptor 2
CSR	Class switch recombination
CXCL10	C-X-C motif chemokine 10
DAB	3,3′-Diaminobenzidine
DAPI 1 and 2	4′,6-Diamidino-2-phenylindole 1 and 2
DLBCL	Diffuse large B-cell lymphoma
DNA	Deoxyribonucleic acid
DZ	Dark zone
EAD	Epstein-Barr early antigen protein D
EAR	Epstein-Barr early antigen protein R
EBER	Epstein-Barr virus-encoded RNA
EBNA1	Epstein-Barr nuclear antigen 1
EBNA2	Epstein-Barr nuclear antigen 2

EBNA3	Epstein-Barr nuclear antigen 3
EBNA-LP	Epstein-Barr nuclear antigen leader protein
EBV	Epstein-Barr virus
EMA	Epithelial membrane antigen
EphA2	Ephrin receptor A2
EPOCH	Chemotherapy regimen consisting of etoposide, prednisone, vincristine (Oncovin), cyclophosphamide and doxorubicin hydrochloride
FFPE	Formalin-fixed paraffin wax-embedded
FISH	Fluorescent *in situ* hybridisation
GAr	Glycine alanine repeat
GC	Germinal centre
Gly	Glycine
GP350/220	Glycoprotein 350/220
GSH	Groote Schuur Hospital
H&E	Haematoxylin and Eosin
HCl	Hydrochloric acid
HHV4	Human herpesvirus 4
HHV8	Human herpesvirus 8
HIER	Heat induced epitope recovery
HIV	Human Immunodeficiency Virus
HNL	Head and Neck Lymphomas
HREC	Human Research Ethics Committee
HRP	Horseradish Peroxidase
IG	Immunoglobulin
IGEPAL	Octylphenoxypolyethoxyethanol
IgH	Immunoglobulin heavy chain
IgK	Immunoglobulin kappa light chain
IgL	Immunoglobulin lambda light chain
IHC	Immunohistochemistry
IRF4/MUM1	Interferon regulatory factor 4
ISH	*In situ* hybridisation
LANA1	Latency associated nuclear antigen 1
LBCL	Large B-cell lymphoma
LMP1	Latent membrane protein 1
LMP2	Latent membrane protein 2
LZ	Light zone
MAGEA4	Melanoma-associated antigen 4
MALT1	Mucosa-associated lymphoid tissue lymphoma translocation protein 1
MAX	Myc-associated factor X
MCD	Multicentric Castleman disease
MHC	Major histocompatibility complex
miRNA	Micro ribonucleic acid
mRNA	Messenger ribonucleic acid
MUM1/IRF4	Multiple myeloma 1
MYC	V-*Myc* Avian Myelocytomatosis Viral Oncogene Homolog

NaSCN	Sodium thiocyanate
NHL	Non-Hodgkin's lymphoma
NHLS	National Health Laboratory Service
NPC	Nasopharyngeal carcinoma
OS	Overall survival
P53/TP53	Tumour protein 53
PAX5	Paired box protein 5
PBL	Plasmablastic lymphoma
PBS	Phosphate buffered saline
PBS/Tween	Phosphate buffered saline tween
PCM	Plasma cell myeloma
PEL	Primary effusion lymphoma
PRDM1	BLIMP1. B lymphocyte induced maturation protein
qPCR	Quantitative polymerase chain reaction
RNA	Ribonucleic acid
RT	Room temperature
SA	South Africa
SHM	Somatic hypermutation
SMT	Smooth muscle tumour
SSA	Sub-Saharan Africa
SSC	Sodium Chloride Sodium Citrate
Tris/EDTA	Tris ethylenediaminetetraacetic acid
UCT	University of Cape Town
WHO	World Health Organisation
XBP1	X-box binding protein 1

PRESENTATIONS/PUBLICATIONS ARISING FROM THIS STUDY

Event: Department of Pathology research day 2018.

Participation: MSc project presentation.

Title: An investigation of *Epstein-Barr Virus* (EBV) latency type in plasmablastic lymphoma diagnosed at GSH.

Abstract

Introduction: Plasmablastic lymphoma (PBL) is a rare, aggressive, AIDS-associated non-Hodgkin lymphoma. The pathogenesis of PBL is incompletely understood, however association with the *Epstein-Barr virus (EBV)* and the *MYC* gene, have been identified as important pathogenic mechanisms.

Aims and objectives: To characterise the EBV latency in a cohort of patients diagnosed with PBL at Groote Schuur Hospital (GSH), by means of immunohistochemistry. To determine *MYC* gene aberrations using fluorescent *in situ* hybridisation (FISH).

Materials and methods: The cohort comprised PBL cases diagnosed from 2005-2017. EBER ISH was used to confirm EBV infection. Manual immunohistochemistry using three monoclonal antibodies for EBV latent proteins, (EBNA1, EBNA2 and LMP1) was used to determine the latency type. Manual *MYC* FISH was performed on all PBL cases using a dual colour break apart rearrangement probe.

Results: Forty-nine cases of PBL were included in this study. Forty-one cases were positive for EBER ISH. Thirty-seven (78.7%) cases showed HIV/EBV coinfection. Latency 0 was observed in 29 (70.7%) cases, latency 1 in 8 (19.5%) and latency 2 in 4 (9.8%) cases. *MYC* FISH was performed on all 49 PBL cases, of which 30 (61.2%) yielded a result. *MYC* was intact in 11 (36.7%), translocated in 8 (26.7%) and 11 (36.7 %) cases showed copy number variations.

Conclusion: Our research demonstrated 37 (90.2%) of the EBV positive PBL cases showed a restricted latency pattern of 0 or 1. Furthermore we found that *MYC* gene aberrations consisting of translocations and copy number variations occurred in 19 cases (63.3%) , with copy number variations being higher than cited in current literature. Our study is also the first to investigate PBL EBV latency in SA. An uncommon finding was the existence of *MYC* gene aberrations in HIV positive, EBV negative PBL cases.

CHAPTER 1

INTRODUCTION

1.1 Plasmablastic lymphoma epidemiology and clinical features

Plasmablastic lymphoma (PBL) is a rare, aggressive B-cell, non-Hodgkin's lymphoma (NHL) commonly associated with the *Human Immunodeficiency Virus* (HIV) (Castillo et al., 2015, Campo et al., 2017). It was originally described as presenting in the jaw and oral mucosa of HIV positive patients by Delecluse et al in 1997 (Delecluse et al., 1997). Based on its morphological and clinical features, PBL was classified as a distinct sub-type of diffuse large B-cell lymphoma (DLBCL) (Elyamany et al., 2015a), but in the 2008 edition of the World Health Organisation (WHO) classification of "Tumours of Haematopoietic and Lymphoid Tissues", PBL was reclassified as a distinct separate entity from DLBCL (Bibas and Castillo, 2014).

PBL makes up approximately 2.6% of all HIV related lymphomas (Castillo et al., 2015, Chetty et al., 2003) and is described as either an Acquired Immune Deficiency Syndrome (AIDS) defining disease or as an AIDS associated lymphoma. Despite being associated with HIV/AIDS, PBL also presents in immunocompetent, the elderly and patients on iatrogenic immunosuppression following organ transplant (Campo et al., 2017, Elyamany et al., 2015a, Bibas and Castillo, 2014, Harmon and Smith, 2016, Vaubell et al., 2014). South Africa (SA) has the highest global HIV rate (Alli and Meer, 2017, Boy et al., 2015) and according to a 2018 StatsSA report that of the 57.73 million population, 13.1% are HIV positive. For adults between the ages of 15 and 49, 19% are HIV positive (StatsSA, 2018). HIV/AIDS has been associated with an increased risk for the development of NHLs, but the proportion and incidence of PBL in SA is relatively unknown. There have been some single institute studies and reviews of the effect of HIV, on particularly NHL as well as head and neck lymphomas (HNL) that have given a better understanding as to effect of this virus in a SA context. The effect of HIV on NHL in a SA perspective is evident based on a study in 2015 conducted at the Chris Hani Baragwanath Academic Hospital (CHBAH). This retrospective study found an increase in previously rare lymphomas such as PBL. It was also found that HIV positive patients presented with more aggressive, high-grade B-cell lymphomas

than HIV negative counterparts (Patel et al., 2015). An important observation garnered from this study highlighted the effect that lack of access to antiretroviral therapy had on the progression and aggression of NHLs such as PBL. Combined anti-retroviral therapy (c-ART) was slower to reach certain SA areas than other areas in the rest of the world (Patel et al., 2015). Lymphomas of the head and neck (HNL) are the second most frequently reported extranodal lymphomas. HNL have shown an increase with the advent of the HIV epidemic, particularly in SA. A study of HNL in the Department of Oral Pathology of the University of Witwaterstrand (WITS) found a marked increase in high-grade B-cell lymphomas such as PBL in HIV positive patients (Alli and Meer, 2017).

PBL shows a strong male predominance with approximately 70 - 80% of cases occurring in men (Castillo et al., 2015). The median age of presentation in adults who are HIV positive is about 39 years and 58 years in HIV negative adults. Paediatric cases are very rare, with the first case being described in 2004 by Colomo et al and later by Vaubell et al in a SA context (Vaubell et al., 2014, Castillo et al., 2015, Colomo et al., 2004). In the 2017 WHO, PBL may present in children with immunodeficiency, particularly HIV associated (Campo et al., 2017). Despite originally being diagnosed in the oral cavity of HIV positive patients, PBL may frequently be found extra-orally, (Wang et al., 2014). It is primarily an extranodal disease and presents in sites such as the gastrointestinal tract, lung, omentum, bone marrow, gall bladder or skin (Bibas and Castillo, 2014, Castillo et al., 2015, Castillo et al., 2008, Castillo and Reagan, 2011, Campo et al., 2017). Nodal or primary lymph node disease is rare (Ikpatt et al., 2012), and accounts for less than 10% of PBL cases, but may occur in up to 30% of post-transplant cases (Campo et al., 2017).

1.1.1 Prognosis and treatment

Most patients present with advanced stage disease and due to the aggressive nature of PBL, the overall prognosis of patients is very poor. (Lopez and Abrisqueta, 2018). The median overall survival (OS) is between 8 and 15 months (Castillo et al., 2008). This is however dependant on the immune status of the patient, with HIV positive patients surviving about 10 months, while with HIV negative patients the overall survival (OS) is about 11 months (Morscio

et al., 2014, Lopez and Abrisqueta, 2018). In patients with post-transplant immune suppression, the OS decreases to about 7 months. Some studies have suggested that HIV positive patients on antiretroviral treatment such as combined antiretroviral therapy (cHART) had a better outcome and OS than HIV negative patients with the same lymphoma (Misra et al., 2017). This was attributed to the possible involvement of antiretroviral treatment in restoring the body's immunological status (Lopez and Abrisqueta, 2018, Carroll and Garzino-Demo, 2015). However, one of the main challenges remains is that cHART is not always available to HIV positive patients in Sub-Saharan Africa (SSA) where the incidences of HIV and AIDS are at the highest levels in the world (Carbone et al., 2014). PBL is most commonly treated with a regimen that includes cyclophosphamide, doxorubicin, vincristine and prednisone or etoposide, vincristine and doxorubicin with bolus cyclophosphamide and prednisone (EPOCH) (Castillo et al., 2015). In the case of HIV positive PBL, the treatment would involve EPOCH and cHART (Castillo et al., 2015).

1.1.2 Morphology

PBL shows diffuse infiltrates of discohesive uniform large cells, with a prominent starry sky appearance. The tumour cells have a high nuclear to cytoplasmic ratio with large vesicular nuclei, distinct smooth nuclear membrane, immature chromatin and multiple prominent nucleoli. There are frequent mitotic figures present with occasional atypical forms. The cytoplasm varies from bright to pale eosinophilic. Most cells have distinct paranuclear hofs (Harmon and Smith, 2016, Swerdlow et al., 2016, Campo et al., 2017) (Figure 1.1A) A paranuclear hof is the Golgi apparatus, which in plasma cells demonstrates the areas where protein synthesis and immunoglobin production takes place. The morphologic features of PBLs may vary slightly depending on the site of disease. PBLs occurring in HIV negative patients, lymph nodes or extranodal sites other than the oral cavity, may display a higher degree of plasmacytic differentiation. This may be characterised by smaller round eccentric nuclei with course chromatin, often described as "clock-faced". There is also abundant basophilic cytoplasm (Harmon and Smith, 2016) (Figure 1.1B). Areas of necrosis, mitotic figures, apoptotic bodies and tingible body macrophages may also be present in both variants. Tingible body macrophages are not however a diagnostic criterion, as they may be observed in other lymphomas as well and are an indicator of the rate of "mopping up" of apoptotic bodies and

cell debris. The occurrence of these tingible body macrophages often leads to the description of a “starry sky” appearance when viewing under a microscope (Campo et al., 2017).

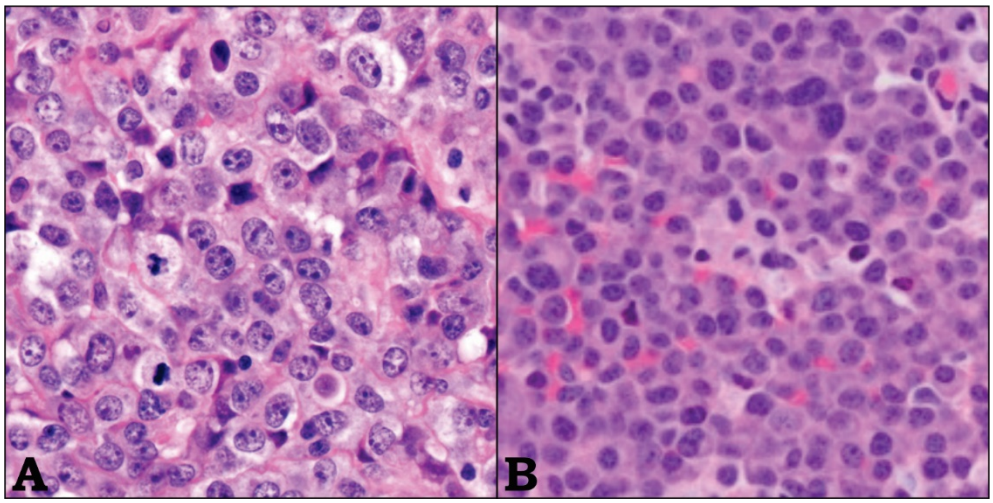

Figure 1.1: Photomicrograph of PBL. A. PBL of oral cavity (H&E x 30) B. PBL with plasmacytic differentiation (H&E x30) (Saraceni et al., 2013, Ramnani, 2016)

1.1.3 Immunophenotype

The immunohistochemical expression pattern of several B-cell and plasma cell markers are essential for the diagnosis of PBL. Even though PBL is a B-cell lymphoma, mature B-cell markers such as CD19, CD20, CD45 and PAX5 are not expressed. Additionally, B-cell lymphoma 2 (BCL2) and B-cell lymphoma 6 (BCL6) proteins, which are B-cell markers linked to germinal centre cell origin, are also expected to be negative. Plasmacytic differentiation markers such as MUM1, CD38, CD138 and VS38C are however expressed (Fernandez-Alvarez et al., 2016). Other markers such as CD79a are positive in 40% of PBL cases with CD56 and CD10 expressed in 25% and 20% of the cases respectively. EMA and CD30 are also frequently expressed. Ki67, which is a proliferation index is often very high (~80-90%).

Differential markers such as LANA-1, which is a latency protein expressed by human herpesvirus (HHV-8), is expected to be negative in order to exclude the plasmablastic variant of HHV-8 positive multicentric Castleman disease (MCD). MCD is however also EBV negative, but may be HIV positive or negative (Said et al., 2017). Another differential marker is ALK

(anaplastic lymphoma kinase), which is used to excluded ALK-positive large B-cell lymphoma (ALK-positive LBCL) (Dupin et al., 2000).

1.1.4 Diagnostic challenges

Based on its immunohistochemical and morphological profile, the diagnosis of PBL may be sometimes be difficult , as it shares features which overlap with other B-cell lymphomas with plasmablastic morphology (Castillo et al., 2015) such as plasmablastic plasma cell myeloma (PCM) , primary effusion lymphoma (PEL) and ALK-positive LBCL. In the setting of HIV infection, both PCM and PBL can be associated with EBV, thus making their distinction challenging. The morphological features of PCM and PBL are almost identical, and other diagnostic aids such as radiographic and clinical presentation need to be considered. For example, PCM shows diffuse bone/bone marrow involvement while PBL is largely associated with EBV and HIV infections (Bibas and Castillo, 2014, Harmon and Smith, 2016, Castillo et al., 2015). Another hallmark clinicopathological characteristic is that PCM exhibits monoclonal para-proteinemia, which is not present in PBL (Taddesse-Heath et al., 2010). For PEL, the clinical history involves the presence of cavity serous effusion. However, this may be complicated though in the rare cases where PEL presents as solid tumour masses (extracavity PEL). Extracavity PEL, which may display immunoblastic or plasmablastic morphology is also associated with HIV infection (Harmon and Smith, 2016). The immunophenotypes are also very similar, but extracavity PEL is positive for HHV-8 (Harmon and Smith, 2016) while PBL is not.

ALK-positive LBCL are rare and often exhibit a diffuse pattern with immunoblastic or plasmablastic cells. Immunohistochemically they are also negative for CD20 and positive for plasma cell markers such as CD38, CD138 and VS38C. The distinguishing factor is that PBL is not positive for the ALK marker, which is positive in cases of ALK-positive LBCL (Harmon and Smith, 2016, Katchi and Liu, 2017, Castillo et al., 2015, Pan et al., 2017). MCD is often associated with the development of other B-cell lymphomas. HHV-8 positive DLBCL may arise in association with HHV-8 positive MCD. HHV-8 infection has been associated with some, but not all cases of MCD (Bower et al., 2011) where the morphology is characterised by the presence of plasmablasts, predominantly in the mantle zones. As a result of the cells morphologically

resembling plasmablasts, the diagnosis of PBL should be excluded. HHV-8 positive DLBCL is however usually associated with HIV positivity. Additionally, the plasmablasts may stain CD20 -/+, CD79a -/+, MUM1 +, CD138 - and CD38-/+. However, EBER for EBV detection is negative (Dupin et al., 2000, Wang et al., 2016) .

1.1.5 Pathogenesis

The pathogenesis of PBL is incompletely understood, but the V-Myc Avian Myelocytomatosis Viral Oncogene Homolog (*MYC)* gene, *Epstein-bar virus* and HIV may be significant role players in the development of PBL. These role players all have oncogenic potential and can influence the body's immune response and the development of various lymphomas. In HIV associated lymphomas such as PBL, the virus is thought to impair the body's immune system and normal B-cell function. This may allow uncontrolled B-cell proliferation and possible secondary oncogenic viral infection by viruses such as EBV (Gloghini et al., 2013), which together with *MYC* rearrangements are observed as the main pathogenic route in PBL (Boy et al., 2011). Particularly in HIV associated PBL, the cell of origin is thought to be derived from post-germinal centre B-cells which have undergone antigen stimulation and are in the process of developing into plasma cells (Castillo and Reagan, 2011).

1.2 Lymph nodes, germinal centre process and plasmablast formation

Lymph nodes show slight variation in their structure depending on their anatomical site. Basic structures include lymphoid follicles, paracortex, medullary cords and sinuses. Lymphoid follicles are regions responsible for T-cell dependant immune responses and are made up of primary and secondary follicles. These are the structures within a lymph node where antibody diversity and isotype switching occurs. Primary follicles contain B-cells and follicular dendritic cells (Ashton-Key et al., 2016).

Germinal centres (GC) form within secondary lymphoid organs including the spleen, tonsils and lymph nodes (Klein and Dalla-Favera, 2008). Secondary follicles show the presences of germinal centres which contain two distinct compartments or zones. These are the dark zone

(DZ) and the light zone (LZ) (Figure 1.2) (Victora, 2014, Suan et al., 2017). In the dark zones one finds large rapidly dividing centroblasts (activated B-cells) while centrocytes, which are post proliferation B-cells with cleaved nuclei, are found in the light zone. The germinal centre is surrounded by the mantle zone (Ashton-Key et al., 2016, Castillo et al., 2015).

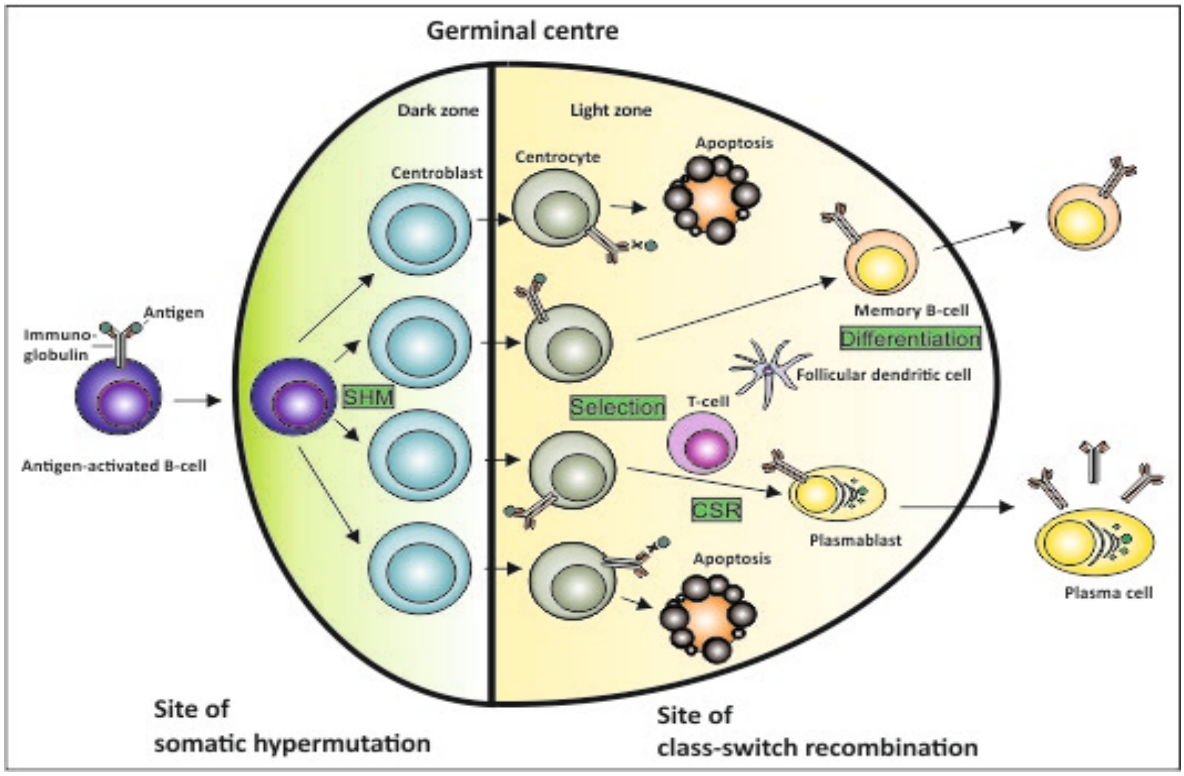

Figure 1.2: Diagram of germinal centre reaction, showing site of somatic hypermutation and class-switch recombination. Adapted from Klein and Dalla-Favera, 2008 (Klein and Dalla-Favera, 2008).

The formation of germinal centres is transient and begins with the acquisition of antigen by the resting B-cells (Calado et al., 2012, Scheller et al., 2009, Mesin et al., 2016). These B-cells move to the T-cell rich area known as the T-cell zone, where they receive stimulatory signals from the CD4+ helper T cells. This triggers a period of intense proliferation (Mesin et al., 2016). The proliferating B-cell's immunoglobulin genes are altered by means of somatic hypermutation and class switching (Scheller et al., 2009, Sampath et al., 2019, Dong et al., 2005). Plasmablasts are circulating, short lived, antibody secreting differentiated B-cells. Their formation is associated with changes in cellular morphology and gene expression. The expression of immunoglobulin heavy chain (IgH), immunoglobulin kappa light chain (IgK) and

immunoglobulin lambda light chain (IgL) is greatly increased in plasmablasts, which leads to an increased secretion of immunoglobulin proteins (Minnich et al., 2016).

Activation-induced cytidine deaminase (AID), which may act directly on DNA, drives somatic hypermutation of the immunoglobulin genes, class switch recombination and proliferation in the dark zone (DZ) of the germinal centre (Klein and Dalla-Favera, 2008, De Silva and Klein, 2015). This leads to the production of B-cells that express B-cell receptors (BCR) with an affinity for initiating antigen. These B-cells leave the DZ and enter the LZ where they are tested by the follicular dendritic cells for their ability to engage antigen (Suan et al., 2017). B-cells may also re-enter the DZ and begin additional cycles of SHM. This is known as cyclic re-entry (Figure 1.2). B-cells may then be selected to produce long lived plasma cells or memory B-cells. Non-selected B-cells are eliminated by means of apoptosis (Dominguez-Sola et al., 2012, Suan et al., 2017). B-cell lymphoma 6 (BCL6) is the master transcriptional regulator and together with B-lymphocyte induced maturation protein (BLIMP) are responsible for both plasma cell and memory B-cell differentiation in the germinal centre (Klein and Dalla-Favera, 2008, De Silva and Klein, 2015).

1.2.1 AID mode of action in SHM and CSR

To create antibody diversity in B-cells, immunoglobulin (*IG)* genes need to undergo several regulated alterations or controlled mutations. This *IG* remodelling occurs during the GC process and is essential for the humoral immunity response (Smit et al., 2003). In the GC DZ, AID is essential for SHM and CSR in the B-cells (Scheller et al., 2009). SHM is the mutation that occurs in the variable regions of the immunoglobulin genes to create greater antigen affinity. Class switching, also known isotype switching, is a mechanism that changes the B-cells production of immunoglobulin. AID deaminates cytosine to produce uracil in DNA. Mismatches that occur may be repaired by mismatch repair genes but may also be processed to produce double-stranded breaks that lead to class switch recombination or translocations. The translocations that may occur during SHM and CSR can be prevented or repaired by the activation of damage signalling proteins such as P53 (McBride et al., 2006). Most non-Hodgkin lymphomas (NHL) are of B-cell origin and many exhibit GC or post GC phenotype. Many B-cell

related NHL show *IG* gene related chromosomal translocations which would indicate a likelihood of DNA diversification mistakes in the GC, particularly during SHM and CSR (Smit et al., 2003, Ramiro et al., 2006). Chromosomal translocations associated with GC related non-Hodgkin lymphoma, show that the most frequent oncogenic translocation involves *MYC* and *IgH* created by AID. This occurs during CSR and SHM (Smit et al., 2003).

1.3 *MYC* gene function and regulation

The V-Myc Avian Myelocytomatosis Viral Oncogene Homolog (MYC) gene located on chromosome 8q24 is part of a gene family that comprises *N-MYC*, *L-MYC* and *S-MYC*. All of these *MYC* genes may code for MYC proteins (Tansey, 2014). MYC is a nuclear phosphoprotein which functions as a transcription factor and has both gene activating and gene repressing capabilities. MYC forms a heterodimer with another transcription factor, Myc-associated factor X (MAX) and regulates between 10-15% of all genes within the human genome. MYC has diverse biologic activities which include cell growth promotion and gene activation. These activated genes may function by increasing cellular metabolism, mitochondrial biogenesis, and biosynthesis of nucleic acids, ribosomes, and various proteins. MYC also functions as an important mediator of cell cycle progression, and the activation of proliferative genes that could encode for proteins such as cyclin D1 (CCND1) and inhibiting antiproliferative proteins such as cyclin-dependent kinase inhibitors. In so doing, MYC can drive the cell from the G0/G1 phase to the S phase of the cell cycle. MYC also plays a role in apoptosis, but the precise mechanism is unknown. MYC is however known to stabilise P53, which is a proapoptotic protein and tumour suppressor. MYC is therefore indirectly involved in inhibiting the antiapoptotic proteins BCLXL and BCL2. This in turn may induce the expression of BIM, which is a proapoptotic protein involved in the stimulation of cytochrome c release from mitochondria (Slack and Gascoyne, 2011) (Figure 1.3).

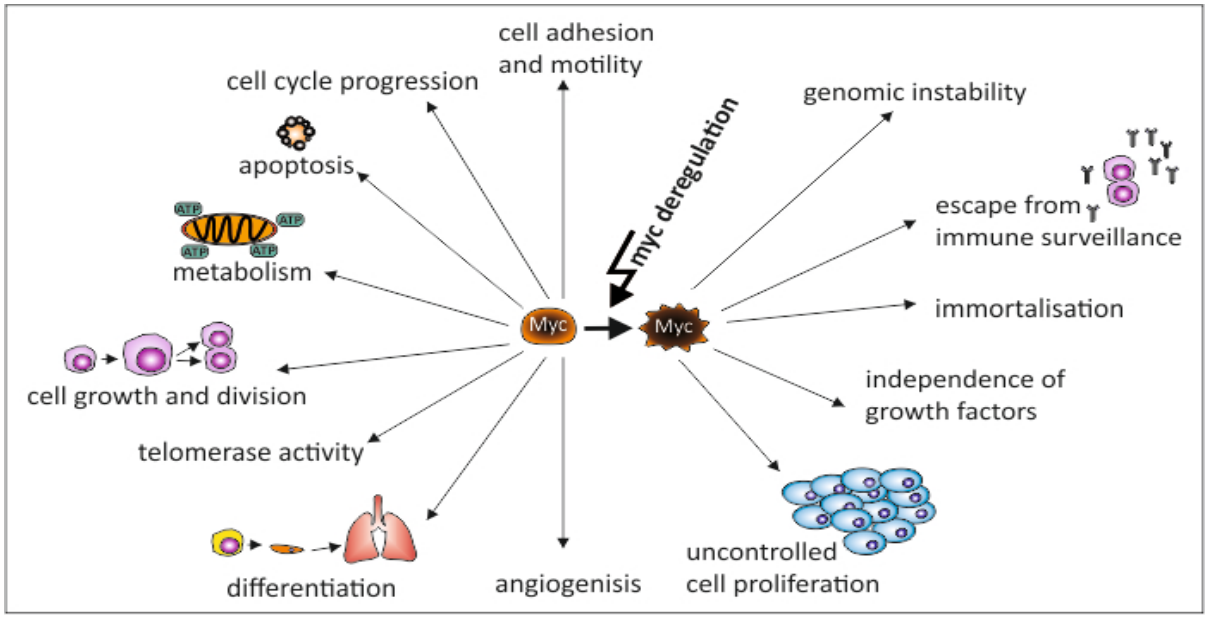

Figure 1.3: Role of the *MYC* gene and protein expression in normal and abnormal cell function. Adapted from Reisfeld, 2015 (Reisfeld, 2015).

In addition, MYC can amplify some of the transcribed genes within a cell (Ott et al., 2013). The primary function of normally regulated MYC is in cellular metabolism and growth regulation control. MYC expression and function are tightly regulated by mitogenic signals. MYC mRNA expression, present in normal cells has a very short half-life in the absence of positive regulatory signals. If these regulatory signals are absent, MYC protein levels become low, and provide no proliferative drive (Miller et al., 2012). MYC expression activates cell death pathways and affects apoptosis when inducing rapid DNA replication, which may lead to potential DNA damage. This would elicit the activation of *TP53*, which is a tumour protein gene coding for P53 (Ott et al., 2013). The P53 protein is a tumour repair protein which attempts to repair potentially damaged DNA from rapid replication. Failing that, P53 prevents the cell from dividing, thereby inducing apoptosis. *MYC* also encodes for a transcription factor that accelerates cell metabolism, proliferation and cell growth (Lynnhtun et al., 2014, Haikala et al., 2017). In normal cells, MYC coordinates acquisition of nutrients to produce ATP, which is a key component in cellular metabolism. MYC protein is important in the regulation of glycolysis by means of regulation of glucose metabolism genes (Miller et al., 2012). MYC plays an important role in the formation of the lymphoid follicle and the germinal centre. Naïve B-cells do not express MYC, but may do so as a result of antigen stimulation (Karube and Campo, 2015). MYC

is expressed in mature B-cells that initiate GC formation but is absent in the highly proliferative cells in the GC dark zone. MYC is upregulated in a few B-cells before BCL6 is expressed. BCL6 expression and binding to the MYC promoter, leads to the repression of MYC. The interplay between *MYC* and *BCL6* is associated with the dark zone of the GC and expansion of proliferating centroblasts, which are antigen activated B-cells. MYC negative cells in the light zone, may exit the germinal centre as memory cells or "immature" plasmablasts. BLIMP1 expression in these cells and MYC repression may lead to plasma cell differentiation (Ott et al., 2013). When the oncogenic potential of MYC is unlocked, and it is over expressed, it can drive metabolic genes and amplify gene expression in a non-linear way. This distorted gene expression leads to silencing of certain cell cycle checkpoints, and the uncontrolled growth creates dependence on MYC driven metabolic pathways, such as its effect on ATP production and glycolysis (Stine et al., 2015). This abnormal metabolic function also leads to the promotion of lipid, nucleotide and protein synthesis by MYC (Haikala et al., 2017). Oncogenic MYC expression can induce growth factor dependant cell cycle entry and prevent the cell cycle exit (Stine et al., 2015).

1.3.1 *MYC* and other gene aberrations in PBL

The oncogenic potential of *MYC* was first demonstrated in 1985, when it was discovered coupled with the immunoglobulin enhancer in mice, resulting in the formation of mature B-cell neoplasms (Vennstrom et al., 1982, Morton and Sansom, 2013, Nguyen et al., 2017). The t(8;14) (q24;q32) translocation involving *MYC* (8q24) and the *IGH* gene (14q32), is the most common genetic aberration observed in PBL, and is observed in about 60% of all PBL cases (Valera et al., 2010, Montes-Moreno et al., 2017, Bogusz et al., 2009) (Figure 1.4). This led to the suggestion that *MYC* activation plays an important role in PBL pathogenesis, and possible over expression of MYC protein (Harmon and Smith, 2016, Montes-Moreno et al., 2017). It is also however evident that MYC protein may be over expressed in PBL irrespective of whether there were *MYC* translocations, or any other *MYC* genetic alterations present. The overall survival rate of PBL patients decreases substantially when there are *MYC* aberrations present. (Montes-Moreno et al., 2017, Elyamany et al., 2015b). Besides translocations of the *MYC* gene, PBL may also be characterised by *MYC* gains in multiple chromosomal loci (Valera et al., 2010).

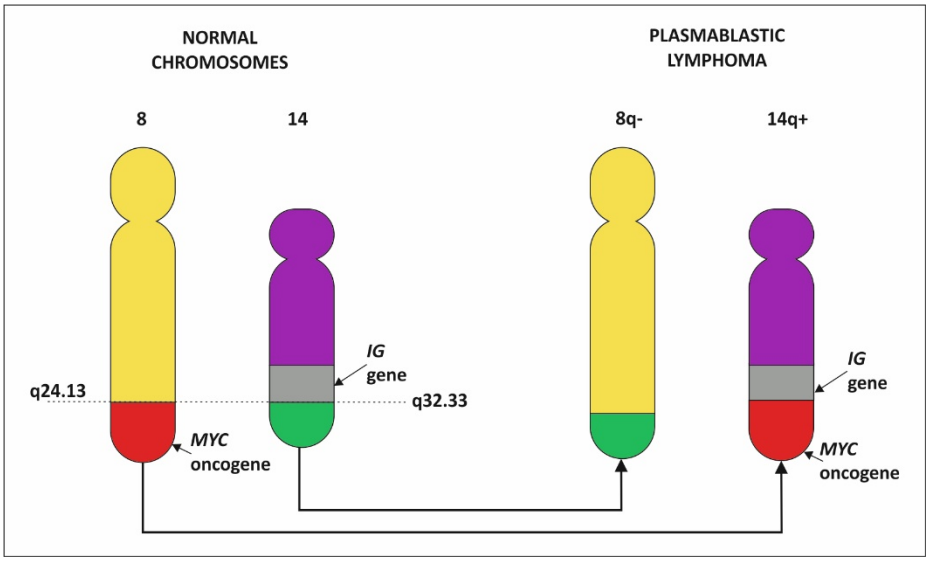

Figure 1.4: Diagrammatic representation of the reciprocal translocation of *MYC* gene on chromosome 8 with the *IGH* gene on chromosome 14. This translocation is frequently found in PBL.

Despite *MYC* gene aberrations being considered the primary driving force in PBL pathogenesis other genes such as BCL*2*, *BCL6*, *MALT1*, *PAX5*, *CCND1* and *PRDM1* (*BLIMP1*) have also been investigated. These studies yielded mix results, with rearrangements in these genes rarely being detected. However, gains of as much as 40%, were observed in some of these genes (Valera et al., 2010, Boy et al., 2011). *CCND1* gene gains were identified for the first time in PBL and resulted in an increased expression of the protein cyclin D1. Cyclin D1 is a key cell cycle regulatory protein involved in uncontrolled cell proliferation and is observed as a possible determining factor in the aggressive nature of NHL such as PBL (Boy et al., 2011). "Double-hit" (DH) phenomena, which may be found in DLBCL, are rarely found in PBL. Only one case has been reported thus far, showing *MYC and BCL2 translocations* (Boy et al., 2011). *PRDM1*, encodes for BLIMP1, which regulates plasma cell differentiation and may be expressed in PBL. *PRDM1* mutations are prevalent in PBL and may be associated with *MYC* translocation, gains and over expression. *PRDM1* mutations may be considered by some as a second genetic aberration in many PBLs and could possibly lead to the over expression of BLIMP1 protein (Montes-Moreno et al., 2017).

1.3.2 *MYC* aberrations in other lymphomas

MYC dysregulation in B-cell lymphomas may occur as either a primary or secondary event. In Burkitt lymphoma (BL) it presents as a primary event, while PBL, mantle cell lymphoma (MCL) and DLBCL it presents as a secondary event (Nguyen et al., 2017). Primary effusion lymphoma (PEL) with plasmablastic phenotype, which is a differential diagnosis for PBL, does not exhibit either primary or secondary *MYC* aberrations (Campo et al., 2017). BL was the first lymphoma that described *MYC* rearrangement and are observed in about 90% of cases (Adams et al., 1983, Alamri et al., 2017). In most cases of BL, *IGH* is the translocation partner, with a small percentage being associated with immunoglobulin light chains (Dawson et al., 2007). In BL, *MYC* rearrangements are therefore a useful diagnostic aid, and is most often associated with a simple karyotype (Slack and Gascoyne, 2011). *MYC* translocations have been identified in about 5-14% of DLBCL. As with many B-cell lymphomas, the *IG* breakpoints occur in the class switching regions which provides evidence that the *IG/MYC* translocations may occur in the germinal centre (Pedersen et al., 2019). In DLBCLs rearrangements in the *MYC* gene may be accompanied by re-arrangements in other genes such as *BCL2* and *BCL6*. In cases where *MYC* rearrangements occur together with rearrangements in *BCL2* or *BCL6,* they are referred to as double , and triple hit lymphomas if all three genes are re-arranged (Swerdlow, 2014, Rosenthal and Younes, 2017, Slack and Gascoyne, 2011). These phenomena are however uncommon in PBL.

1.3.3 Detection of *MYC* gene aberrations

There are two methods clinically available for *MYC* gene analysis, conventional karyotyping and fluorescent *in situ* hybridisation (FISH), with FISH being the most commonly used methodology (Nguyen et al., 2017). For diagnostic FISH in Anatomical Pathology, formal fixed paraffin embedded (FFPE) tissue is the preferred method, as conventional karyotyping requires fresh tissue (Nguyen et al., 2017) . There are two types of FISH probes used to detect *MYC* translocations. These are dual colour break apart rearrangement probes and dual colour dual fusion probes. The dual colour break apart rearrangement probe detects a *MYC* translocation without identifying the partner gene, while the dual colour dual fusion probe is

able to detect a *MYC* translocation and the partner gene involved (Dawson et al., 2007, Nguyen et al., 2017).

1.4 *Epstein-Barr virus* (EBV)

EBV or *human herpesvirus - 4* (HHV-4) is a human *gamma* herpesvirus. EBV is a double stranded DNA virus and it is estimated that approximately 90% of the human population is infected by the age of 40 years (Rezk et al., 2018). EBV was first discovered more than 50 years ago by Anthony Epstein and Yvonne Barr in BL cell lines (Epstein et al., 1964, Young et al., 2016).

1.4.1 Initial infection

Infection with EBV in humans usually occurs via contact with infected saliva, but may also be transmitted through blood, semen and organ transplants. EBV infects the epithelial cells and resting B -cells of the Waldeyer's ring of the oropharynx and tonsillar crypts, where replication takes place (Longnecker et al., 2013) (Figure 1.5).

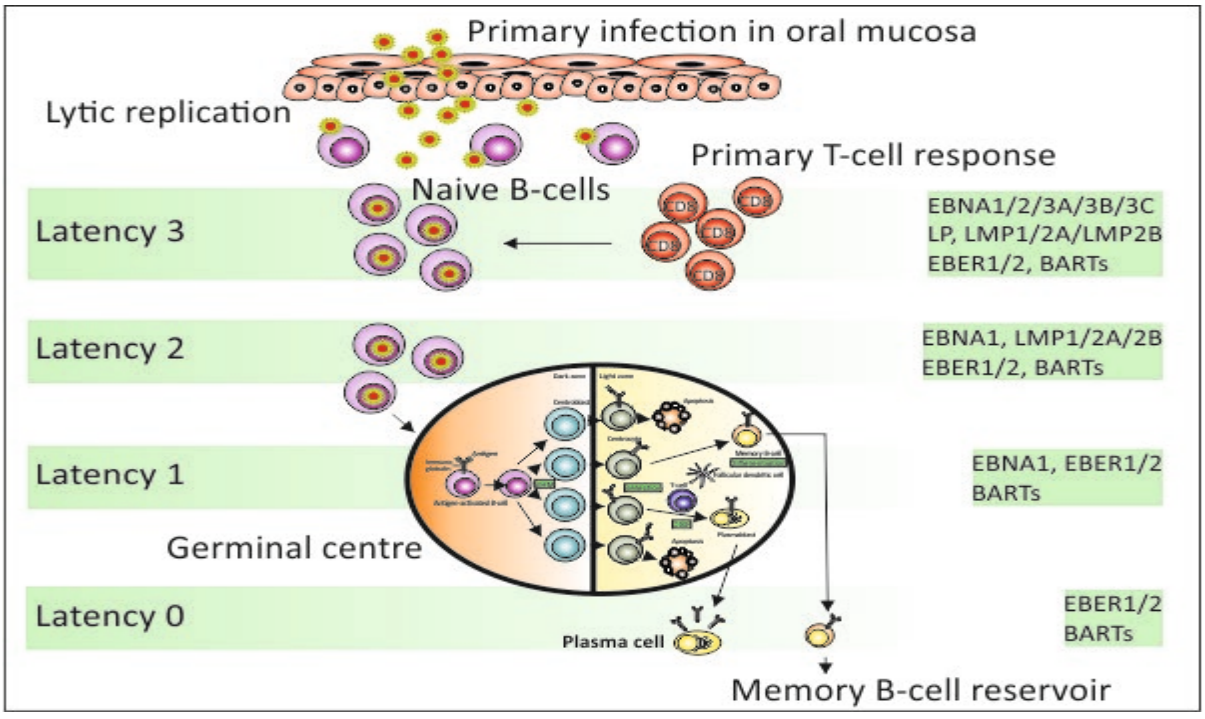

Figure 1.5: EBV primary route of infection and expected latency patterns.

Two different routes exist by which EBV glycoprotein binds to human epithelial cells and B-cell receptors. The infection of B-cells by EBV is well documented, however, EBV's entry into mucosal epithelium was not fully understood. The first route of infection is of the epithelial cells, and involves the EBV membrane glycoprotein BMRF2, which binds to the *beta*1 family integrins on the cell surface (Xiao et al., 2008). Ephrin receptor A2 (EphA2) on epithelial cells is responsible for EBV glycoprotein binding to these cells, and upregulation of EphA2 leads to an increase in epithelial cell infection by EBV (Chen et al., 2018, Zhang et al., 2018). However, it is also known that tonsillar epithelial cells may express CD21 on their surface, which would satisfy the more B-cell like route of infection, described below (Longnecker et al., 2013).

The second route is of infecting the B-cells, which is the primary objective of EBV. This infection enables EBV of maintaining a lifelong persistent infection. The binding mechanism of EBV to resting B-cells is facilitated by CD21 and MHC class II molecules on the surface of these cells. CD21, also known as complement receptor 2 (CR2), binds to EBV membrane glycoprotein GP350/220 (Longnecker et al., 2013, Hutt-Fletcher, 2017, Hutt-Fletcher, 2014, Hutt-Fletcher, 2007). After these initial fusions with the plasma membranes of epithelial cells or endocytic membranes of B-cells, the viral capsid is released into the cytoplasm and the linear viral genome is transported to and enters the nucleus via the nuclear pores. The viral genome then circularises and assembles into chromatin, and is often referred to as a viral episome, resembling a small human chromosome (Longnecker et al., 2013, Lieberman, 2015), with host chromosomal integration very rarely occurring (Morissette and Flamand, 2010). In the human host, EBV may exist in certain cells in either the latent phase or the lytic phase. During the latent phase only, certain latent proteins are expressed, while during the lytic phase, viral replication occurs. During either of these phases, the viral genetic material is preserved in the form of circular extrachromosomal DNA. Circularisation occurs in many herpes viruses and is thought to protect the ends against the effect of cellular nucleases (Takayuki and Tatsuya, 2014, Morissette and Flamand, 2010).

Indicators of initial infection include episodes of typical cold like symptoms, characterised by fever, sore throat and headaches. In teenagers and/or adults, EBV can cause infectious mononucleosis (IM), also known as mono or kissing disease (Louten, 2016). EBV infection is

typically asymptomatic in healthy individuals and is controlled by the immune system, particularly the CD8+ cytotoxic T-cells. EBV is however also associated with malignancies such as PBL, BL and nasopharyngeal carcinoma (NPC) (Hatton et al., 2014).

1.4.2 Latent Infection

During the EBV latency program up to 8 different EBV encoded proteins and non-coding RNAs are expressed. A pre-latent phase begins soon after initial infection, and thereafter four traditional latent phases occur. These are latency 0, 1, 2 and 3, and each of these latent phases results in the expression of various latent proteins and the repression of lytic genes. During the pre-latent phase, certain lytic and latent genes are expressed and EBV infects both epithelial and resting B-cells. Replication does not occur in the epithelial cells but takes place in the resting B-cells. These infected B-cells start to enlarge into blast cells and begin proliferation, with viral DNA becoming detectable. It is also during this phase that cellular chromatin is acquired, and eventually lytic genes are silenced. The pre-latent phase is complete about 14 days post infection (Hammerschmidt, 2015, Kempkes and Robertson, 2015, Price and Luftig, 2015).

EBV then enters a latency 3 phase (also referred to as the growth program) during which time all the protein encoding genes are expressed. These include the Epstein-Barr virus nuclear antigens (EBNA1, 2, 3A, 3B, 3C), latent membrane proteins (LMP1, LMP2a and LMP2b), the Epstein-Barr virus encoded RNAs (EBERs) and miRNAs. During latency 3, EBV drives the proliferation and differentiation of the B-cells into memory B-cells and expresses proteins that allow for bypassing of the normal host B-cell differentiation (Table 1.1). This proliferation of B-cells is curtailed to a certain degree by CD4+ helper and CD8+ cytotoxic T-cells (Heuts et al., 2014). The expression of all the EBV gene products during latency 3 allows for escape of normal immune surveillance in post-transplant and HIV associated immune suppressed patients (Cameron et al., 2008).

Table 1.1: The proteins expressed during the EBV latency types.

Latency 0	Latency 1	Latency 2	Latency 3
			EBNA-LP
	EBNA1	EBNA1	EBNA1
			EBNA2
			EBNA3
		LMP1	LMP1
		LMP2	LMP2
EBER	EBER	EBER	EBER
BART miRNA	BART miRNA	BART miRNA	BART miRNA

It is believed that all the other latency programs are generated from type 3 latency infected B-cells that pass through into the germinal centres of lymph nodes. This leads to the expression of latent proteins EBNA1, LMP1, LMP2 and EBER, which is in keeping with a type 2a latency pattern (Heuts et al., 2014). Even though latency type 2 is categorised as type 2a and 2b, they do not necessarily occur concurrently. Latency 2b was first observed in the primary infection of B-cells in patients with chronic lymphocytic leukaemia and was named latency 2b because the protein expression was directly opposite to that of latency type 2a. Further research showed that type 2b latency actually occurred just before latency 3 (Price and Luftig, 2015). After exiting the germinal centres of the lymph nodes and entering circulation, the latently infected B-cells express only EBER's and miRNAs. No other EBV proteins are expressed and this is referred to as latency 0. Latency 1 occurs when only EBNA1 is expressed briefly during the cell cycle. Latency 0/1 is sometimes also referred to as restricted or true latency, and results in complete immune surveillance evasion (Kliszczewska et al., 2017).

1.4.3 EBV Latent protein location and function

1.4.3.1 EBNA1

Epstein-Barr nuclear antigen 1 (EBNA1) is expressed during latency 1, 2 and 3. EBNA1 is however not expressed in latency 0 which occurs in resting memory B-cells. It is thought to be expressed briefly during the cell cycle, resulting in EBV latency 1 for a brief period (Rezk et al., 2018). It is expressed in the nucleus and is considered the viral genome maintenance protein and may be expressed in both lytic and latent EBV infection. EBNA1 depletion in latently infected cells may lead to EBV reactivation and is credited as the driving force in EBV moving

from a latency cycle to a lytic one (Frappier, 2012, Sivachandran et al., 2012). EBNA1 also plays a role in the transcriptional regulation of other latent nuclear and membranous proteins and is not recognised by the cytotoxic T-cells (Rezk et al., 2018, Sivachandran et al., 2012).

1.4.3.2 EBNA2

Epstein-Barr nuclear antigen 2 (EBNA2) and Epstein-Barr nuclear antigen leader protein (EBNA-LP) are co-expressed soon after EBV infection of B-cells. EBNA2 is expressed during latency 3 only in the nucleus of infected cells and is essential for B-cell transformation. Both EBNA2 and EBNA-LP are associated with binding to upstream elements of *MYC* and *MYC* regulated genes. This may result in an increased *MYC* driven cellular proliferation (Rezk et al., 2018, Kang and Kieff, 2015).

1.4.3.3 EBNA3 Family

Epstein-Barr nuclear antigens 3A/3B/3C (EBNA3A/3B/3C) belong to a family of genes that have the same promoter, have similar gene structures and are similarly regulated. The EBNA3 family is expressed during latency 3 only and is expressed in the nucleus of infected B-cells. The entire EBNA3 family functions as coactivators of EBNA2. EBNA3A functions as a transcriptional regulator that influences viral and cellular gene expression. EBNA3A may also play a role in B-cell transformation. The inactivation of EBNA3B, which is the EBV-encoded tumour suppressor drives lymphomagenesis and immune evasion. EBNA3B also upregulates CXCL10 and has a growth inhibitory role. Among the 6 latent nuclear proteins, EBNA3B is the only dispensable protein for B-cell transformation. EBNA3C coactivates the LMP1 promoter with EBNA2, and induces disturbances of various cell-cycle checkpoints, which promotes cell proliferation and induces G1 arrests. These are essential for EBV mediated B-cell transformation (Rezk et al., 2018, Kang and Kieff, 2015).

1.4.3.4 EBNA-LP

Epstein-Barr nuclear antigen leader protein (EBNA-LP), is also sometimes referred to as EBNA5, and is expressed during latency 3 only. EBNA-LP is expressed in the nucleus of infected cells.

EBNA-LP is one of the first viral proteins produced by EBV. The main function of EBNA-LP is coactivator of EBNA2 and is also responsible for driving resting B-cells into the G1 or growth phase of the cell cycle by binding and inactivating cellular P53 (Kang and Kieff, 2015, Rezk et al., 2018, Thompson and Kurzrock, 2004).

1.4.3.5 LMP1

Latent membrane protein 1 (LMP1) is expressed during latency 2 and 3. LMP1 is expressed in the cytoplasmic membrane of infected B-cells. LMP1 is involved in B-cell transformation and can mimic the active receptor CD40 by associating with the same tumour necrosis factors. LMP1 has also been recognised as the primary transforming gene product of EBV. LMP1 is expressed in many EBV associated lymphoproliferative diseases and is directly linked to oncogenesis. LMP1 is also linked to enhanced expression of B-cell adhesion molecules, enhanced expression of B-cell activation molecules and cellular clumping. By causing the overexpression of BCL2, it protects infected B-cells from P53 induced apoptosis (Thompson and Kurzrock, 2004, Kieser and Sterz, 2015, Rezk et al., 2018).

1.4.3.6 LMP-2A and LMP-2B

Latent membrane protein 2A/2B (LMP-2A/2B) is expressed during latency 2 and 3. Both LMP-2A and 2B are coded by the same *LMP-2* gene. LMP-2A and 2B are expressed in the cytoplasmic membrane of infected B-cells. EBV infected cells are prevented from entering the lytic cycle by LMP2A, which can sequester tyrosine kinase from BCR and thereby result in the inhibition of BCR signalling. LMP2A is therefore able to mimic BCR and replace survival signals for B-cells. LMP-2B negatively regulates LMP-2A functions in preventing the switch from latent to lytic replication. LMP-2A and 2B modifies normal B-cell development in favour of an EBV latency program (Rezk et al., 2018, Thompson and Kurzrock, 2004).

1.4.3.7 EBER-1 and EBER-2

EBER 1 and 2 are expressed abundantly in the nuclei of almost all EBV infected B-cells, during all latency programs. The EBER's are non-polyadenylated RNAs that are not essential for the

EBV-induced transformation of B-cells. They also play a role in inducing the production of IL-10, which might suppress cytotoxic T cells and stimulate growth of infected B-cells. EBERs have also been thought to play a modulatory role of the pathways important in interferon response (Thompson and Kurzrock, 2004, Rezk et al., 2018).

1.4.3.8 BARTs

*Bam*HI fragment A rightward transcripts (BARTs) are EBV miRNAs that are expressed in the nucleus of EBV infected cells during all forms of latency. The main function of BARTs are to act as epigenetic regulators of the microenvironment which is conducive for EBV latency. BARTs also enable EBV to evade the host immune response. The exact role of BART in tumourigenesis and possible treatment target is subject of much research (Verhoeven et al., 2019).

1.4.4 Lytic infection and reactivation

After initial infection the virus embarks on a short lytic program before adopting a lasting or persistent latent infection. Only a small percentage of infected cells switch from the latent to the lytic phase (Takayuki and Tatsuya, 2014). During the latent phase in infected B-cells, EBV exists as a nuclear episome, which is replicated once per cell cycle with the aid of the hosts DNA polymerase (Kenney and Mertz, 2014). During the lytic cycle, all the viral lytic genes are expressed, including the virus's transcription factors BZLF1 and BRLF1 as well as a viral DNA polymerase catalytic subunit (Takayuki and Tatsuya, 2014, Kenney and Mertz, 2014).

The life cycle of EBV may be referred to as biphasic since the virus may alternate between a latent or lytic phase (Hammerschmidt, 2015, Takayuki and Tatsuya, 2014). Reactivation may be divided into three phases viz intermediate early (IE), early (E) and late (L). During IE, two transcription factors are expressed. Two viral genes *BZLF1* and *BRLF* are transcribed to encode the transactivator proteins BZLF1 also known Zta and BRLF1, also known as Rta (Li et al., 2016). The entire EBV reactivation and drive to the lytic phase may be triggered by BZLF/Zta and BRLF/Rta, which belong to the same transcription factor family. These transcription factors are never expressed during the latent phase, due to silencing by transcriptional repressors (Kenney

and Mertz, 2014). This is followed by an early phase (E) during which time the proteins involved in DNA replication are produced. The last phase is the late phase (L), during which time the virions are formed (Thorley-Lawson et al., 2013). Activation of the lytic program and replication of EBV appears to take place in the circulating B-cells that move through the lymphoid tissue in the oropharyngeal epithelial cell mucosa. The virus then passes into the epithelial cells, where it is amplified and shed in the saliva for possible infection (new host or present host B-cells) to establish a lifelong persistence (Hutt-Fletcher, 2014, Hutt-Fletcher, 2017).

1.4.4.1 Mechanism of reactivation

BZLF1/Zta, also sometimes referred to as ZEB1, is the major trigger of the EBV lytic cycle of events and may be activated in B-cells by a variety of physiological stimuli as well as chemical agents (Kenney and Mertz, 2014). The amount of BZLF1 expression determines whether EBV is in a latent form or in a reactivated form (Murata, 2014, Takayuki and Tatsuya, 2014). Surface B-cell receptor (BCR) is stimulated, which results in signal transmission to the latent virus in the nucleus. This BCR signal activation causes the expression of BZLF1. When there is sufficient circulating antibodies, BCR is not stimulated and EBV remains in latency (Takayuki and Tatsuya, 2014). When there is a decrease in serum antibodies or increase in antigens, this is thought to simulate EBV lytic reactivation (Takayuki and Tatsuya, 2014). However, the precise method of reactivation is the topic of much research, and another widely accepted theory is that lytic replication may be linked to differentiation of cells that are latently infected by EBV. It is further purported that when B-cells differentiate into plasma cells, the lytic phase is induced by the plasma cell differentiation factor XBP-1. However, it has also been suggested that when LMP1 down-regulates the B-lymphocyte - induced maturation protein 1, (BLIMP1), plasma cell differentiation is disrupted which leads to EBV lytic replication regulation (Longnecker et al., 2013). It should also be considered though, that LMP1 which may be detected in EBV positive PBL, is only expressed during latency 2 and 3.

1.4.5 Oncogenesis

EBV needs to maintain its viral genome in the infected B-cell but must avoid killing the cell, in order to remain oncogenic. Furthermore, EBV must prevent the infected cell from being

targeted by the human immune response, by means of cellular growth control pathway intervention (Thompson and Kurzrock, 2004, Price and Luftig, 2015). When EBV establishes true latency and the only EBV proteins expressed are EBERs and or EBNA1, the host immune surveillance is evaded, and the cells are not pathogenic (Price and Luftig, 2015). Viral DNA, which exists as an extra chromosomal episome in the nucleus, still needs to be maintained, and is transmitted via cell progeny when B-cells replicate. Although these cells are not transformed or acquire oncogenic mutations, they may become neoplastic (Thompson and Kurzrock, 2004). Potential oncogenesis by EBV occurs in a multistep approach. It is thought to occur during latency 3, when the full repertoire of EBV proteins are expressed (Murata et al., 2014). LMP1 and LMP2A, which are two known and frequently identifiable and studied EBV oncogenes, are encoded and act in concert. The function of LMP1 is to elicit growth promoting signals by mimicking the CD40 signalling pathway. LMP2A is structurally like and functions identically to the BCR. It is likely that due to LMP1's ability to mimic CD40 and LMP2A's ability to mimic BCR in the germinal centre, also allows for the deregulation of the host immune system (Murata et al., 2014). EBNA 3A and 3C play a critical role in the maintenance and formation of neoplastic cells by silencing tumour suppressor genes (Vega et al., 2004, Murata et al., 2014).

EBER, which is present during all latencies is constantly under investigation and has also been implicated in oncogenesis, but its precise role needs further research.
The escape from the host immunity, by virtue of a systematic suppression of the immune system by HIV, may result in the emergence of certain EBV positive B-cell lymphomas such as PBL (Murata et al., 2014). The role of immune suppression contributes to latently infected cells in the peripheral blood to increase in number. EBV is also able to activate intracellular signalling involved in the control of cell proliferation (Thompson and Kurzrock, 2004). A further method of immune evasion by EBV, involves the expression of EBNA1 Gly/Ala repeat sequence, which has the ability of impairing antigen presentation.

1.4.6 Latency in PBL

The EBV latency pattern most commonly reported in PBL is latency type 1, but latency 2 and latency 3 have also been reported. In latency 1, EBER, EBNA1 and miRNAs (BARTs) are the only EBV proteins expressed and complete host immune evasion is maintained (Rezk et al., 2018, Rezk and Weiss, 2007). EBV Latency type 2 was reported in a study by Ambrosio et al., 2017, when EBER, EBNA1 and LMP2 proteins were expressed (Ambrosio et al., 2017). However, latency 3, where all EBV latent proteins are expressed, has been reported in cases of HIV positive oral cavity PBL and post-transplant immunosuppression (Bibas and Castillo, 2014, Castillo et al., 2015).

1.4.7 EBV Latency in other lymphomas and malignancies

The table below (Table 1.2), provides a summary of the various EBV associated disorders and the EBV latent protein expression. Many of these EBV related disorders are often associated with a coinfection with HIV as in the case of DLBCL, immunodeficiency associated BL and EBV associated smooth muscle tumour (EBV-SMT). EBV related disorders may also be associated with other pathogens such as the malaria parasite *plasmodium falciparum* in the case of endemic BL.

Table 1.2: EBV Latency in other lymphomas and malignancies *(Rezk, 2018)*

Disease	EBV Frequency	EBV Latency	Latent protein expression pattern
Hodgkin lymphoma	40%	Latency 2	EBNA1, LMP1, LMP2
Burkitt lymphoma	20-95%	Latency 1	EBNA1
Primary effusion lymphoma	>90%	Latency 1/2	EBNA1 and or LMP1, LMP2
Diffuse large B-cell lymphoma	30-60%	Latency 3	EBNA1, 2, 3, LP, LMP1, LMP2
Primary CNS lymphoma	>95%	Latency 3	EBNA1, 2, 3, LP, LMP1, LMP2
Nasopharyngeal carcinoma	>80%	Latency 3	EBNA1, 2, 3, LP, LMP1, LMP2
EBV associated smooth muscle tumour	100%	Latency 3	EBNA1, 2, 3, LP, LMP1, LMP2

1.5 Rationale for doing this research

The rationale for doing this research is to gain a better understanding of the pathogenesis of PBL in the context of EBV infection. To understand how each EBV gene product during the latent phase contributes (if at all) to the pathogenesis of PBL and to determine if these correlate with any clinical or histopathological parameters. The goal is to understand EBV-related diseases with a view to effective prevention and treatment strategies. In the SA context, EBV latency in PBL has not been previously investigated. Determining the *MYC* gene status will provide some insight with regards to the prognostic value of this marker in our setting. Patients may be stratified according to their *MYC* gene status to receive targeted treatment or closer follow-up. It is also observed that the median survival of patients is greatly reduced when *MYC* rearrangements were present.

1.6 Aims and objectives

1. To characterise the EBV latency in a cohort of patients diagnosed with PBL at GSH, by means of immunohistochemistry.
2. To determine the *MYC* gene aberrations in the same cohort, using fluorescent *in situ* hybridisation (FISH).

CHAPTER 2

MATERIALS AND METHODS

2.1 Ethics approval

Scientific approval for the study was obtained from the Department of Pathology Research Committee, Faculty of Health Sciences, University of Cape Town. Thereafter, the protocol was approved by the Human Research Ethics Committee (HREC) of the Faculty of Health Sciences, University of Cape Town (HREC Ref Number: 533/2017).

2.2 Study design

A search of the National Health Laboratory Service (NHLS) laboratory information systems (DISA and Trak) in the Division of Anatomical Pathology, Groote Schuur Hospital (GSH) was performed for all cases diagnosed as PBL from 2005 to 2017. Patient information such as age, gender and HIV status were recorded, in addition to all diagnostic immunohistochemistry (IHC) results. This information was collated into a Microsoft Excel (Microsoft, Redmond, Washington, USA) spreadsheet and patient identifiers were removed to ensure patient confidentiality. The cases were then assigned a randomised study number. All study information and material were securely stored for the duration of the study. SPSS (IBM, New York, USA) statistical software was used to analyse all patient demographic information as well as EBV and *MYC* test results.

2.3 Sample selection

The slides for the selected cases were retrieved from the archives of the Division of Anatomical Pathology, NHLS, Groote Schuur Hospital. The PBL diagnosis was reviewed, confirmed and thereafter the wax blocks were retrieved. The inclusion criteria included a confirmed diagnosis of PBL and adequate, well preserved tissue. Cases with insufficient or poorly preserved tissue, ALK+ immunohistochemistry as well as duplicate cases were excluded.

2.4 Immunohistochemical staining

To determine the EBV latency status, 3 immunohistochemical stains were performed on each EBV positive case, using three primary antibodies viz., EBNA1, EBNA2 and LMP1. In order to rule out ALK-positive LBCL, which exhibits a similar immunophenotype as PBL, ALK IHC was performed on selected cases (all EBV negative cases and a random selection of EBV positive cases)

2.5 Immunohistochemical staining protocol

Immunohistochemistry was performed using the commercially available Envision+ HRP System Labelled Polymer Anti-Mouse kit (DAKO/Agilent, Santa Clara, CA, USA). The preparation of all buffers and reagents used in the staining protocol are listed in Appendix 1. Three-micron tissue sections were cut on a Leica Rotary Microtome RM2125 RTS (Leica Biosystems Inc GmbH, Wetzlar, Germany), floated on a water bath (Sakura Finetek, Nihonbashi-Hamacho, Chuo-ku, Tokyo, Japan) and picked up on coated HISTOBOND® slides (Paul Marienfeld GmbH & Co, Lauda-Königshofen, Germany). The sections were then heat fixed on a hotplate (Hospital and Laboratory Supplies Ltd, London, England) at 60^{o}C for 10-15 minutes. Thereafter, the sections were dewaxed through a series of xylene baths, cleared in ethanol and hydrated in running tap water for 5 minutes. Antigen retrieval was performed using the conventional pressure cooker method. Each antibody required a specific buffer solution for antigen retrieval (Appendix 1, Table 2.1), but the process of antigen retrieval remained the same. Either a citric acid buffer (pH6) or Tris/EDTA buffer (pH9) was used. The antigen retrieval buffer was poured into the pot of the pressure cooker and was placed on a heating plate (J.P. Selecta S.A, Autovia, Barcelona, Spain), to get to a rolling boil. The slides were placed into a stainless-steel slide rack and submerged in the boiling solution. The pressure cooker lid was placed on the cooker and the timer was set. After 1 minute and 30 seconds, the pressure cooker was removed from the heating plate and placed under a stream of running tap water to allow the pressure to drop for the lid to be removed safely. The slides were then allowed to cool down in the buffer solution for a further 30 minutes and then washed in running tap water for 2-3 minutes.

Table 2.1: Immunohistochemistry antibody staining information

Primary Antibody/ Manufacturer	Clone	Clonality/ Species	Antigen retrieval	Dilution	Incubation time (minutes)	Positive control tissue
EBNA1 (Biorad)	E1-2.5	Monoclonal mouse	Citric acid	1:10	60	EBV-SMT
EBNA2 (Novus Biologicals)	PE2	Monoclonal mouse	Citric acid	1:250	60	EBV-SMT
LMP1 (DAKO/ Agilent)	CS.1-4	Monoclonal mouse	T/EDTA	1:300	60	NPC
ALK (DAKO/ Agilent)	ALK1	Monoclonal mouse	CC1	1:20	36	ALK-positive anaplastic large cell lymphoma (ALK-positive ALCL)

Key: ALK=Anaplastic lymphoma kinase, EBV=Epstein-Barr virus, EBNA1=Epstein-Barr nuclear antigen 1, EBNA2=Epstein-Barr nuclear antigen 2, LMP1=Latent membrane protein 1, T/EDTA - Tris EDTA, PBS=Phosphate buffered saline

The sections were then flooded with a 3% solution of H_2O_2 (Appendix 1) and incubated for 10 minutes at room temperature (RT) to block endogenous peroxidase activity. The sections were then washed in running water for 2-5 minutes and then with PBS/Tween (Appendix 1) for 5 minutes. A 5% solution of normal goat serum (Appendix 1) was applied to the sections and allowed to incubate for 15 minutes at RT to block nonspecific antibody binding. The goat serum was wiped from around the sections and edges of the and marker pen (DAKO/Agilent, Santa Clara, CA, USA) was used to circle around the sections to prevent antibody run off. One hundred microliters of diluted primary antibody was applied to each section (Table 2.1), and allowed to incubate for 1 hour at RT. After 1 hour, each slide was rinsed off with PBS (Appendix 1) and then washed for a further 5 minutes in PBS/Tween. Two drops of Envision+ HRP System Labelled Polymer Anti-Mouse (DAKO/Agilent, Santa Clara, CA, USA) was applied to each section and incubated for 30 minutes at RT. Each slide was then rinsed with PBS and washed for a further 5 minutes in PBS/Tween. The working DAB solution (Appendix 1) was then prepared. Two drops of DAB solution was applied to each section and incubated at RT for 10 minutes.

After staining with DAB, the sections were washed in running tap water for 5 minutes and then counterstained with Mayer's haematoxylin (Appendix 1) for 3 minutes. Thereafter, the sections were rinsed in running tap water and the nuclei were blued in bluing solution (Appendix 1) for 30 seconds. The slides were dehydrated in alcohol and cleared in xylene (Merck KGaA, Darmstadt, Germany). The slides were then cover slipped using glass coverslips (Paul Marienfeld GmbH & Co, Lauda-Königshofen, Germany) and Entellan (Merck KGaA, Darmstadt, Germany). A positive and negative control was included in each batch of immunohistochemical stains. The positive control was either NPC tissue or EBV-SMT, while the negative control excluded the application of the primary antibody with PBS used as a substitute (Appendix 3).

2.5.1 Interpretation of EBV immunohistochemical stains

The immunohistochemical stains were evaluated using an Olympus BX43F (Olympus, Shinjuku, Tokyo, Japan) microscope. Staining was scored as either positive, showing a brown DAB staining reaction, or negative, when showing the lack thereof. EBNA1 and EBNA2 have a nuclear localisation while LMP1 has cytoplasmic or membranous localisation in the tumour cells.

2.5.2 Immunohistochemistry optimisation

The optimisation strategy for each antibody included determining the optimal dilution, and antigen retrieval solution (Table 2.1).

2.6 CD246, ALK Protein (Anaplastic Lymphoma Kinase) ALK1 clone

The selected FFPE wax blocks were sectioned at 3µm, using a Leica Rotary Microtome RM2125 RTS (Leica Biosystems Inc GmbH, Wetzlar, Germany). The sections were heat fixed on a hotplate (Hospital and Laboratory Supplies Ltd, London, England) at 60^{o}C for 10-15 minutes. The slides were then placed on the Ventana XT auto-stainer (Roche Diagnostics, Basel, Switzerland). The protocol included dewaxing using EZ Prep (Roche Diagnostics, Basel, Switzerland), antigen retrieval for 64 minutes in CC1 (Roche Diagnostics, Basel, Switzerland), primary antibody incubation for 36 minutes and detection using Optiview DAB. On completion

of the protocol, the slides were removed from the auto-stainer, washed briefly in diluted detergent and water, and then stained in haematoxylin for 3 minutes. The slides were washed in water, placed in bluing solution (Appendix 1) for 30 seconds and rinsed in running tap water for another minute. The slides were dehydrated in alcohol and cleared in xylene (Merck KGaA, Darmstadt, Germany). The slides were then cover slipped using glass coverslips (Paul Marienfeld GmbH & Co, Lauda-Königshofen, Germany) and mounted in Entellan (Merck KGaA, Darmstadt, Germany). A positive and negative control was included in each batch of immunohistochemical stains. The positive control was ALK-positive ALCL tissue while the negative control excluded the application of the primary antibody with PBS used as a substitute (Appendix 3).

2.6.1 Interpretation of ALK staining

The processed slides were evaluated using an Olympus BX43F (Olympus, Shinjuku, Tokyo, Japan) microscope. Staining was interpreted as positive when brown DAB staining was observed in the nuclei and/or cytoplasm of the tumour tissue.

2.7 EBER *In Situ* Hybridisation

EBER ISH was performed on earlier cases when EBER ISH was not available on the diagnostic platform. This test was performed on the Roche Ventana XT auto-stainer (Roche Diagnostics, Basel, Switzerland). The FFPE wax blocks were sectioned at 3µm, using a Leica Rotary Microtome RM2125 RTS (Leica Biosystems Inc GmbH, Wetzlar, Germany) and mounted on coated HISTOBOND® slides (Paul Marienfeld GmbH & Co, Lauda-Königshofen, Germany). The slides were then heat fixed on the hotplate (Hospital and Laboratory Supplies Ltd, London, England) at 60^{o}C for 10-15 minutes. Thereafter slides were placed on the Roche Ventana XT auto-stainer (Roche Diagnostics, Basel, Switzerland). The protocol included dewaxing with EZ Prep (Roche Diagnostics, Basel, Switzerland), antigen retrieval using CC2 (Roche Diagnostics, Basel, Switzerland), probe denaturation and hybridisation and detection. The indirect detection method involved the use of an antibody and substrate-chromogen linked enzyme system. After completion of the protocol, the slides were removed and placed in a stainless-steel rack for the post staining dehydration procedure. The liquid coverslip (LCS) was removed

from the slide by washing in a mild detergent and the slides were then washed in running tap water for about a minute. After washing in water, the slides were then washed in grade alcohols (80-100%) for about 2 minutes each and then dipped into acetone briefly for 10 times. The slides were cleared in three baths of xylene (Merck KGaA, Darmstadt, Germany) for 30 seconds each. After clearing in xylene, the slides were cover-slipped using Entellan mounting media (Merck KGaA, Darmstadt, Germany). A positive control was included with each batch of EBER ISH. The positive control was either EBV-SMT or NPC tissue.

2.7.1 Analysis of EBER ISH

The processed slides were analysed using an Olympus BX43F (Olympus, Shinjuku, Tokyo, Japan) light microscope. A dark blue stain present in nuclei of the tumour cells indicated a positive EBER result.

2.8 Fluorescence *in situ* hybridisation (FISH)

FISH was performed on all cases in the cohort. The H&E and/or most recent immunohistochemical stained slide were used to identify the most suitable area to perform FISH, as the whole section was not used. Areas of necrosis, traction distortion and haemorrhage were avoided and an area 5mm x 5mm was identified and circled with a fine liner. Using a Leica Rotary Microtome RM2125 RTS (Leica Biosystems Inc GmbH, Wetzlar, Germany), 4µm sections were cut and mounted on HISTOBOND® slides (Paul Marienfeld GmbH & Co, Lauda-Königshofen, Germany). The slides were then dried in an incubator (Memmert GmbH, Schwabach, Germany) at 37^{o} C overnight. The next day, the slides were dewaxed in three changes of xylene for 5 minutes each and then three changes of graded alcohol of 70%, 85%, 100% concentrations (Appendix 1) for 2 minutes each. The slides were air dried and then treated in 0.2N HCl at 37^{o}C in a water bath for 20 minutes. Thereafter, the slides were washed in deionised water for 5 minutes followed by a wash in 2xSSC (Appendix 1) for 5 minutes at RT. Antigen retrieval was performed using 1M sodium thiocyanate (NaSCN) at 80^{o}C in a water-bath for 30 minutes. (Appendix 1) After antigen retrieval, the slides were washed in 2xSSC for 10 minutes at RT and then for 5 minutes in deionised water. The tissue sections were then digested in 0.05% pepsin/0.01N HCl at 37^{o}C in a water bath for between 16-30 minutes. At

the end of the digestion, the slides were washed in deionised water for 2 minutes, dehydrated in graded alcohols for 2 minutes and allowed to air dry in a darkened cupboard. Thereafter, the probe, Vysis LSI *MYC* Dual Colour Break Apart Rearrangement Probe (Abbott Laboratories, Illinois, USA) (Table 2.1), was prepared according to manufacturer instructions (Appendix 1, Table 5.1). Five microliters of the probe mix was applied to each section and coverslipped. The edges of the coverslip were sealed using Fixogum rubber cement (Marabu GmbH & Co. KG, Bietigheim-Bissingen, Germany). The slides were then placed on a slide hybridiser (DAKO/Agilent, Santa Clara, CA, USA). The denaturation and hydridisation conditions for the *MYC* probe were as follows: Denaturation at 73^{o}C for 5 minutes and then hybridisation at 37^{o}C for 24hrs. After hybridisation, the coverslip of the section was gently removed, and the slides were washed in 2X SSC/0.3% IGEPAL CA-630 post hybridization buffer at RT for 2 minutes. Thereafter, slides were washed in 2X SSC/0.3% IGEPAL CA-630 post hybridisation buffer at 72^{o}C in a water bath for 2 minutes and 10 seconds. The slides were then removed, the edges and around the sections were dried and the slides were placed in a darkened cupboard to dry completely. Thereafter, the sections were mounted in 5 µl of DAPI II counterstain (Abbott Laboratories, Illinois, USA) and coverslipped. The edges of the coverslip were sealed using clear nail polish and allowed to dry in a dark cupboard. A DLBCL with a *MYC* translocation served as the positive control while a reactive lymph node served as the negative control.

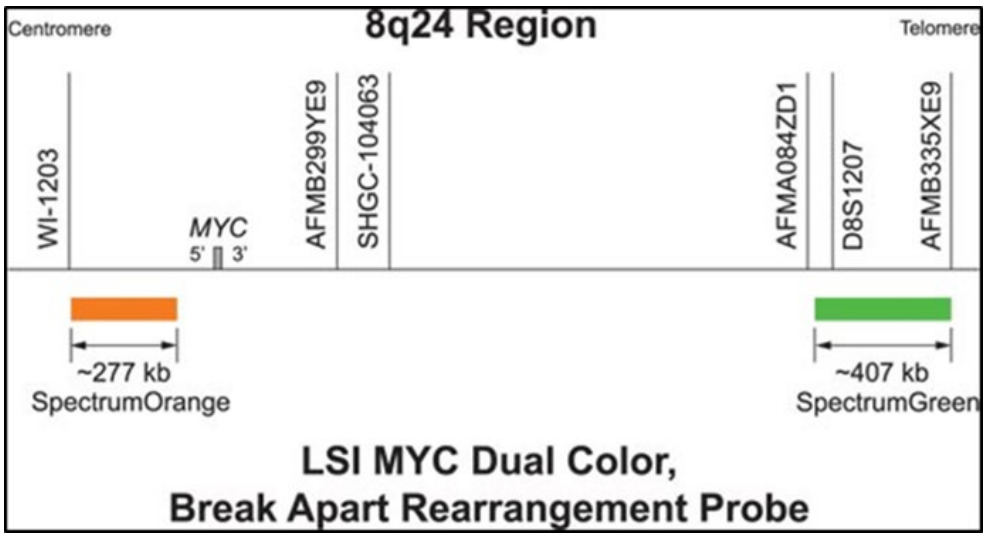

Figure 2.1: Diagrammatic representation of the *MYC* FISH probe map. The 277kb SpectrumOrange probe is designed to anneal centromerically to the 5' end, while the 407kb SpectrumGreen probe is designed to anneal telomerically to the 3' end of the *MYC* gene.

2.8.1 Analysis of *MYC* FISH

The processed slides were viewed, analysed and photographed on a Zeiss Axioskop 40FL fluorescent microscope (HBO 100) fitted with the appropriate excitation and emission filters (Carl Zeiss AG, Oberkochen, Germany). At least 100-200 non-overlapping, intact nuclei in an area of tumour tissue were assessed. Nuclei containing two orange/green (yellow) fusion signals indicated an intact *MYC* gene while nuclei showing one orange, one green and one orange/green (yellow) signal indicated MYC translocation. *MYC* gain was observed as 3-4 orange/green (yellow) signals while *MYC* amplification was observed as >4 orange/green (yellow) signals. When scoring, a cut-off for structural and numerical aberrations of ≥5% was applied. The expected FISH signal patterns are found in Figure 2.2 (Ventura et al., 2006).

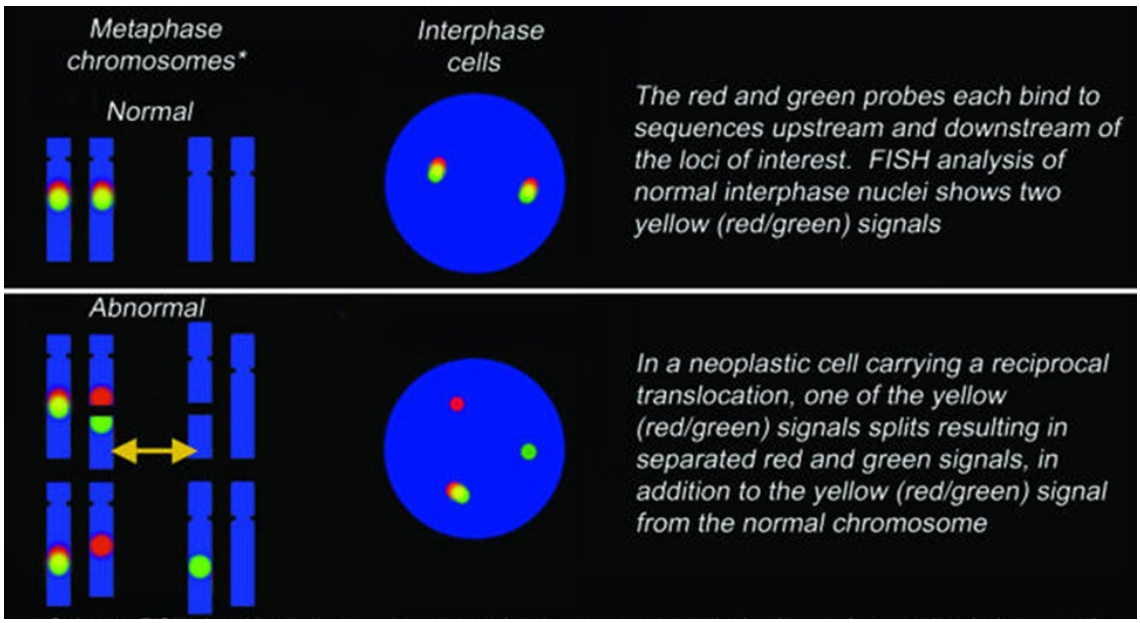

Figure 2.2: Anticipated FISH hybridisation pattern. Normal intact signal (top) and abnormal broken apart signal (bottom) (Ventura et al., 2006).

2.8.2 Troubleshooting and optimisation

Several parameters such as the appropriate pre-treatment procedure, digestion time and hybridisation time were optimised.

2.9 Statistical analysis

Descriptive statistics were reported as frequencies or medians. Distributions of immunohistochemical scoring or FISH data with clinicopathological data was compared using the Chi-squared test or Fisher's exact test. Differences were considered significant when the P value was less than 0.05 (two-side). The Statistical Package for Social Sciences (SPSS) v 26.0.0.0 (IBM, New York, USA) was used for the statistical analysis.

CHAPTER 3

RESULTS

3.1 Case selection

A search of the TRAK and DISA laboratory information system databases, over a period of 13 years, yielded 182 patients who were diagnosed with PBL at Groote Schuur Hospital. First, the reports were retrieved and information such as clinical history, macroscopy, microscopy, immunohistochemistry and pathological diagnosis were examined and confirmed. At this stage, 12 duplicate cases and 57 referrals were excluded. One additional case was excluded as it was positive for HHV8, which was in keeping with a diagnosis of PBL variant of MCD. Thereafter, the slides of 112 cases were requested from the archives of the Division of Anatomical Pathology; NHLS/UCT. The slides were examined by a histopathologist to confirm the diagnosis and assess tissue fixation. Core biopsies and poorly fixed tissue were excluded which resulted in 64 FFPE tissue blocks being requested from archives. Sixty blocks were received and re-examined during which time, another 11 blocks were excluded, leaving a cohort size of 49 cases.

3.2 Patient clinical characteristics

The PBL cohort comprised 49 cases of which 30/49 (61.2%) were male and 19/49 (38.8%) were female (Table 3.1). The median age of the patients was 39 years while the ages ranged from 24 to 64 years with most patients being between 30 and 49 years of age (Figure 3.1).

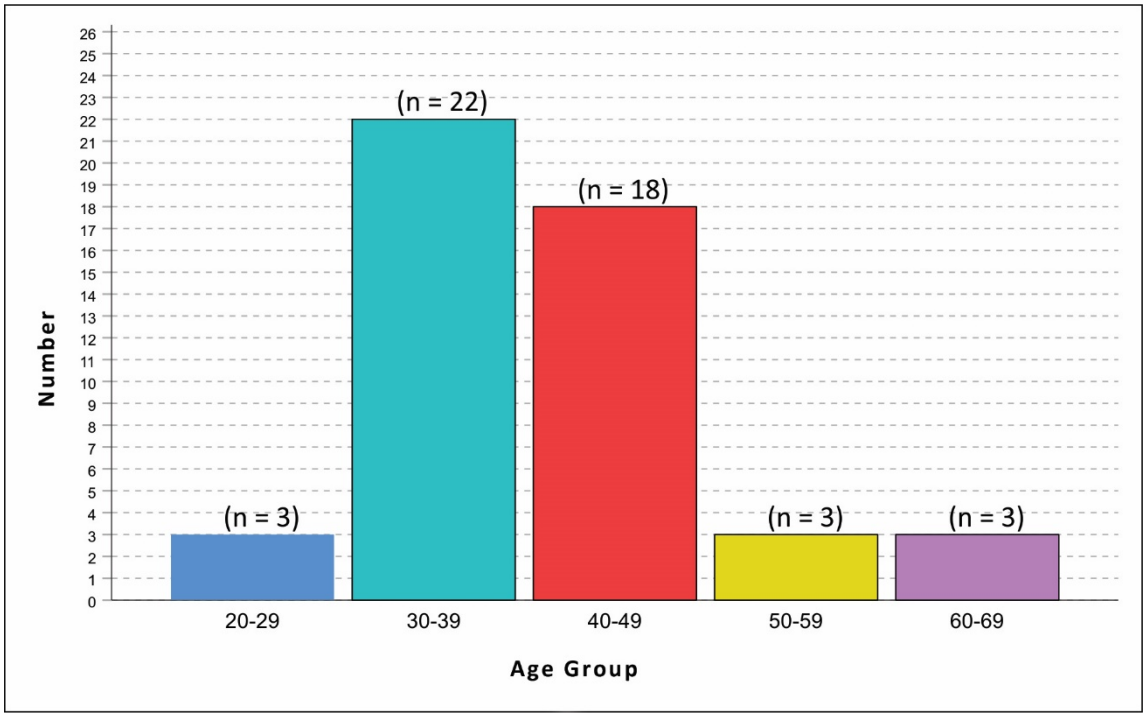

Figure 3.1: Age distribution of PBL cases

Of the 49 patients, the HIV status of 47 patients were known. Of these 44/49 (89.8%) were HIV positive and 3/49 (6.1%) were HIV negative. Two cases were unknown. The site of tumour biopsy in 12/49 (24.5%) cases was nodal and 37/49 (75.5%) were extranodal. The most common extra nodal site was the upper aerodigestive tract (54.1%) followed by pelvis (18.9%) and the thorax (8.1%) (Table 3.1).

Table 3.1: Summary of PBL case information

Patient demographics		Total
Gender	Male	30
	Female	19
Age	Median	39
	Range	24-64
HIV Status	Positive	44
	Negative	3
	Unknown	2
Site of biopsy	Nodal	12
	Extranodal	37
	Upper aerodigestive tract	11
	Oral cavity	9
	Pelvis	7
	Thorax	3
	Abdomen	2
	Lower limb	2
	Neck	2
	Upper limb	1

3.3 Pathological features

3.3.1 Immunophenotype

The diagnosis of PBL was in keeping with the WHO criteria i.e. the neoplastic cells expressed at least one plasma cell marker (CD38, CD138 or VS38C) and was negative for B-cell markers (CD20 and PAX5). Further, MUM1/IRF4 was positive in 22/49 (44.9%) of the cases. HHV8 was negative for the 12 cases that were tested thereby excluding the diagnosis of HHV-8 positive plasmablastic variant of MCD.

3.4 Immunohistochemical analysis

3.4.1 CD246, ALK Protein expression

An ALK-positive ALCL served as the positive control for the ALK immunohistochemistry. Assessment of the processed slides showed a DAB staining reaction in the nuclei and cytoplasm of the tumour cells (Figure 3.2A). In addition, there was no non-specific background staining.

This staining pattern was consistent with manufacturer specification. Of the 4 EBV positive and 6 EBV negative PBL cases, none were positive for ALK (Figure 3.2B). In total, 18 cases were ALK negative including cases that were processed during the routine diagnostic workup.

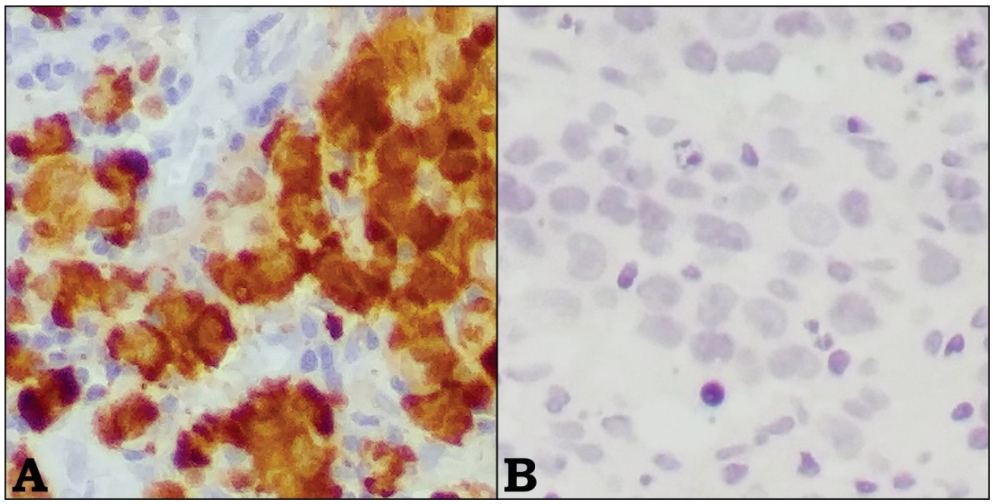

Figure 3.2: Anaplastic lymphoma kinase (ALK) staining in control and PBL cases. **A.** ALK-positive ALCL positive control (20x mag). **B.** ALK negative staining PBL case 12 (20x mag).

3.4.2 EBER ISH

An EBV positive NPC served as the positive control. Assessment of the processed slides showed a dark blue, circumscribed homogenous nuclear staining pattern in all EBV infected cells (Figure 3.3A). The background showed only the red/pink counterstain. A negative EBER ISH was confirmed by the absence of the dark blue nuclear staining. EBER ISH was performed on 27 cases. Twenty-two cases were EBER positive, showing positivity in more than 5% of the tumour cells (Figure 3.3B) while 5 cases were considered negative (Figure 3.3C). In total, including cases that were processed during the diagnostic work up, 41/49 (83.7%) cases were EBV positive and 8/49 (16.3%) cases were EBV negative (Table 5).

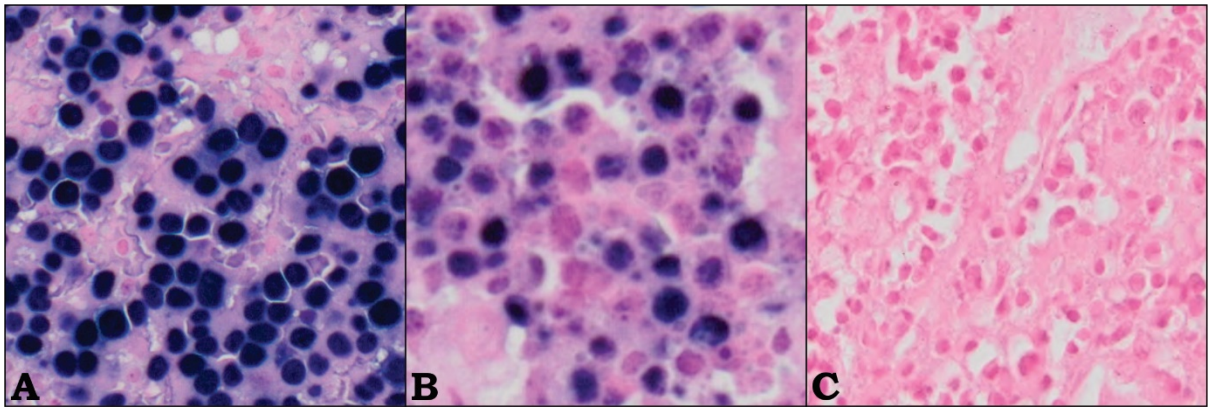

Figure 3.3: EBER ISH staining in control and PBL cases. **A.** EBV positive NPC positive control (20x mag). **B.** Positive PBL case 12 (20x mag). **C.** Negative PBL case 16 (20x mag).

3.4.3 EBNA1

EBV positive NPC tissue served as the positive control and showed a DAB staining reaction in the nuclei of the tumour cells (Figure 3.4A). There was no non-specific background staining in any of the slides processed including the negative control (Figure 3.4B). This staining pattern was consistent with the manufacturer specification. EBNA1 was positive in 11/41 (26.8%) of 41 EBER positive PBL cases (Figure 3.4C), while the remaining 30/41 (73.2%) were negative (Figure 3.4D).

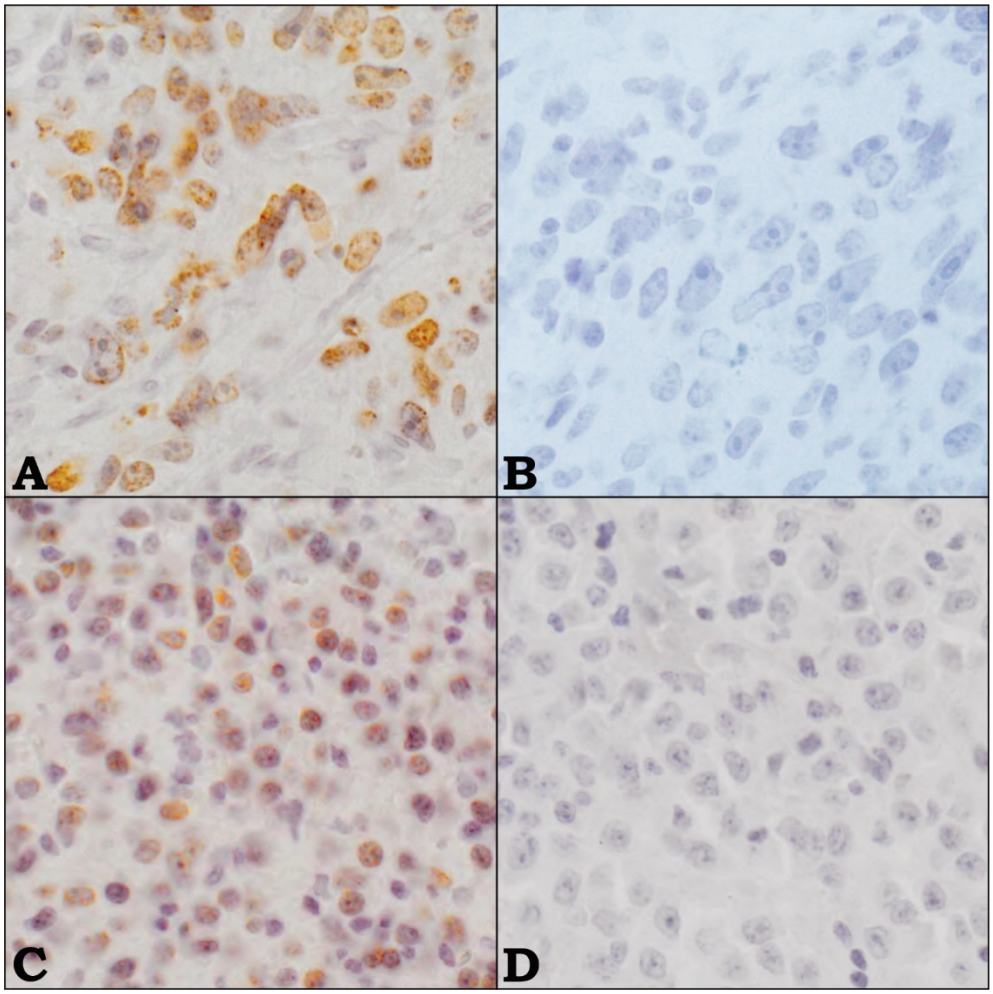

Figure 3.4: EBNA1 immunohistochemical staining in control and PBL cases. **A.** Positive control showing nuclear staining in the EBV positive NPC cells. (20x mag) **B.** Negative control (20x mag). **C.** EBNA1 positive PBL case 25 (10x mag). **D.** EBNA1 negative PBL case 2 (20x mag).

3.4.4 EBNA2

EBV positive NPC tissue served as the positive control and showed a DAB staining reaction in the nuclei of the tumour cells (Figure 3.5A). there was no cytoplasmic or non-specific background staining in any of the slides processed including the negative control (Figure 3.5B). This staining pattern was consistent with the manufacturer specification. All 41 cases were EBNA2 negative (Figure 3.5C).

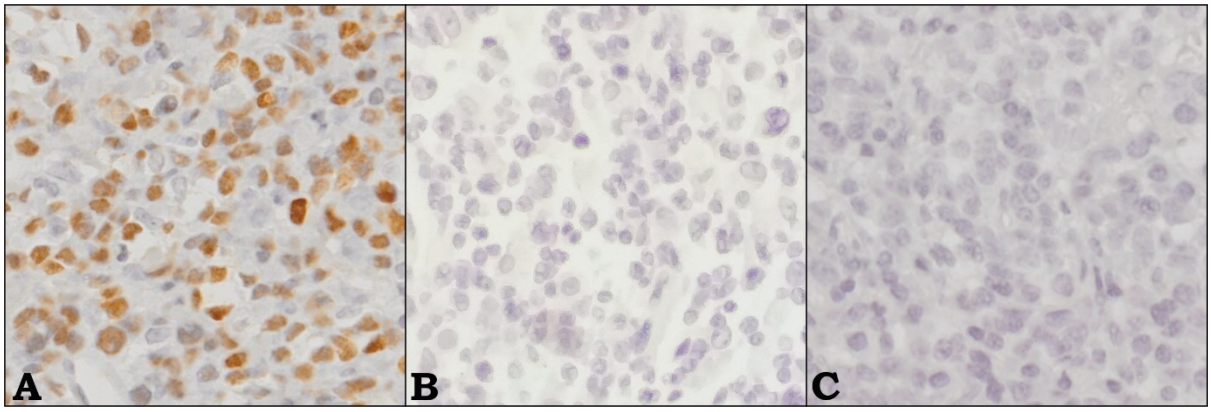

Figure 3.5: EBNA2 immunohistochemical staining in control and PBL cases. A. Positive control showing nuclear staining in the EBV positive NPC cells. (20x mag) B. Negative control (20x mag). C. EBNA2 negative PBL case 2 (20x mag).

3.4.5 LMP1

EBV positive NPC tissue served as the positive control and showed strong membranous and cytoplasmic DAB staining reaction in the tumour cells (Figure 3.6A). There was no nuclear or other background staining present in any of the slides processed including thenegative control (Figure 3.6B). This staining pattern was consistent with the manufacturer specification. Of the 41 cases, 4/41 (9.8%) were positive for LMP1 (Figure 3.6C) and the remaining 37/41 (90.2%) cases were negative (Figure 3.6D).

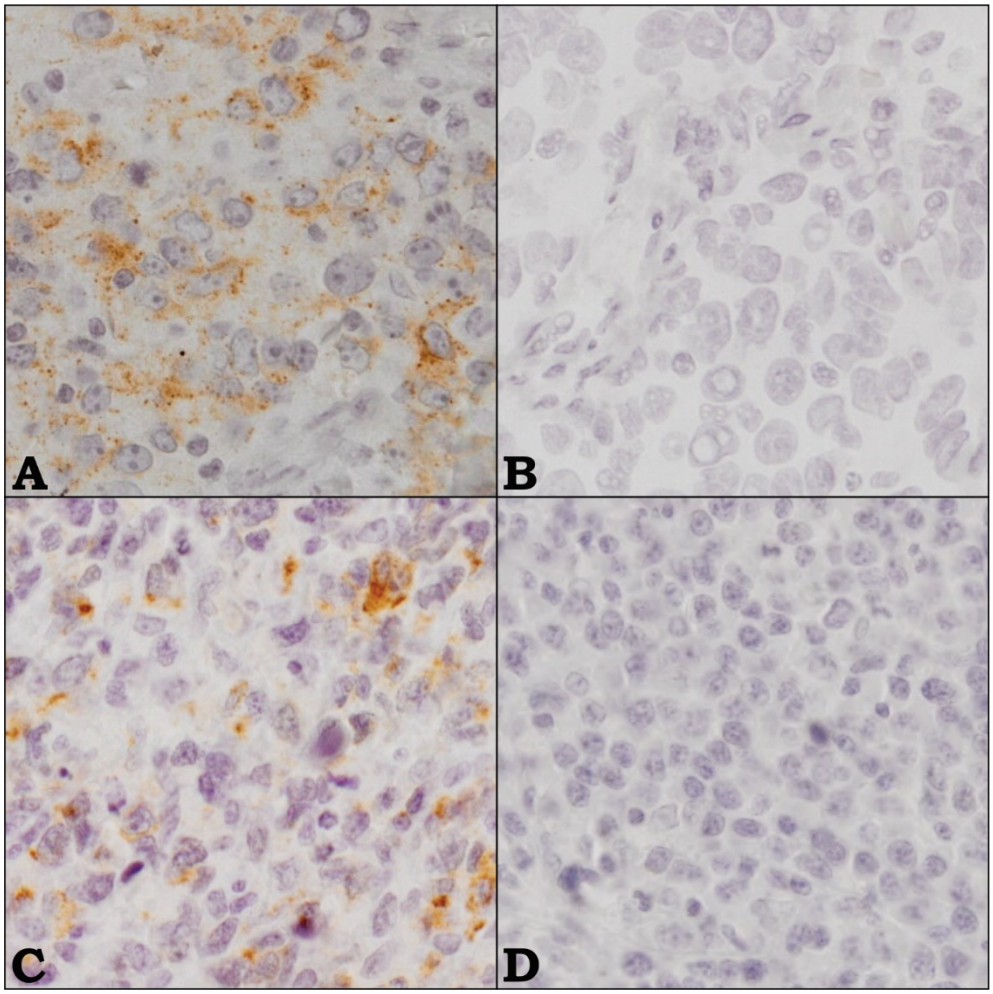

Figure 3.6: LMP1 immunohistochemical staining in control and PBL cases. A. Positive control showing staining in the cytoplasm and cell membrane of the EBV positive NPC cells (20x mag). B. Negative control. C. LMP1 positive PBL case 21 (20x mag). D. LMP1 negative PBL case 14 (20x mag).

3.5 EBV latency determination

The expression of the latency proteins (EBNA1, EBNA2 and LMP1) and EBER was then used to determine the EBV latency type in each case. Latency 0 was observed in 29/41 (70.7%) of PBL cases (Figure 3.7) where only EBER was positive. Latency 1 was observed in 8/41 (19.5%) cases (Figure 3.8) where EBER and EBNA1 were expressed. Lastly, latency 2 (Figure 3.9) was observed in 4/41 (9.8%) cases where EBER/EBNA1/LMP1 or EBER/LMP1 was expressed. Table 3.2 provides summary of EBV latency study.

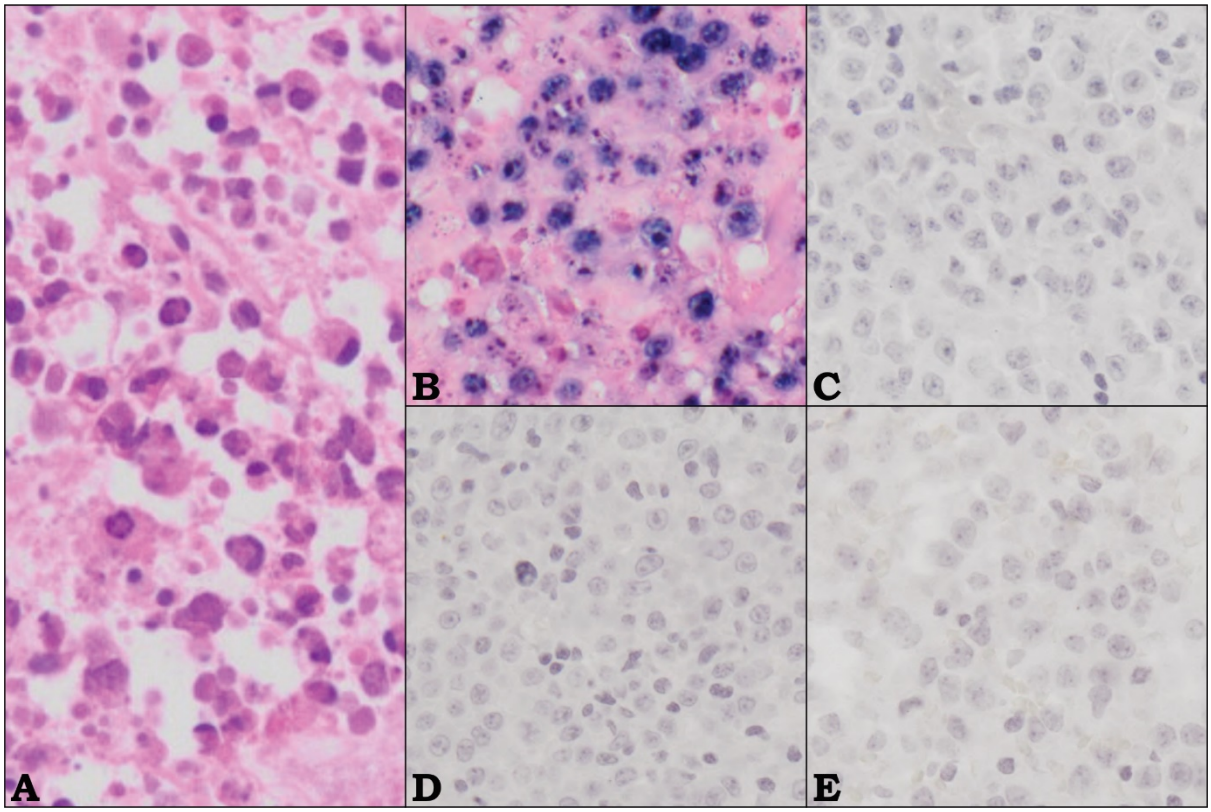

Figure 3.7: PBL case 5 showing EBV latency 0. A. H&E (20x mag). B. EBER positive (20x mag). C. EBNA1 negative (20x mag). D. EBNA2 negative (20x mag). E. LMP1 negative (20x mag).

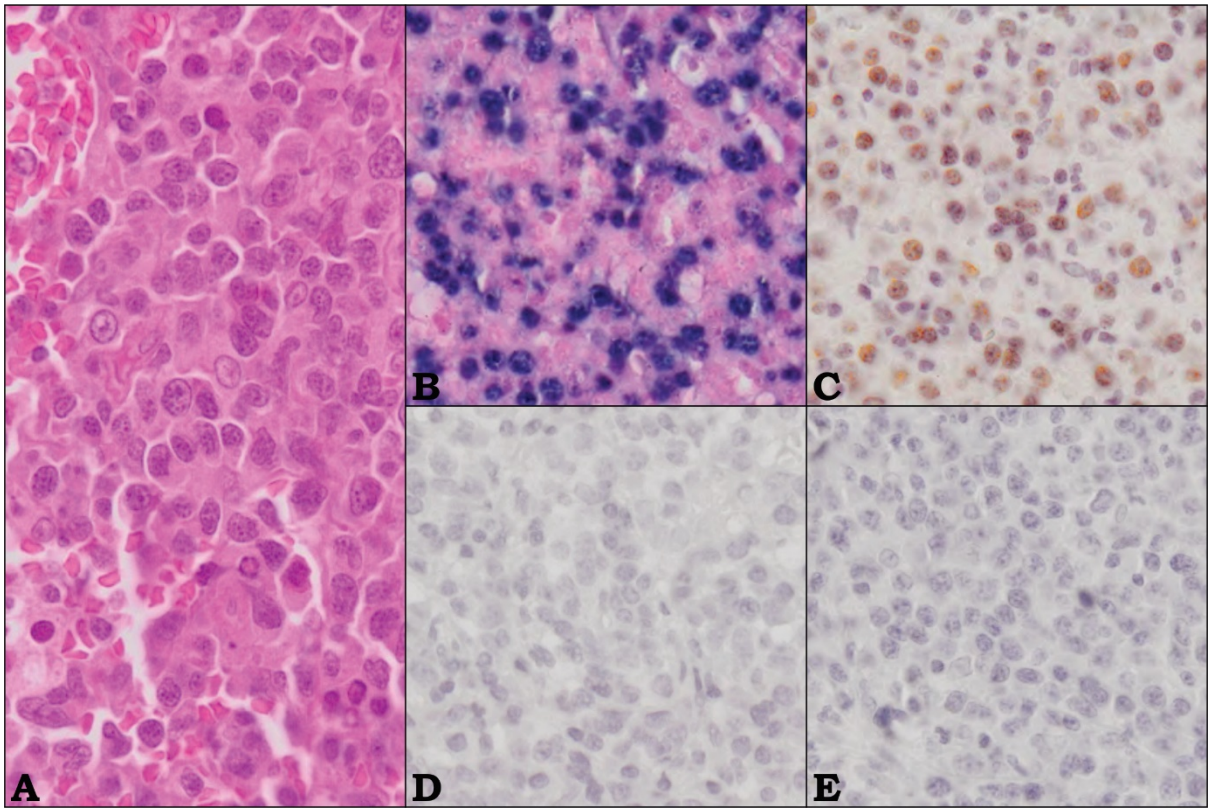

Figure 3.8: PBL case 34 showing EBV latency 1. **A.** H&E (20x mag). **B.** EBER positive (20x mag). **C.** EBNA1 positive (20x mag). **D.** EBNA2 negative (20x mag). **E.** LMP1 negative (20x mag).

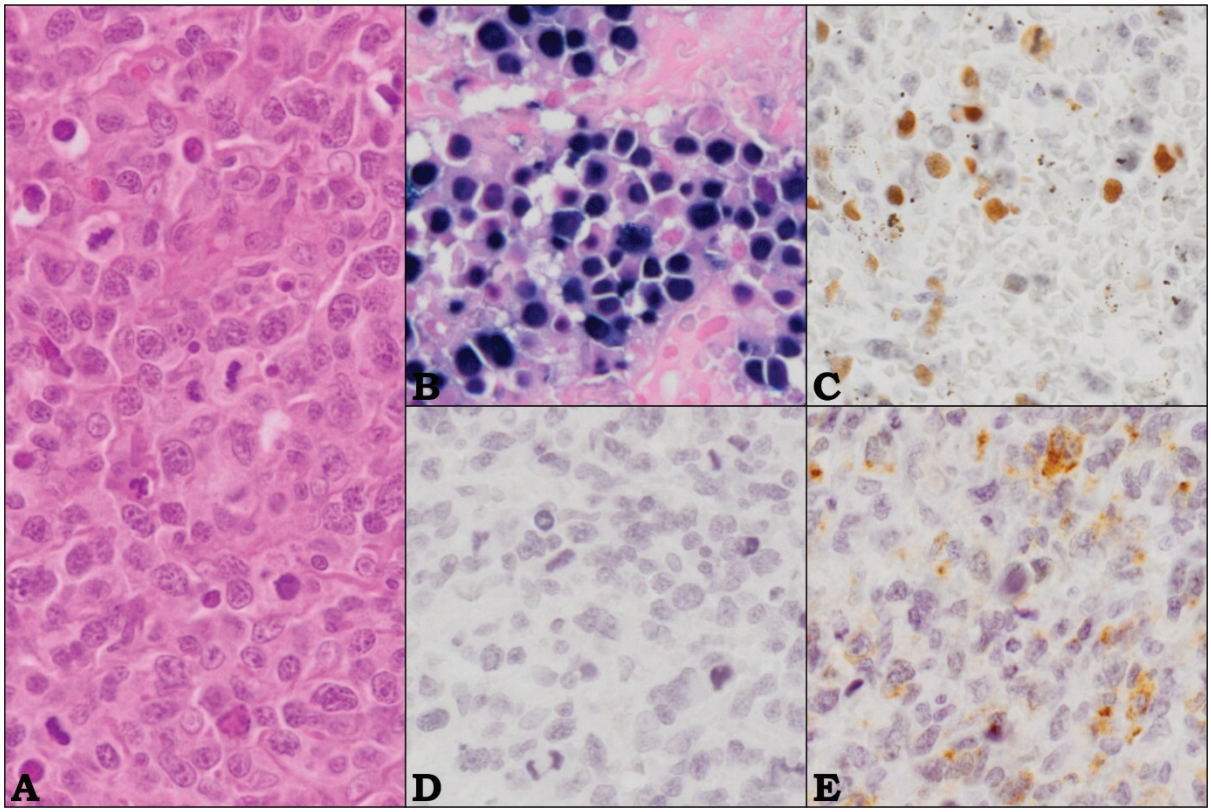

Figure 3.9: PBL case 35 showing EBV latency 2. **A.** H&E (20x mag). **B.** EBER positive (20x mag). **C.** EBNA1 positive (20x mag). **D.** EBNA2 negative (20x mag). **E.** LMP1 positive (20x mag).

Table 3.2: EBV study summary

EBV parameters	Measured values	Obtained values
EBV status	Positive	41 (83.7%)
	Negative	8 (16.3%)
EBNA1	Positive	11 (26.8%)
	Negative	30 (73.2%)
EBNA2	Positive	0 (0%)
	Negative	41 (100%)
LMP1	Positive	4 (9.8%)
	Negative	37 (90.2%)
Latency	0	29 (70.7%)
	1	8 (19.5%)
	2	4 (9.8%)

3.6 *MYC* FISH

MYC FISH was performed on all 49 PBL cases using a *MYC* dual colour break apart probe (BAP). To verify the probe, a DLBCL with a *MYC* translocation served as the positive control (Figure 3.10A) while a reactive lymph node served as the negative control (Figure 3.10B). The signal patterns observed in the controls were consistent with expected results.

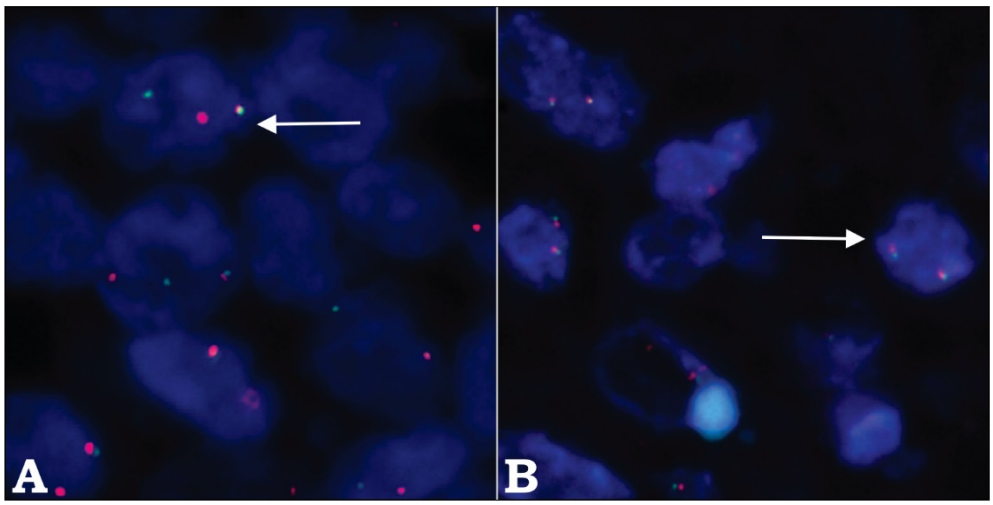

Figure 3.10: Photomicrographs showing *MYC* FISH controls. **A.** Translocated *MYC* FISH positive control showing one yellow or fused orange/green signal and one separate orange and green signal in the tumour cell nuclei (white arrow). **B.** Intact *MYC* FISH negative control showing two yellow or fused orange/green signals (white arrow).

Of the cases tested, 30/49 (61.2%) yielded a result. In 11/30 (36.7%) cases the *MYC* gene was intact (Figure 3.11B). *MYC* translocation was observed in 8/30 (26.7%) (Figure 3.12B), while combined copy number variations were identified in 11/30 (36.7%) cases. Copy number variations consist of 10/11 (90.0%) cases showing a *MYC* gain (Figure 3.13B) and 1/10 (10.0%) case showing *MYC* amplification (Figure 3.13D). Table 3.3 provides detailed information of the all the *MYC* FISH analysis.

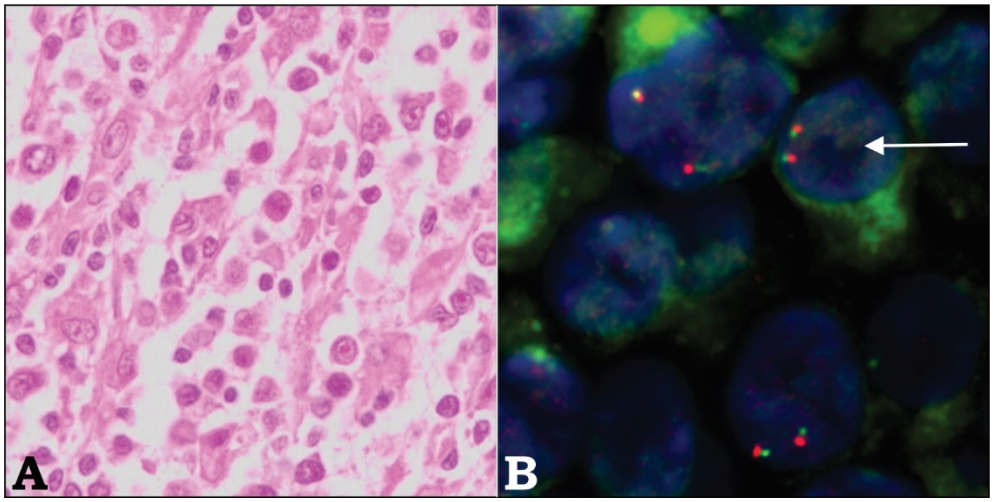

Figure 3.11: Photomicrographs showing comparative H&E and corresponding *MYC* FISH on case 3. **A.** H&E (20x mag). **B.** Intact *MYC* showing two yellow or fused orange/green signals (white arrow).

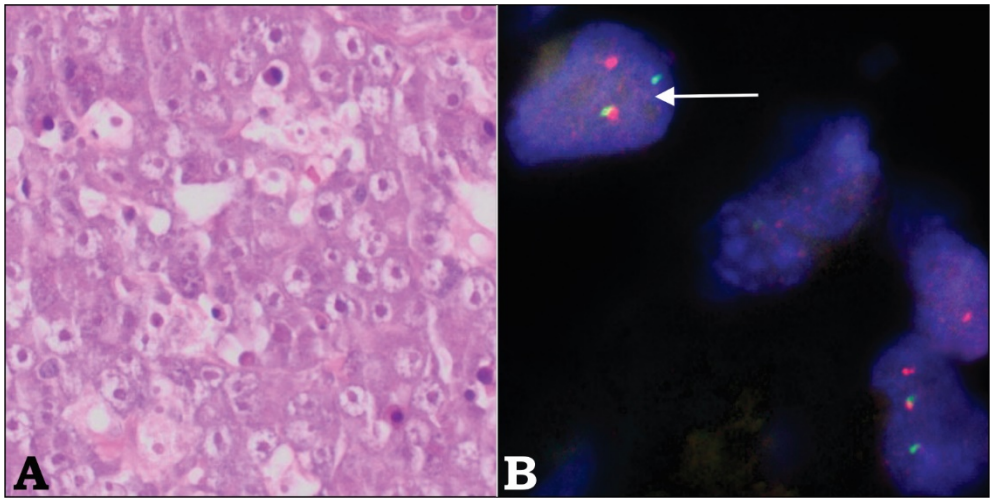

Figure 3.12: Photomicrographs showing comparative H&E and corresponding *MYC* FISH result of case 9. **A.** H&E (20x mag). **B.** Translocated *MYC* showing one yellow or fused orange/green signal and one separate orange and green signal in the tumour cell nuclei (white arrow).

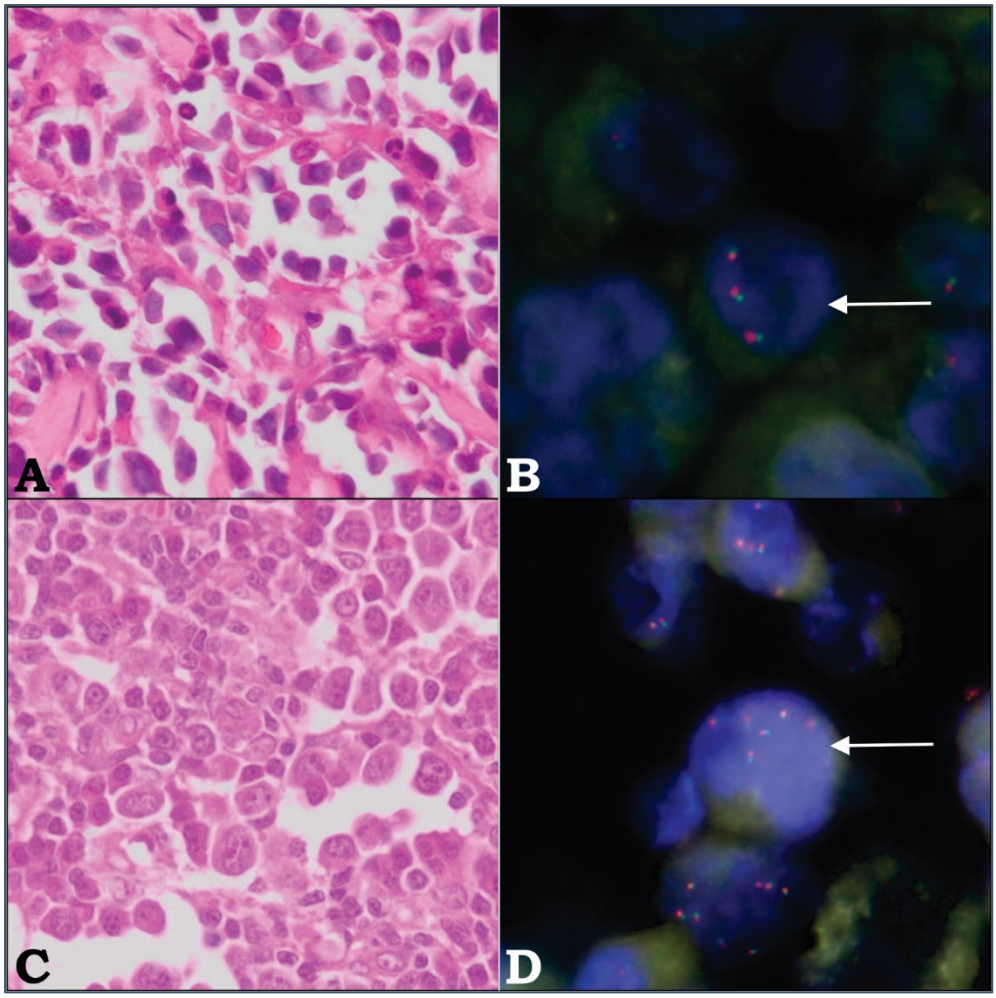

Figure 3.13: Photomicrographs of comparative H&E stain and *MYC* copy number variation *MYC* results for case 17 (gain, **A** and **B**) and case 44 (amplified, **C** and **D**). **A.** H&E stain. **B.** *MYC* gain showing 3 yellow or fused orange/green signals **C**. H&E stain. **D.** *MYC* amplification showing >4 yellow or fused orange/green signals in one PBL case.

Table 3.3: Detailed results of *MYC* study

MYC gene status	Measured values	Obtained values
Number=49	Translocation	8 (16.3%)
	Gain	10 (20.4%)
	Amplification	1 (2.0%)
	Intact	11 (22.4%)
	Tissue not suitable	19 (38.8%)

3.7 Statistical analysis

Due to the nature of the data that was obtained from this study, particularly with regards the small numbers of both EBV and HIV negative cases as well as dichotomous input variables, a detailed statistical analysis and "p" value determination and interpretation was only performed on certain data. Where applicable, the *MYC* results for translocation and copy number variation were combined as *MYC* aberration. Statistical analysis on EBNA1 and *MYC* showed that among EBNA1 positive cases (n=10), *MYC* was intact in 3, and showed aberrations in 7 cases ($p = 0.402$, Fisher's exact test).

3.8 Interesting observations

Thirty-seven cases showed HIV/EBV coinfection, 7 cases were positive for HIV only, 2 cases were positive for EBV only, and 1 case was negative for both viruses. In HIV/EBV coinfection cases, 27 were latency 0, 6 were latency 1 and 4 were latency 2. In HIV/EBV coinfection cases (n=21), *MYC* was intact in 9 cases, translocated in 5 and showed copy number variations in 7 cases. In HIV positive, EBV negative cases (n=7), *MYC* was intact in 1, translocated in 4 and showed copy number variations in 2 cases.

CHAPTER 4

DISCUSSION

PBL is a rare aggressive high-grade B-cell NHL, with a very poor outcome and thought to account for about 2.6% of AIDS-related lymphomas. SA is recognised as having the highest number of people living with HIV and AIDS. This ultimately results in a high incidence of AIDS related diseases, particularly PBL (Boy et al., 2011, Boy et al., 2010). A better understanding of PBL, particularly with regards to the role of EBV and *MYC* in its pathogenesis, would potentially allow for better treatment strategies for patients.

Patient clinical characteristics

Age and gender

The median age in this study was 39 years, where 81.6% of the patients were between the ages of 30 and 49 years. PBL occurs mainly in adults with HIV infection or age related immunosenescence, with cases of paediatric PBL rarely being reported (Vaubell et al., 2014, Campo et al., 2017). The median age may be affected by HIV infection, where one study found that in HIV positive patients the age dropped from 50 to 38 years (Harmon and Smith, 2016), which is very much in keeping with what we observed in our predominantly HIV positive cohort. In our study the youngest adult patient was 24 years old. GSH does not have a paediatric department and as such paediatric cases have been excluded from this study.

Patient immune status

Our study revealed that 89.9% of patients were HIV positive, three were HIV negative, and 4.1% had unknown HIV status. One of the unknown cases was a post-transplant patient. PBL occurs in immunocompetent, post-transplant and immunocompromised patients, and given the high incidence of HIV and AIDS in SA, this may contribute to the increase in cases of aggressive lymphomas such as PBL (Campo et al., 2017, Boy et al., 2011). The current setting

of HIV/AIDS epidemic in SA has also seen an increase in HNL, where PBL was identified as the most common histological subtype (Alli and Meer, 2017).

Site involvement

In this study, 75.5% of the cases were extranodal, and 24.5% were nodal. Of the extranodal cases, more than half (54.1%) originated from the upper aerodigestive tract, which included sites such as the oral cavity, maxilla and mandible. PBL presents mainly as an extranodal disease, and was originally described in the oral cavity by Delecluse et al., in 1997 in a cohort of 16 HIV positive patients (Delecluse et al., 1997, Campo et al., 2017). Extranodal involvement may be as high as 90% in reported PBL cases, with only about 10% reported in lymph nodes (Campo et al., 2017, Rafaniello Raviele et al., 2009). In post-transplant patients however, lymph node involvement was found to increase to 30% (Campo et al., 2017). In our study we observed an usually higher nodal involvement of 24.5%, which may possibly be attributed to case selection criteria. These criteria allowed for the inclusion of only cases with adequate, well preserved tissue. In the lymph node cases, the tissue was considerably larger, well preserved, and had more residual tissue left over when compared to the smaller biopsy fragments. Another factor that should also be considered is that we did not know the PBL disease progression status in our cohort. We were therefore unable to determine if our samples were from primary or secondary tumour site involvement.

Pathogenesis

Overall, the pathogenesis of PBL remains poorly understood and it may be difficult to distinguish from other neoplasms with plasmablastic morphology such as PEL and PCM. PBL is thought to occur post germinal centre, where the antigen activated B-cells developed into plasma cells after undergoing somatic hypermutation and class switch recombination (Castillo and Reagan, 2011). The development of PBL is likely dependant on various factors such as immunodeficiency (HIV infection), coinfection by oncogenic viruses such as EBV and molecular events relating to *MYC* aberrations (Ambrosio et al., 2017).

ALK

In our study, all the EBV negative and a random selection of EBV positive cases showed no ALK staining patterns. PBL shares a similar immunophenotypic staining profile as ALK-positive LBCL. It was therefore necessary to perform this assay to show that we indeed had a clean cohort of PBL cases.

Epstein-Barr virus

EBV was first identified as a human tumour virus more than 50 years ago. It is one of 7 known oncogenic viruses and is responsible for more than 1.8% of cancer cases worldwide each year. These cancers include BL, gastric carcinoma, NPC and PBL (Dawson et al., 2012). EBV infection of tumour cells is found in almost all cases of endemic BL (Aguilar et al., 2017). EBV is the most common viral infection in humans and after initial infection, persists as a lifelong latent infection (Young et al., 2016). More than 90% of the population is infected with EBV by the age of 40 years (Münz, 2016). EBV positive infection was described in up to 80% of HIV positive PBL cases and in approximately 50% of HIV negative cases (Lopez and Abrisqueta, 2018). However, not everyone infected by EBV goes on to develop cancers, as the human body's immune response is crucial in preventing this. It appears to be that in PBL where EBV and HIV are involved, EBV is the initial viral infector, which then goes into latency. HIV is a secondary viral infector which compromises the body's immune system, allowing EBV to sporadically come out of latency and take advantage of this compromised immunity. This is very similar to what is found in endemic BL, where the initial infector is also EBV, and secondary infector is plasmodium falciparum, which is also able to compromise the body's immune system. Again, this compromised immunity allows EBV to selectively come out of latency (Pannone et al., 2014). In both lymphomas, EBV appears to be an opportunistic infective agent which after initial infection hides from the immune system through lack of latent protein expression. It is then able to move between latent and lytic reactivation as suitable conditions arise. During this "hit and run" latent and lytic infection either initially or later when the immunity is compromised, it is possible that the transcription factor *MYC* may be affected.

EBER ISH

EBER ISH was used to determine EBV infection in all our cases where EBV status was not known. This resulted in 83.7% cases being EBER positive, and 16.3% being negative. Southern blot hybridisation was one of the early methods used for the detection of EBV DNA before the use of EBER ISH since 1990 (Wu et al., 1990). At GSH, prior to the implementation of EBER ISH, LMP1 IHC was the method of choice. EBER ISH was later identified as a more accurate, reliable and specific test for the presence of EBER viral transcripts in the nucleus of tumour cells infected by EBV. EBER ISH positive staining of non-tumour cells should however not be included in the scoring process. Despite the great benefits of choosing EBER ISH as a method of EBV detection, when compared with EBV DNA quantification using qPCR, EBV DNA was found in EBER negative cases. It is therefore crucial that great care needs to be taken when interpreting EBER ISH results, particularly regarding the location and intensity of positive staining. qPCR demonstrates a high sensitivity and may potentially produce false positives when detecting viral DNA in non-malignant cells (Okamoto et al., 2017, Gulley and Tang, 2008).

EBNA1

EBNA1 was expressed in 26.8% of our cases that were positive for the expression of EBER as well. The use of EBNA1 IHC is not commonplace in EBV latency studies, with some researchers choosing the more sensitive qPCR method instead. This was brought about by sensitivity issues with a certain clone of EBNA1 antibody (clone 2B4) when doing IHC. This subsequently resulted in qPCR being used instead, as the methodology was considered to be more sensitive (Gulley and Tang, 2008, Ambrosio et al., 2017). In one such study using qPCR , of the cases tested, 92.3% were EBNA1 positive (Ambrosio et al., 2017). We did not however experience any issues with our antibody choice, which was validated using NPC or EBV-positive SMT tissue and stained as per expectation. EBNA1, whose main function is that of preservation and maintenance of EBV DNA and replication of the virus during cell division, may sporadically be expressed (Kliszczewska et al., 2017). EBNA1 is expressed during all EBV latencies except latency 0, and with this knowledge we were able to provide a distinction between latency 0 and 1.

EBNA2

EBNA2 expression was not detected in any of our cases. These findings compared well to other studies where EBNA2 expression was also negative (Valera et al., 2010, Liu et al., 2012). Together with EBV-LP, EBNA2 is the first EBV protein that is expressed soon after B-cell infection, and then expressed later in latency 3 (Schlee et al., 2004). The lack of EBNA2 expression was also confirmed in previous studies by qPCR (Ambrosio et al., 2017). Only one study showed 1 EBNA2 positive case using conventional IHC (Morscio et al., 2014). In our study, NPC and EBV-positive SMT were used as the control tissue for the detection of EBNA2 expression. Both malignancies exhibit EBV latency 3 infection, and as a result showed EBNA2 positive staining in the tumour tissue as per manufacturers insert (Rezk and Weiss, 2007, Rezk et al., 2018).

Although not a contributor to the EBNA2 negative results in our study, EBV positive PBL has never been tested before for the possibilities of EBV strain variation or its influence on disease progression. EBV type 1 and type 2 strains are determined by variations in the coding regions of EBNA2 and EBNA3 family of genes. EBV type 2 strain has been found to be more frequently associated with HIV positive patients and has more efficient B-cell transformation properties (Santos et al., 2014, Young and Murray, 2003).

LMP1

In our study 9.8% of the cases were positive for LMP1. LMP1 is expressed only during latency 2 and 3. LMP1 is reported to have a higher prevalence in immunocompromised patients when immune surveillance is absent, but this was however not the case in our study. EBNA2 is responsible for the upregulation of LMP1, and may potentially be the reason why LMP1 was not expressed in some of our EBV positive PBL (Gulley and Tang, 2008, Niedobitek et al., 1997). Both LMP1 and EBNA1 can provide resistance to the effect of P53 related death signals in genetically damaged cells and thereby promote lymphomageneses. This is however mostly evident in classic HL and NPC, where LMP1 is readily expressed and might not be the case in PBL (Middeldorp and Pegtel, 2008).

Latency 0

Our study found that 70.7% of the cases showed an EBV latency 0, which was defined in our research by the expression of only EBER. Latency 0 is also referred to as true or restricted latency and results in a state of complete immune evasion by EBV. It is possible that EBV exhibits this reduced latent protein expression in B-cells post GC, when undergoing terminal differentiation into plasma cells. This results in the cells not being recognised by the T-cell immune response (Price and Luftig, 2015, Rezk et al., 2018). Latency 0 has been reported in reviews to occur in EBV positive PBL, but research confirming this is lacking (Rezk and Weiss, 2007).

Latency 1

Our study found 19.5% of the cases showed an EBV latency of 1. Latency 1 was defined in our research by the expression of EBER and EBNA1 and is also referred to as a restricted latency pattern. Latency 1 is the most frequently reported latency to occur in EBV positive PBL (Valera et al., 2010, Ambrosio et al., 2017). The sporadic expression of EBNA1, possibly during cell division, provides the distinction between latency 0 and latency 1. In many studies latency 1 has been determined by using the lack of expression of EBNA2 and LMP1, with very few using EBNA1 in their methodology (Valera et al., 2010, Liu et al., 2012). One could however argue as to the relevance of distinguishing between latency 0 and 1. Both are restricted latencies and occur post GC when the B-cells are undergoing differentiation into plasma cells, which also coincides with the EBV life cycle (Shannon-Lowe and Rickinson, 2019). However, it is important as more recent research has identified a more complicated role of EBNA1 in tumourigenesis, which would warrant further investigation. The expression of EBNA1 in latency 1 has also been investigated as a potential target for therapy against EBV related cancers due to its effect of the cells growth-promoting pathways (Wilson et al., 2018).

Latency 2

Our study found that 9.8% of cases showed and EBV latency of 2. Latency 2 was defined in our research by the expression of EBER, EBNA1 and LMP1. In the EBV life cycle, latency 2 is referred to as the default latency program and is thought to occur in the GC. Thorley-Lawsone et al.,

2015 stated that “EBV is B lymphotropic and that its biology closely follows that of normal B-cells” (Thorley-Lawson, 2015). This may provide evidence of the stepwise latency program adopted by EBV after initial infection via tonsillar epithelium, which is followed by an abortive lytic or pre-latent state (Price and Luftig, 2015). Following this, a post GC latency 0/1 is observed (Rezk et al., 2018). Evidence of this was found in a study by Ambrosio et al., 2017, where the authors made use of IHC and qPCR to study the latent and lytic cycles of EBV positive PBL. In their study they found the expression of proteins which characterised latency 2, and importantly found evidence of an abortive lytic cycle. Lytic protein expression pattern indicated an aborted lytic reactivation, which is thought to contribute to EBV associated neoplasms (Price et al., 2017, Ambrosio et al., 2017). We did not however conduct any detailed studies into the EBV lytic cycle, but our findings of latency 2 may however provide some evidence of an attempted EBV reactivation or a transition period from GC latency 2 to post GC latency 0/1.

Latency 3

No cases in our study showed an EBV latency 3 pattern, due to the lack of co-expression of EBER, EBNA1, EBNA2 and LMP1. Latency 3 is also referred to as the EBV growth program and is the most immunogenic of all the latencies. It is characterised by the expression of all EBV latent proteins and occurs soon after infection (Kliszczewska et al., 2017). It is evidential that all latencies originate from latency 3, and EBV embarks on a latency 3 program soon after lytic infection or reactivation (Shannon-Lowe and Rickinson, 2019). As mentioned earlier the EBV lytic cycle or reactivation was not investigated in this study, which would make it difficult to observe latency 3 in PBL. Literature reports that latency 3 occurs in HIV positive patients as well as immunosuppression in posttransplant PBL when there is T-cell immune suppression (Castillo et al., 2015, Ambrosio et al., 2017, Price and Luftig, 2015). Latency 3 was not observed in our study which included mainly HIV positive cases with one post-transplant patient.

EBV study methodology

This study made use of standard manual immunohistochemical staining on FFPE tissue, using EBNA1, EBNA2 and LMP1 primary antibodies. We made these antibody choices based on which proteins are expressed by EBV during the various latencies. The most common available

methods of EBV latency determination are ISH for the detection of EBER, automated or manual IHC staining using primary monoclonal or polyclonal antibodies, and qPCR using commercially available primers. Due to its ease of use, affordability and quick turnaround time, IHC is often employed when the case material is FFPE (Rezk et al., 2018, Ambrosio et al., 2017, Wu et al., 1990). In many earlier studies, EBNA2 and LMP1 were often the antibodies of choice in determining EBV latency, as both expressed proteins have recognised oncogenic potential. EBNA2 prevents cell death and is critical in EBV related B-cell transformation and is responsible for the upregulation of LMP1 (Niedobitek et al., 1997). LMP1 is an oncogene whose primary role is inhibiting apoptosis and mimicking CD40 induced signalling pathway (Linke-Serinsöz et al., 2017, Liu et al., 2012, Rezk and Weiss, 2007, Valera et al., 2010). Other reasons for these antibody choices may be due to antibody availability, or literature stating that latency 3 may be found in HIV associated PBL, which may be proven by the expression of EBNA2 (Castillo et al., 2015, Bibas and Castillo, 2014). EBV latent proteins do however remain difficult to study because of their ability to hide from detection by the body's immune system, and different cells expressing varying stages of latency.

MYC

The transcription factor MYC regulates the expression of several target genes (Rosenthal and Younes, 2017), is associated with apoptosis, lipid synthesis, glucose metabolism and has strong oncogenic potential (Karube and Campo, 2015, Ambrosio et al., 2017). *MYC,* a proto-oncogene is frequently activated in human cancers. If *MYC* is deregulated, and uncontrolled by check-points such as P53, it could possibly contribute to tumorigenesis by virtue of its ability to promote metabolic and proliferation activities (Dang, 2013).

MYC intact

In our study we found *MYC* intact in 36.7% of the cases. In normal cell function, *MYC* expression is tightly regulated. *MYC* may be found in almost all cells in the human body, where its main function is the regulation of cell growth. In PBL, *MYC* status alone does not form part of the diagnostic criteria (Castillo et al., 2015, Boy et al., 2011). Our study showed a higher than reported intact *MYC*, and a possible reason for this may relate to a limitation of the probe type

that was used. BAP FISH probes are only able to identify translocations and amplifications of an assigned region of the *MYC* gene. The probes are not able to detect other possible *MYC* mutations such as insertions, deletions, frameshifts, and a recently discussed cryptic insertion of *MYC* exons into the *IGH* locus (Wagener et al., 2019). Salaverria et al., 2013 discussed the scattering of *MYC* and *IGH* break points which potentially rendered breaks in the *MYC* gene undetectable when using FISH. That study was conducted on BL, so the results should be viewed with caution despite the fact that PBL and BL share a common cytogenic abnormality (Salaverria et al., 2014).

MYC translocated

We reported *MYC* translocations in 26.7% of our cases. This is slightly lower than what was found in a study by Valera et al., 2010 using a BAP, where *MYC* translocations were detected in 49% of the PBL cases (Valera et al., 2010). In the present study we found *MYC* intact more than translocated. This finding may warrant further investigation, but *MYC* translocations alone do not cause lymphoma (Ott et al., 2013). *MYC* translocations, which are commonly found in PBL, also occur in other diseases and are often associated with an aggressive progression of that disease. Some studies do however suggest that there may not be a significant difference in OS in patients with translocated *MYC* or not, with *MYC* rearrangements seen as a late genetic alteration acquired during disease progression (Nguyen et al., 2017, Valera et al., 2010). Of importance were reported findings that in PBL, there were histological differences in cases with *MYC* translocation as opposed to cases where there was no *MYC* translocation present (Taddesse-Heath et al., 2010). When using FISH to identify *MYC* translocations, consideration should be taken with regards to the location of the break points on chromosome 8, which may vary from patient to patient. These variations may be as much as 300kb upstream or downstream of the *MYC* loci and may be missed in FISH cytogenetic studies. It is therefore essential that the correct probe with flanking regions is chosen in order to identify these translocations (Veronese et al., 1995). As mentioned earlier pertaining to FISH methodology, is that the sensitivity of *MYC* detection may be improved with the use of dual colour dual fusion probes. A SA study employed BAP for *MYC* status screening then dual colour dual fusion probes to determine *MYC* status and possible translocation partner gene. In this study the authors reported *MYC* translocations in 60% of their oral PBL cases. This study was however very

homogenous in that all the cases were HIV related oral PBL (Boy et al., 2011). This was unlike an earlier study conducted by Valera et al., 2010, where the cases were more heterogenous in origin representing various nodal and extranodal sites and reported translocations in 49% of their cases (Valera et al., 2010).

MYC copy number variations

We reported copy number variations in 36.7% of our cases, which consisted of both gains and amplification of the *MYC* gene. Copy number variations are not uncommon in PBL, with gains reported in up to 30% of the cases, (Valera et al., 2010) and amplifications observed in up to 23.1% of the cases (Miao et al., 2019). However, it should be noted that *MYC* gains or amplifications detected by FISH, may also be as a result of an increase in the number of copies of chromosome 8 or structural abnormalities of that chromosome. In the setting of aggressive B-cell NHLs such as PBL, it is not clear if *MYC* gains or amplification have any prognostic significance, particularly regarding MYC protein expression. In the present study we did not however investigate this possibility. In studies conducted to compare MYC protein expression to *MYC* FISH results, all the cases showed increases in MYC protein expression, but it was not restricted to *MYC* translocation or *MYC* amplified cases alone (Montes-Moreno et al., 2017, Laurent et al., 2016). This and other studies support that MYC protein expression is not a surrogate for *MYC* gene aberrations (Chisholm et al., 2015). More interestingly though it was also found that a relationship may exist between mutations in the *PRDM1* gene and the regulation of *MYC*. The normal expression of *PRDM1*/BLIMP1 leads to suppression of MYC protein expression, which may be lost when *PRDM1* gene is mutated. It was also found that the relationship between *MYC* and *PRDM1* does not necessarily affect terminal B-cell differentiation into plasma cell but may contribute more to its oncogenicity (Montes-Moreno et al., 2017, Valera et al., 2010).

Recently a direct link between EBNA1 and *MYC* expression was reported to exist, with the identification of a mechanism mediated by the glycine alanine repeat region (GAr) of *EBNA1.* The *EBNA1* GAr may cause translation stress which may bring about the induction of *MYC* (Wilson et al., 2018). This may provide a possible explanation of the potential relationship

between EBNA1 and *MYC* in our study. We found that EBNA1 was positive in 26.8% cases, with most of those showing *MYC* aberrations consisting of either translocations or copy number variations. However, when a detailed statistical analysis was conducted on the full EBNA1 result, a "p" value equal to 0.402 was obtained. Even though this indicates no significant statistical relationship, it may prompt for further study into the possible effect of EBNA1 on *MYC* in PBL. Ambrosio et al., 2017 used qPCR very effectively to confirm EBNA1 expression, with results of 92.3% in their EBV infected cases (Ambrosio et al., 2017). The use of a sensitive technology such as qPCR may possibly provide a better opportunity for correlation with *MYC* FISH results to see if a relationship exists between these two pathogenic entities.

MYC study methodology

This study made use of dual colour break apart probes (BAP) for the main reason that *MYC* gene aberrations were of interest, but the translocation partner was not. Dual colour/dual fusion probes are employed in FISH where more detailed information regarding gene activity is required. In PBL and BL, *MYC* dual colour/dual fusion probes can detect a translocation affecting the *MYC* gene on chromosome 8 and the *IGH* gene on chromosome 14. Dual fusion probes are more sensitive and have a very low chance of obtaining false-positive results. BAP on the other hand are useful in cases where there may be various translocation partners associated with a known break-point (Liew et al., 2016). Most studies used one or the other probe and rarely use both due to cost implications.

Unsuccessful *MYC* FISH

In this study, 38.8% of the cases did not yield a result despite optimising the methodology and validating the probe. The reason for the high failure may be related to tissue conditions. Tissue fixation is often not standardised, and there is no assurance that all samples are fixed for the optimal time. Areas of haemorrhage may have caused autofluorescence in certain tissue, while areas of necrosis possibly lead to high degree of non-specific background staining in others (Bancroft, 2013).

FISH limitations

Although FISH is considered the gold standard method for *MYC* investigation, some limitations do exist. FISH probes are very expensive. Analysis also requires the use of specialised microscopes with the correct emission and excitation filters fitted in order to view the fluorescent signal. Furthermore, special cameras and imaging analysis software also contribute to this expense. Despite these limitations, FISH remains one of the preferred methods for cytogenetic analyses.

HIV/EBV coinfection and other observations

Even though PBL is a HIV/AIDS associated lymphoma, coinfection with viruses such as EBV occur frequently. HIV with EBV coinfection may be found in over 60% of PBL cases, but the full pathogenic effect of this coinfection is not fully understood (Boy et al., 2011). In our study we showed an HIV/EBV coinfection of 78.7%. This compares well to the 68.9% obtained by Boy et al., 2011, where although the cases lacked homogeneity, it was the only report to detail HIV/EBV coinfection in PBL (Boy et al., 2011). Furthermore, in our coinfected cases, latency 0 was determined in 73.0% of the cases. Latency 1 and latency 2 were found in a further 16.2% and 10.8% of the cases respectively. Our study reported an unusually higher number of latency 0 cases in the HIV/EBV coinfection cohort. This prompted the question of how HIV/EBV as a coinfection contributed to PBL. There are only a few EBV proteins that are of great importance when establishing latency in B-cells. These are EBNA1, EBNA2 and LMP1, which were the proteins which we used in our study and are expressed in various latent stages. EBNA1 binds EBV genome to the host cell, LMP1 drives B-cell activation and proliferation, while EBNA2 promotes B-cell activation and replication. In healthy individuals with functional immunity, latently infected B-cells may eventually be eliminated by the immune system. This is not the case in patients with compromised immunity such as HIV or post-transplant immune suppression, where reactivation of EBV is very possible. This could result in an uncontrolled B-cell proliferation and a multistep progress towards B-cell lymphoma (Kumar V, 2014). Evidence of this reactivation or lytic reactivation has been reported previously (Ambrosio et al., 2014, Ambrosio et al., 2017, Price and Luftig, 2015). It is therefore possible in our study that under the right HIV immune suppressive conditions, EBV can embark on a brief reactivation cycle, before resuming a complete latency again. In the present study, this could account for latency

0/1 in the HIV/EBV coinfection PBL cases, where the only difference is the expression of EBNA1 in latency 1. In the coinfected PBL cases where LMP1 was expressed in latency 2, the oncogenic role of LMP1 is already established but this finding possibly gives credence to the notion of the step wise latency program by EBV (Price and Luftig, 2015). According to Delecluse et al., 2007, EBER is expressed in many HIV/EBV positive PBL cases, but LMP1 is however rarely expressed (Delecluse et al., 2007). What is encouraging in our study where LMP1 was expressed in 4 cases, 2 showed translocations, 1 was intact and 1 did not work.

We however also have one PBL patient that was both HIV and EBV negative but has lung cancer. The treatment status for the lung cancer is unknown, but cancer may cause a compromised immune system, which may contribute to PBL lymphomagenesis (Gonzalez et al., 2018). In 7 cases, which again is a small dataset in our study, we observed PBL cases that were HIV positive and EBV negative. In this small subset, *MYC* was intact in 14.3% of the cases, was translocated in 28.6% of the case and showed copy number variations in the remaining 57.1% of the cases. This is an unusual finding, because *MYC* rearrangements are more commonly observed in EBV positive PBL patients (Valera et al., 2010). It is uncommon that HIV infection alone would result in *MYC* rearrangements or copy number variations PBL. It is therefore clear that further investigation with a more representative viral infection status is needed.

The role of EBNA1, particularly in relation to *MYC* behaviour, requires more elucidation. EBNA1 is expressed during all latencies except latency 0, and its primary role is to ensure extra chromosomal replication of the viral episome during cell division. Delecluse et al., 2007 stated that EBNA1 protein detection would be a good alternative to the gold standard of EBER ISH for the detection of EBV infection (Delecluse et al., 2007). Only our study and another conducted by Ambrosio et al., 2017, used EBNA1 as part of their latency determination. In data extracted from the tables provided in their study 92.3% cases were EBV positive, and all were EBNA1 positive as well, by means of qPCR analysis. In those cases, 61.5% showed *MYC* translocations (Ambrosio et al., 2017). EBV is recognised as a class one carcinogen by the WHO, and EBNA1, which is expressed during all but one EBV latency, is thought to act as an oncoprotein (Boudreault et al., 2019, Niedobitek, 1999).

Importance of EBV and *MYC* research in PBL

There is much ongoing research into EBV-directed therapies, but a major drawback is that antiviral agents are not as effective due to EBV's immune evasion capabilities. A study was conducted on the effect of the antiviral drug ganciclovir, with arginine butyrate to induce the EBV lytic phase. By inducing the lytic phase, EBV would be identifiable by the body's immune system, resulting in an immune response. This however showed limited efficacy in EBV associated lymphomas (Lopez and Abrisqueta, 2018). Despite *MYC* translocation being found in many PBL cases, the *MYC* gene does not support a targetable binding domain for possible directed therapy (Lopez and Abrisqueta, 2018, Boy et al., 2011). Currently, standard treatment and therapy is the only option for PBL patients. As a result, the overall survival (OS) may be as low as 15 months, due to a relatively poor overall efficacy of standard treatment and therapy. This OS may decrease to about 10 months in HIV positive patients.

Future directions

An observation in our study which was also found in two others, was that EBNA2 was not expressed in the EBV positive PBL cases (Valera et al., 2010, Liu et al., 2012). Only one study showed EBNA2 in one case, resulting in a latency 3 infection (Morscio et al., 2014). EBNA2, which is only expressed in latency 3, is a transcriptional activator for LMP1 which also targeted *MYC*. In 2019, a study investigated EBNA2 in the two different strains of EBV (strain 1 and 2). Variation in the nucleotide sequence of EBNA2 defined EBV strain 1 and 2, which furthermore affected the way in which EBNA2 acts on B-cells (Young et al., 2016). EBV type 2 strain tends to transform B-cells less efficiently than strain 1. To date, the effect of EBV EBNA2 strain variation has not formed part of a detailed study on PBL. The use of sensitive sequencing techniques to identify the differences in the nucleotide sequences of EBNA2 would possibly allow for a better understanding as to which of these are present in the cases of PBL in this study.

Besides a distinction between the restrictive EBV latency 0 and 1, the role of EBNA 1 appears to be poorly understood in PBL. Some researchers allude to the possibility of EBNA1 having minimal immunological host effect, restricted expression, responsible for viral episomal

maintenance and EBV retention in dividing B-cells (Wilson et al., 2018). The effect of EBNA1 on the behaviour of *MYC* also certainly warrants further investigation.

Limitations of the present study

A lack of adequate and preserved extranodal tissue led to a greater than expected nodal PBL representation. Not having more representative HIV and EBV negative PBL cases in our sample cohort contributed to an inability to perform a suitable correlation of these two viruses and the effect they may have on PBL or *MYC* status. A MYC protein expression analysis was not performed in order to investigate a possible relationship between MYC protein expression and *MYC* gene translocations or *MYC* copy number variations. Only *MYC* BA FISH probes were used in this study, which would detect almost all translocations in the *MYC* gene, but the translocation partner was not identified. Dual colour dual fusion probes may be used in order to identify or eliminate the translocation partner gene.

CHAPTER 5

CONCLUSION

We achieved the aim of this study, which was an investigation of *Epstein-Barr Virus* (EBV) latency type and *MYC* gene status in PBL diagnosed at Groote Schuur Hospital. We demonstrated a restricted latency pattern of 0/1 in most of our PBL cases, during which time only EBER and or EBNA1 were expressed. With the occurrence of latency 2 in some of the cases, we demonstrated a possible step wise latency program that EBV embarks on following infection or reactivation. To the best of our knowledge, this was also the first study in a SA context to investigate EBV latency patterns in PBL. We were the first in our institution to perform *MYC* FISH on a cohort of PBL and found a higher than cited amount of copy number variations. Another finding to come out of this research was a small subset of HIV positive and EBV negative PBL cases that showed *MYC* gene aberrations. This uncommon finding does however require further investigation as to another possible effector besides EBV on the *MYC* gene in B-cell lymphomas such as PBL. With these achievements we provided sound foundation for further study into the poorly understood pathogenesis of PBL.

6. REFERENCES

ADAMS, J. M., GERONDAKIS, S., WEBB, E., CORCORAN, L. M. & CORY, S. 1983. Cellular myc oncogene is altered by chromosome translocation to an immunoglobulin locus in murine plasmacytomas and is rearranged similarly in human Burkitt lymphomas. *Proceedings of the National Academy of Sciences of the United States of America,* 80**,** 1982-1986.

AGUILAR, R., CASABONNE, D., O'CALLAGHAN-GORDO, C., VIDAL, M., CAMPO, J. J., MUTALIMA, N., ANGOV, E., DUTTA, S., GAUR, D., CHITNIS, C. E., CHAUHAN, V., MICHEL, A., DE SANJOSÉ, S., WATERBOER, T., KOGEVINAS, M., NEWTON, R. & DOBAÑO, C. 2017. Assessment of the Combined Effect of Epstein–Barr Virus and Plasmodium falciparum Infections on Endemic Burkitt Lymphoma Using a Multiplex Serological Approach. *Frontiers in Immunology,* 8.

ALAMRI, A., NAM, J. Y. & BLANCATO, J. K. 2017. Fluorescence In Situ Hybridization of Cells, Chromosomes, and Formalin-Fixed Paraffin-Embedded Tissues. *Methods in molecular biology (Clifton, N.J.),* 1606**,** 265-279.

ALLI, N. & MEER, S. 2017. Head and neck lymphomas: A 20-year review in an Oral Pathology Unit, Johannesburg, South Africa, a country with the highest global incidence of HIV/AIDS. *Oral Oncology,* 67**,** 17-23.

AMBROSIO, M., MUNDO, L., GAZANEO, S., PICCIOLINI, M., VARA, P., SAYED, S., GINORI, A., LO BELLO, G., DEL PORO, L., NAVARI, M., ASCANI, S., YONIS, A., LEONCINI, L., PICCALUGA, P. P. & LAZZI, S. 2017. MicroRNAs sequencing unveils distinct molecular subgroups of plasmablastic lymphoma. *Octotarget,* 8**,** 107356-107373.

AMBROSIO, M. R., DE FALCO, G., GOZZETTI, A., ROCCA, B. J., AMATO, T., MOURMOURAS, V., GAZANEO, S., MUNDO, L., CANDI, V., PICCALUGA, P. P., CUSI, M. G., LEONCINI, L. & LAZZI, S. 2014. Plasmablastic transformation of a pre-existing plasmacytoma: a possible role for reactivation of Epstein Barr virus infection. *Haematologica,* 99**,** e235-e237.

ASHTON-KEY, M., WRIGHT, P. & WRIGHT, D. 2016. Normal/reactive lymph nodes: Structure and cells. *Diagnostic Lymph Node Pathology.* CRC Taylor and Francis Group.

BANCROFT 2013. Molecular pathology. *Bancroft's Theory and Practice of Histological Techniques.* 7 ed.: Churchill Livingstone.

BIBAS, M. & CASTILLO, J. 2014. Current knowledge on HIV-associated Plasmablastic Lymphoma. *Mediterranean Journal Of Hematology and Infectious Diseases,* 6.

BOGUSZ, A. M., SEEGMILLER, A. C., GARCIA, R., SHANG, P., ASHFAQ, R. & CHEN, W. 2009. Plasmablastic Lymphomas With MYC/IgH RearrangementReport of Three Cases and Review of the Literature. *American Journal of Clinical Pathology,* 132**,** 597-605.

BOUDREAULT, S., ARMERO, V. E. S., SCOTT, M. S., PERREAULT, J.-P. & BISAILLON, M. 2019. The Epstein-Barr virus EBNA1 protein modulates the alternative splicing of cellular genes. *Virology Journal,* 16**,** 29.

BOWER, M., NEWSOM-DAVIS, T., NARESH, K., MERCHANT, S., LEE, B., GAZZARD, B., STEBBING, J. & NELSON, M. 2011. Clinical Features and Outcome in HIV-Associated Multicentric Castleman's Disease. *J Clin Oncol,* 29**,** 2481-6.

BOY, S., VAN HEERDEN, M., BABB, C., VAN HEERDEN, W. & WILLEM, P. 2011. Dominant genetic aberrations and coexistent EBV infection in HIV-related oral plasmablastic lymphomas. *Journal of Oral Oncology,* 47.

BOY, S., VAN HEERDEN, M., POOL, R., WILLEM, P. & SLAVIK, T. 2015. Plasmablastic lymphoma versus diffuse large B cell lymphoma with plasmablastic differentiation: proposal for a novel diagnostic scoring system. *Journal of Hematology***,** 3-11.

BOY, S., VAN HEERDEN, M., RAUBENHEIMER, E. & VAN HEEREDEN, W. 2010. Plasmablastic lymphomas with light chain restriction – plasmablastic extramedullary plasmacytomas? *Journal of Oral Pathology,* 39.

CALADO, D. P., SASAKI, Y., GODINHO, S. A., PELLERIN, A., KOCHERT, K., SLECKMAN, B. P., DE ALBORAN, I. M., JANZ, M., RODIG, S. & RAJEWSKY, K. 2012. The cell-cycle regulator c-

Myc is essential for the formation and maintenance of germinal centers. *Nat Immunol,* 13**,** 1092-100.

CAMERON, J. E., FEWELL, C., YIN, Q., MCBRIDE, J., WANG, X., LIN, Z. & FLEMINGTON, E. K. 2008. Epstein–Barr virus growth/latency III program alters cellular microRNA expression. *Virology,* 382**,** 257-266.

CAMPO, E., STEIN, H. & HARRIS, N. 2017. Plasmablastic Lymphoma. *In:* SWERDLOW, S., CAMPO, E., HARRIS, N., JAFFE, E., PILERI, S., STEIN, H., THIELE, J., ARBER, D., HASSERJIAN, R., LE BEAU, M., ORAZI, A. & SIEBERT, R. (eds.) *WHO Classification of Tumours of Haematopoietic and Lymphoid Tissues.* Lyon: IARC.

CARBONE, A., VACCHER, E., GLOGHINI, A., PANTANOWITZ, L., ABAYOMI, A., DE PAOLI, P. & FRANCESCHI, S. 2014. Diagnosis and management of lymphomas and other cancers in HIV-infected patients. *Nature Reviews Clinical Oncology,* 11**,** 223-238.

CARROLL, V. & GARZINO-DEMO, A. 2015. HIV-associated lymphoma in the era of combination antiretroviral therapy: shifting the immunological landscape. *Pathogens and disease,* 73**,** ftv044.

CASTILLO, J., BIBAS, M. & MIRANDA, R. 2015. The biology and treatment of plasmablastic lymphoma. *Blood Journal,* 125.

CASTILLO, J., PANTANOWITZ, L. & DEZUBE, B. 2008. HIV-associated plasmablastic lymphoma: Lessons learned from 112 published cases. *American Journal of Hematology***,** 804-809.

CASTILLO, J. & REAGAN, J. 2011. Plasmablastic Lymphoma: A systematic Review. *The Scientific World Journal***,** 687-696.

CHEN, J., SATHIYAMOORTHY, K., ZHANG, X., SCHALLER, S., PEREZ WHITE, B. E., JARDETZKY, T. S. & LONGNECKER, R. 2018. Ephrin receptor A2 is a functional entry receptor for Epstein-Barr virus. *Nat Microbiol,* 3**,** 172-180.

CHETTY, R., HLATSWAYO, N., MUC, R., SABARATNAM, R. & GATTER, K. 2003. Plasmablastic lymphoma in HIV+ patients: an expanding spectrum. *Histopathology,* 42**,** 605-609.

CHISHOLM, K. M., BANGS, C. D., BACCHI, C. E., KIRSCH, H. M.-., CHERRY, A. & NATKUNAM, Y. 2015. Expression Profiles of MYC Protein and MYC Gene Rearrangement in Lymphomas. *The American Journal of Surgical Pathology,* 39**,** 294-303.

COLOMO, L., LOONG, F., RIVES, S., PITTALUGA, S., MARTINEZ, A., LOPEZ-GUILLERMO, A., OJANGUREN, J., ROMAGOSA, V., JAFFE, E. & CAMPO, E. 2004. Diffuse Large B-cell Lymphomas With Plasmablastic Differentiation Represent a Heterogeneous Group of Disease Entities *The American Journal of Surgical Pathology,* 28**,** 736-747.

DANG, C. V. 2013. MYC, metabolism, cell growth, and tumorigenesis. *Cold Spring Harbor perspectives in medicine,* 3**,** a014217.

DAWSON, C. W., PORT, R. & YOUNG, L. S. 2012. The role of the EBV-encoded latent membrane proteins LMP1 and LMP2 in the pathogenesis of nasopharyngeal carcinoma (NPC). *Seminars in Cancer Biology,* 22.

DAWSON, M. A., SCHWARER, A. P., MCLEAN, C., OEI, P., CAMPBELL, L. J., WRIGHT, E., SHORTT, J. & STREET, A. M. 2007. Aids-related plasmablastic lymphoma of the oral cavity associated with an IgH/MYC translocation–treatment with autologous stem-cell transplantation in a patient with severe haemophilia-A. 92**,** e11-e12.

DE SILVA, N. S. & KLEIN, U. 2015. Dynamics of B cells in germinal centres. *Nature Reviews Immunology,* 15**,** 137.

DELECLUSE, H., ANAGNOSTOPOULUS, I., DALLENABCH, F., HUMMEL, M., MARAFIOTI, T., SCHNEIDER, U., HUHN, D., SCHMIDT-WESTHAUSEN, A., REICHART, P., GROSS, U. & STEIN, H. 1997. Plasmablastic Lymphomas of the Oral Cavity: A New Entity Associated With the Human Immunodeficiency Virus Infection. *Blood Journal,* 89**,** 1413-1420.

DELECLUSE, H. J., FEEDERLE, R., O'SULLIVAN, B. & TANIERE, P. 2007. Epstein Barr virus-associated tumours: an update for the attention of the working pathologist. *Journal of clinical pathology,* 60**,** 1358-1364.

DOMINGUEZ-SOLA, D., VICTORA, G. D., YING, C. Y., PHAN, R. T., SAITO, M., NUSSENZWEIG, M. C. & DALLA-FAVERA, R. 2012. The proto-oncogene MYC is required for selection in the germinal center and cyclic reentry. *Nature Immunology,* 13**,** 1083.

DONG, H. Y., SCADDEN, D. T., DE LEVAL, L., TANG, Z., ISAACSON, P. G. & HARRIS, N. L. 2005. Plasmablastic lymphoma in HIV-positive patients: an aggressive Epstein-Barr virus-associated extramedullary plasmacytic neoplasm. *Am J Surg Pathol,* 29**,** 1633-41.

DUPIN, N., DISS, T. L., KELLAM, P., TULLIEZ, M., DU, M.-Q., SICARD, D., WEISS, R. A., ISAACSON, P. G. & BOSHOFF, C. 2000. HHV-8 is associated with a plasmablastic variant of Castleman disease that is linked to HHV-8–positive plasmablastic lymphoma. *Blood,* 95**,** 1406-1412.

ELYAMANY, G., AL MUSSAED, E. & MATAR ALZHRANI, A. 2015a. Plasmablastic Lymphoma: A Review of Current Knowledge and Future Directions. *Advances in Hematology,* 2015**,** 1-11.

ELYAMANY, G., ALZAHRANI, A. M., ALJUBOURY, M., MOGADEM, N., REHAN, N., ALSUHAIBANI, O., ALABDULAALY, A., AL-MUSSAED, E., ELHAG, I. & ALFIAAR, A. 2015b. Clinicopathologic features of plasmablastic lymphoma: Single-center series of 8 cases from Saudi Arabia. *Diagnostic pathology,* 10**,** 78-78.

EPSTEIN, M. A., ACHONG, B. G. & BARR, Y. M. 1964. VIRUS PARTICLES IN CULTURED LYMPHOBLASTS FROM BURKITT'S LYMPHOMA. *Lancet,* 1**,** 702-3.

FERNANDEZ-ALVAREZ, R., SANCHO, J.-M. & RIBERA, J.-M. 2016. Plasmablastic lymphoma. *Medicina Clinica*.

FRAPPIER, L. 2012. The Epstein-Barr Virus EBNA1 Protein. *Scientifica,* 2012**,** 15.

GLOGHINI, A., DOLCETTI, R. & CARBONE, A. 2013. Lymphomas occurring specifically in HIV-infected patients: From pathogenesis to pathology. *Seminars in Cancer Biology,* 23**,** 457-467.

GONZALEZ, H., HAGERLING, C. & WERB, Z. 2018. Roles of the immune system in cancer: from tumor initiation to metastatic progression. *Genes Dev***,** 1267-1284.

GULLEY, M. L. & TANG, W. 2008. Laboratory Assays for Epstein-Barr Virus-Related Disease. *The Journal of Molecular Diagnostics,* 10**,** 279-292.

HAIKALA, H. M., ANTTILA, J. M. & KLEFSTRÖM, J. 2017. MYC and AMPK-Save Energy or Die! *Frontiers in cell and developmental biology,* 5**,** 38-38.

HAMMERSCHMIDT, W. 2015. The Epigenetic Life Cycle of Epstein–Barr Virus. *In:* MÜNZ, C. (ed.) *Epstein Barr Virus Volume 1: One Herpes Virus: Many Diseases.* Cham: Springer International Publishing.

HARMON, C. & SMITH, L. 2016. Plasmablastic Lymphoma - A Review of Clinicopathological Features and Differential Diagnosis. *Arch Pathol Lab Med,* 140.

HATTON, O., ARNOLD HARRIS, O., SCHAFFERT, S., KRAMS, S. & MARTINEZ, O. 2014. The Interplay Between Epstein Barr Virus and B Lymphocytes: Implications for Infection, Immunity, and Disease. *Immunol Research*.

HEUTS, F., ROTTENBERG, M. E., SALAMON, D., RASUL, E., ADORI, M., KLEIN, G., KLEIN, E. & NAGY, N. 2014. T Cells Modulate Epstein-Barr Virus Latency Phenotypes during Infection of Humanized Mice. *Journal of Virology,* 88**,** 3235-3245.

HUTT-FLETCHER, L. M. 2007. Epstein-Barr Virus Entry. *Journal of Virology,* 81**,** 7825-7832.

HUTT-FLETCHER, L. M. 2014. Epstein–Barr virus replicating in epithelial cells. *Proceedings of the National Academy of Sciences,* 111**,** 16242-16243.

HUTT-FLETCHER, L. M. 2017. The Long and Complicated Relationship between Epstein-Barr Virus and Epithelial Cells. *Journal of Virology,* 91.

IKPATT, O. F., SUJOY, V. & CIOFFI-LAVINA, M. 2012. Nodal Plasmablastic Lymphoma in an HIV-Positive Man: A Case Report. *AJSP: Reviews & Reports,* 17**,** 75-78.

KANG, M.-S. & KIEFF, E. 2015. Epstein–Barr virus latent genes. *Experimental and Molecular Medicine*.

KARUBE, K. & CAMPO, E. 2015. MYC Alterations in Diffuse Large B-Cell Lymphomas. *Seminars in Hematology,* 52**,** 97-106.

KATCHI, T. & LIU, D. 2017. Diagnosis and treatment of CD20 negative B cell lymphomas. *Biomarker Research,* 5**,** 5.

KEMPKES, B. & ROBERTSON, E. S. 2015. Epstein-Barr virus latency: current and future perspectives. *Current Opinion in Virology,* 14**,** 138-144.

KENNEY, S. C. & MERTZ, J. E. 2014. Regulation of the latent-lytic switch in Epstein–Barr virus. *Seminars in Cancer Biology,* 26**,** 60-68.

KIESER, A. & STERZ, K. 2015. The Latent Membrane Protein 1 (LMP1). *Epstein-Barr Virus Volume 2.* Springer, Cham.

KLEIN, U. & DALLA-FAVERA, R. 2008. Germinal centres: role in B-cell physiology and malignancy. *Nat Rev Immunol,* 8**,** 22-33.

KLISZCZEWSKA, E., JARZYŃSKI, A., BOGUSZEWSKA, A., PASTERNAK, J. & POLZ-DACEWICZ, M. 2017. Epstein-Barr Virus – pathogenesis, latency and cancers. *Journal of Pre-Clinical and Clinical Research,* 11**,** 142-146.

KUMAR V, A. A., ASTER, C 2014. *Robbins and Cotran Pathologic Basis of Disease*.

LAURENT, C., FABIANI, B., DO, C., TCHERNONOG, E., CARTRON, G., GRAVELLE, P., AMARA, N., MALOT, S., PALISOC, M. M., COPIE-BERGMAN, C., GLEHEN, A. T., COPIN, M. C., BROUSSET, P., PITTALUGA, S., JAFFE, E. S. & COPPO, P. 2016. Immune-checkpoint expression in Epstein-Barr virus positive and negative plasmablastic lymphoma: a clinical and pathological study in 82 patients. *Haematologica,* 101**,** 976-84.

LI, H., LIU, S., HU, J., LUO, X., LI, N., M.BODE, A. & CAO, Y. 2016. Epstein-Barr virus lytic reactivation regulation and its pathogenic role in carcinogenesis. *International Journal of Biological Sciences,* 12**,** 1309-1318.

LIEBERMAN, P. 2015. Chromatin Structure of Epstein–Barr Virus Latent Episomes. *Epstein-Barr Virus Volume 1.*

LIEW, M., ROWE, L., CLEMENT, P. W., MILES, R. R. & SALAMA, M. E. 2016. Validation of break-apart and fusion MYC probes using a digital fluorescence in situ hybridization capture and imaging system. *Journal of pathology informatics,* 7**,** 20-20.

LINKE-SERINSÖZ, E., FEND, F. & QUINTANILLA-MARTINEZ, L. 2017. Human immunodeficiency virus (HIV) and Epstein-Barr virus (EBV) related lymphomas, pathology view point. *Seminars in Diagnostic Pathology,* 34**,** 352-363.

LIU, F., ASANO, N., TATEMATSU, A., OYAMA, T., KITAMURA, K., SUZUKI, K., YAMAMOTO, K., SAKAMOTO, N., TANIWAKI, M., KINOSHITA, T. & NAKAMURA, S. 2012. Plasmablastic lymphoma of the elderly: a clinicopathological comparison with age-related Epstein-Barr virus-associated B cell lymphoproliferative disorder. *Histopathology,* 61**,** 1183-97.

LONGNECKER, R., KIEFF, E. & COHEN, J. 2013. Epstein-Barr Virus. *In:* KNIPE, D. & HOWLEY, P. (eds.) *Fields Virology.* Lippincott Williams and Wilkins.

LOPEZ, A. & ABRISQUETA, P. 2018. Plasmablastic lymphoma: current perspectives. *Blood and Lymphatic Cancer: Targets and Therapy,* 8**,** 63-70.

LOUTEN, J. 2016. Herpesviruses. *In:* LEONARD, J. (ed.) *Essential Human Virology.* USA: Sara Tenney.

LYNNHTUN, K., RENTHAWA, J. & VARIKATT, W. 2014. Detection of MYC rearrangement in high grade B cell lymphomas: correlation of MYC immunohistochemistry and FISH analysis. *Pathology,* 46**,** 211-215.

MCBRIDE, K. M., GAZUMYAN, A., WOO, E. M., BARRETO, V. M., ROBBIANI, D. F., CHAIT, B. T. & NUSSENZWEIG, M. C. 2006. Regulation of hypermutation by activation-induced cytidine deaminase phosphorylation. 103**,** 8798-8803.

MESIN, L., ERSCHING, J. & VICTORA, G. D. 2016. Germinal Center B Cell Dynamics. *Immunity,* 45**,** 471-482.

MIAO, L., GUO, N., FENG, Y., RAO, H., WANG, F., HUANG, Q. & HUANG, Y. 2019. High incidence of MYC rearrangement in human immunodeficiency virus-positive plasmablastic lymphoma. *Histopathology,* 0.

MIDDELDORP, J. M. & PEGTEL, D. M. 2008. Multiple roles of LMP1 in Epstein-Barr virus induced immune escape. *Seminars in Cancer Biology,* 18**,** 388-396.

MILLER, D. M., THOMAS, S. D., ISLAM, A., MUENCH, D. & SEDORIS, K. 2012. c-Myc and cancer metabolism. *Clinical cancer research : an official journal of the American Association for Cancer Research,* 18**,** 5546-5553.

MINNICH, M., TAGOH, H., BONELT, P., AXELSSON, E., FISCHER, M., CEBOLLA, B., TARAKHOVSKY, A., NUTT, S. L., JARITZ, M. & BUSSLINGER, M. 2016. Multifunctional role of the transcription factor Blimp-1 in coordinating plasma cell differentiation. *Nature Immunology,* 17**,** 331+.

MISRA, A., BAKHSHI, S., KUMAR, R. & CHOPRA, A. 2017. Pediatric plasmablastic lymphoma: Diagnostic and therapeutic dilemma. 60**,** 303-304.

MONTES-MORENO, S., MARTINEZ-MAGUNACELAYA, N., ZECCHINI-BARRESE, T., GONZALEZ DE VILLAMBROSIA, S., LINARES, E., RANCHAL, T., RODRIGUEZ-PINILLA, M., BATLLE, A., CERECEDA-COMPANY, L., REVERT-ARCE, J., ALMARAZ, C. & PIRIS, M. 2017. Plasmablastic lymphoma phenpotype is determined by genetic alterations in MYC and PRDM1. *Modern Pathology,* 30**,** 85-94.

MORISSETTE, G. & FLAMAND, L. 2010. Herpesviruses and Chromosomal Integration. *Journal of Virology,* 84**,** 12100-12109.

MORSCIO, J., DIERICKX, D., NIJS, J., VERHOEF, G., BITTOUN, E., VANOETEREN, X., WLODARSKA, I., SAGAERT, X. & TOUSSEYN, T. 2014. Clinicopathologic Comparison of Plasmablastic Lymphoma in HIV-positive, Immunocompetent, and Posttransplant Patients. *American Journal of Surgical Pathology,* 38**,** 12.

MORTON, J. P. & SANSOM, O. J. 2013. MYC-y mice: From tumour initiation to therapeutic targeting of endogenous MYC. *Molecular Oncology,* 7**,** 248-258.

MÜNZ, C. 2016. Epstein Barr virus — a tumor virus that needs cytotoxic lymphocytes to persist asymptomatically. *Current Opinion in Virology,* 20**,** 34-39.

MURATA, T. 2014. Regulation of Epstein–Barr virus reactivation from latency. *Microbiology and Immunology,* 58**,** 307-317.

MURATA, T., SATO, Y. & KIMURA, H. 2014. Modes of infection and oncogenesis by the Epstein–Barr virus. *Reviews in Medical Virology,* 24**,** 242-253.

NGUYEN, L., PAPENHAUSEN, P. & SHAO, H. 2017. The Role of c-MYC in B-Cell Lymphomas: Diagnostic and Molecular Aspects. *Genes,* 8**,** 116.

NIEDOBITEK, G. 1999. The Epstein-Barr virus: a group 1 carcinogen? *Virchows Arch,* 435**,** 79-86.

NIEDOBITEK, G., MUTIMER, D. J., WILLIAMS, A., WHITEHEAD, L., WILSON, P., ROONEY, N., YOUNG, L. S. & HÜBSCHER, S. G. 1997. Epstein-Barr virus infection and malignant lymphomas in liver transplant recipients. *International Journal of Cancer,* 73**,** 514-520.

OKAMOTO, A., YANADA, M., INAGUMA, Y., TOKUDA, M., MORISHIMA, S., KANIE, T., YAMAMOTO, Y., MIZUTA, S., AKATSUKA, Y., YOSHIKAWA, T., MIZOGUCHI, Y., NAKAMURA, S., OKAMOTO, M. & EMI, N. 2017. The prognostic significance of EBV DNA load and EBER status in diagnostic specimens from diffuse large B-cell lymphoma patients. *Hematological Oncology,* 35**,** 87-93.

OTT, G., ROSENWALD, A. & CAMPO, E. 2013. Understanding MYC-driven aggressive B-cell lymphomas: pathogenesis and classification. *Blood,* 122**,** 3884-3891.

PAN, Z., HU, S., LI, M., ZHOU, Y., KIM, Y. S., REDDY, V., SANMANN, J. N., SMITH, L. M., CHEN, M., GAO, Z., WANG, H.-Y. & YUAN, J. 2017. ALK-positive Large B-cell Lymphoma: A Clinicopathologic Study of 26 Cases With Review of Additional 108 Cases in the Literature. *The American Journal of Surgical Pathology,* 41**,** 25-38.

PANNONE, G., ZAMPARESE, R., PACE, M., PEDICILLO, M., CAGIANO, S., SOMMA, P., ERRICO, M., DONOFRIO, V., FRANCO, R., DE CHIARA, A., AQUINO, G., BUCCI, E., SANTORO, A. & BUFO, P. 2014. The role of EBV in the pathogenesis of Burkitt's Lymphoma: an Italian hospital based survey. *Infectious Agents and Cancer*.

PATEL, M., PHILIP, V., OMAR, T., TURTON, D., CANDY, G., LAKHA, A. & PATHER, S. 2015. The Impact of Human Immunodeficiency Virus Infection (HIV) on Lymphoma in South Africa. *Journal of Cancer Therapy,* Vol.06**,** 9.

PEDERSEN, M. Ø., GANG, A. O., CLASEN-LINDE, E., BREINHOLT, M. F., KNUDSEN, H., NIELSEN, S. L., POULSEN, T. S., KLAUSEN, T. W., HØGDALL, E. & NØRGAARD, P. 2019. Stratification by MYC expression has prognostic impact in MYC translocated B-cell lymphoma—Identifies a subgroup of patients with poor outcome. *European Journal of Haematology,* 102**,** 395-406.

PRICE, A. & LUFTIG, M. 2015. To Be or Not IIb: A Multi-Step Process for Epstein-Barr Virus Latency Establishmnet and Consequences for B Cell Tumorigenesis. *Plos Pathogens***,** 7.

PRICE, A., MESSINGER, J. & LUFTIG, M. 2017. c-Myc Represses Transcription of the Epstein-Barr Virus Latent Membrane Protein 1 Early After Primary B Cell Infection. *Journal of Virology*.

RAFANIELLO RAVIELE, P., PRUNERI, G. & MAIORANO, E. 2009. Plasmablastic lymphoma: a review. *Oral Diseases,* 15**,** 38-45.

RAMIRO, A. R., JANKOVIC, M., CALLEN, E., DIFILIPPANTONIO, S., CHEN, H. T., MCBRIDE, K. M., EISENREICH, T. R., CHEN, J., DICKINS, R. A., LOWE, S. W., NUSSENZWEIG, A. & NUSSENZWEIG, M. C. 2006. Role of genomic instability and p53 in AID-induced c-myc-Igh translocations. *Nature,* 440**,** 105-9.

RAMNANI, D. 2016. *Plasmablastic Pathology* [Online]. WebPathology. Available: https://www.webpathology.com/image.asp?n=1&Case=828 [Accessed September 1 2020].

REISFELD, M. 2015. *The MYC Transcription Factor* [Online]. United States Documents. Available: https://documents.pub/document/the-myc-transcription-factor-by-michael-reisfeld.html [Accessed September 1 2020].

REZK, S. A. & WEISS, L. M. 2007. Epstein-Barr virus–associated lymphoproliferative disorders. *Human Pathology,* 38**,** 1293-1304.

REZK, S. A., ZHAO, X. & WEISS, L. M. 2018. Epstein-Barr virus (EBV)–associated lymphoid proliferations, a 2018 update. *Human Pathology,* 79**,** 18-41.

ROSENTHAL, A. & YOUNES, A. 2017. High grade B-cell lymphoma with rearrangements of MYC and BCL2 and/or BCL6: Double hit and triple hit lymphomas and double expressing lymphoma. *Blood Reviews,* 31**,** 37-42.

SAID, J., ISAACSON, P. G., CAMPO, E. & HARRIS, N. 2017. HHV8-associated lymphoproliferative disorders. *WHO Classification of Tumours of Haematopoietic and Lymphoid Tissues.* 4th ed.

SALAVERRIA, I., MARTIN-GUERRERO, I., WAGENER, R., KREUZ, M., KOHLER, C. W., RICHTER, J., PIENKOWSKA-GRELA, B., ADAM, P., BURKHARDT, B., CLAVIEZ, A., DAMM-WELK, C., DREXLER, H. G., HUMMEL, M., JAFFE, E. S., KÜPPERS, R., LEFEBVRE, C., LISFELD, J., LÖFFLER, M., MACLEOD, R. A. F., NAGEL, I., OSCHLIES, I., ROSOLOWSKI, M., RUSSELL, R. B., RYMKIEWICZ, G., SCHINDLER, D., SCHLESNER, M., SCHOLTYSIK, R., SCHWAENEN, C., SPANG, R., SZCZEPANOWSKI, M., TRÜMPER, L., VATER, I., WESSENDORF, S., KLAPPER, W., SIEBERT, R., PROJECT, F. T. M. M. I. M. L. N. & GROUP, B.-F.-M. N.-H. L. 2014. A recurrent 11q aberration pattern characterizes a subset of MYC-negative high-grade B-cell lymphomas resembling Burkitt lymphoma. *Blood,* 123**,** 1187-1198.

SAMPATH, R., MANIPADAM, M., NAIR, S., VISWABANDYA, A. & ZACHARIAH, A. 2019. HIV-associated lymphoma: A 5-year clinicopathologic study from India. *Indian Journal of Pathology and Microbiology,* 62**,** 73-78.

SANTOS, L., AZEVEDO, K., SILVA, L. & OLIVEIRA, L. 2014. Epstein-Barr virus in oral mucosa from human immunodeficiency virus positive patients. *Revista da Associação Médica Brasileira,* 60**,** 262-269.

SARACENI, C., AGOSTINO, N., CORNFIELD, D. B. & GUPTA, R. 2013. Plasmablastic lymphoma of the maxillary sinus in an HIV-negative patient: a case report and literature review. *SpringerPlus,* 2**,** 142.

SCHELLER, H., TOBOLLIK, S., KUTZERA, A., EDER, M., UNTERLEHBERG, J., PFEIL, I. & JUNGNICKEL, B. 2009. c-Myc overexpression promotes a germinal center-like program in Burkitt's lymphoma. *Oncogene,* 29**,** 888.

SCHLEE, M., KRUG, T., GIRES, O., ZEIDLER, R., HAMMERSCHMIDT, W., MAILHAMMER, R., LAUX, G., SAUER, G., LOVRIC, J. & BORNKAMM, G. W. 2004. Identification of Epstein-Barr virus (EBV) nuclear antigen 2 (EBNA2) target proteins by proteome analysis: activation of EBNA2 in conditionally immortalized B cells reflects early events after infection of primary B cells by EBV. *Journal of virology,* 78**,** 3941-3952.

SHANNON-LOWE, C. & RICKINSON, A. 2019. The Global Landscape of EBV-Associated Tumors. *Frontiers in Oncology,* 9.

SIVACHANDRAN, N., WANG, X. & FRAPPIER, L. 2012. Functions of the Epstein-Barr Virus EBNA1 Protein in Viral Reactivation and Lytic Infection. *Journal of Virology*.

SLACK, G. & GASCOYNE, R. 2011. MYC and Aggressive B-cell Lymphomas. *Adv Anat Pathol,* 18**,** 219-228.

SMIT, L. A., BENDE, R. J., ATEN, J., GUIKEMA, J. E. J., AARTS, W. M. & VAN NOESEL, C. J. M. 2003. Expression of Activation-induced Cytidine Deaminase Is Confined to B-Cell Non-Hodgkin's Lymphomas of Germinal-Center Phenotype. 63**,** 3894-3898.

STATSSA 2018. Statistical release Statistical release P0302 Mid-year population estimates 2018 1-18.

STINE, Z. E., WALTON, Z. E., ALTMAN, B. J., HSIEH, A. L. & DANG, C. V. 2015. MYC, Metabolism, and Cancer. *Cancer Discovery,* 5**,** 1024-1039.

SUAN, D., SUNDLING, C. & BRINK, R. 2017. Plasma cell and memory B cell differentiation from the germinal center. *Current Opinion in Immunology,* 45**,** 97-102.

SWERDLOW, S. H. 2014. Diagnosis of 'double hit' diffuse large B-cell lymphoma and B-cell lymphoma, unclassifiable, with features intermediate between DLBCL and Burkitt lymphoma: when and how, FISH versus IHC. 2014**,** 90-99.

SWERDLOW, S. H., CAMPO, E., PILERI, S. A., HARRIS, N. L., STEIN, H., SIEBERT, R., ADVANI, R., GHIELMINI, M., SALLES, G. A., ZELENETZ, A. D. & JAFFE, E. S. 2016. The 2016 revision of the World Health Organization classification of lymphoid neoplasms. *Blood,* 127**,** 2375-2390.

TADDESSE-HEATH, L., MELONI-EHRIG, A., SEARLE, J., KELLY, J. & JAFFE, E. 2010. Plasmablastic lymphoma with MYC translocation: evidence for a common pathway in the generation of plasmablastic features. *Modern Pathology,* 23**,** 991-999.

TAKAYUKI, M. & TATSUYA, T. 2014. Switching of EBV cycles between latent and lytic states. *Reviews in Medical Virology,* 24**,** 142-153.

TANSEY, W. P. 2014. Mammalian MYC Proteins and Cancer. *New Journal of Science,* 2014**,** 27.

THOMPSON, M. P. & KURZROCK, R. 2004. Epstein-Barr Virus and Cancer. 10**,** 803-821.

THORLEY-LAWSON, D. A. 2015. EBV Persistence—Introducing the Virus. *In:* MÜNZ, C. (ed.) *Epstein Barr Virus Volume 1: One Herpes Virus: Many Diseases.* Cham: Springer International Publishing.

THORLEY-LAWSON, D. A., HAWKINS, J. B., TRACY, S. I. & SHAPIRO, M. 2013. The pathogenesis of Epstein–Barr virus persistent infection. *Current Opinion in Virology,* 3**,** 227-232.

VALERA, A., BALAGUE, O., COLOMO, L., MARTINEZ, A., DELABIE, J., TADDESSE-HEATH, L., JAFFE, E. & CAMPO, E. 2010. IG/MYC Rearrangements are the Main Cytogenetic Alteration in. *American Journal of Surgical Pathology,* 34**,** 1686-1694.

VAUBELL, J. I., SING, Y., RAMBURAN, A., SEWRAM, V., THEJPAL, R., RAPITI, N. & RAMDIAL, P. K. 2014. Pediatric Plasmablastic Lymphoma:A Clinicopathologic Study. *International Journal of Surgical Pathology,* 22**,** 607-616.

VEGA, F., CHANG, C.-C., MEDEIROS, L. J., UDDEN, M. M., CHO-VEGA, J. H., LAU, C.-C., FINCH, C. J., VILCHEZ, R. A., MCGREGOR, D. & JORGENSEN, J. L. 2004. Plasmablastic lymphomas and plasmablastic plasma cell myelomas have nearly identical immunophenotypic profiles. *Modern Pathology,* 18**,** 806.

VENNSTROM, B., SHEINESS, D., ZABIELSKI, J. & BISHOP, J. M. 1982. Isolation and characterization of c-myc, a cellular homolog of the oncogene (v-myc) of avian myelocytomatosis virus strain 29. *J Virol,* 42**,** 773-9.

VENTURA, R. A., MARTIN-SUBERO, J. I., JONES, M., MCPARLAND, J., GESK, S., MASON, D. Y. & SIEBERT, R. 2006. FISH Analysis for the Detection of Lymphoma-Associated Chromosomal Abnormalities in Routine Paraffin-Embedded Tissue. *The Journal of Molecular Diagnostics,* 8**,** 141-151.

VERHOEVEN, R. J. A., TONG, S., MOK, B. W.-Y., LIU, J., HE, S., ZONG, J., CHEN, Y., TSAO, S.-W., LUNG, M. L. & CHEN, H. 2019. Epstein-Barr Virus BART Long Non-coding RNAs Function as Epigenetic Modulators in Nasopharyngeal Carcinoma. *Frontiers in Oncology,* 9.

VERONESE, M., OHTA, M., FINAN, J., NOWELL, P. & CROCE, C. 1995. Detection of myc translocations in lymphoma cells by fluorescence in situ hybridization with yeast artificial chromosomes. *Blood,* 85**,** 2132-2138.

VICTORA, G. D. 2014. SnapShot: The Germinal Center Reaction. *Cell,* 159**,** 700-700.e1.

WAGENER, R., BENS, S., TOPRAK, U. H., SEUFERT, J., LÓPEZ, C., SCHOLZ, I., HERBRUEGGEN, H., OSCHLIES, I., STILGENBAUER, S., SCHLESNER, M., KLAPPER, W., BURKHARDT, B. & SIEBERT, R. 2019. Cryptic insertion of MYC exons 2 and 3 into the IGH locus detected by whole genome sequencing in a case of MYC-negative Burkitt lymphoma. *Haematologica***,** haematol.2018.208140.

WANG, H.-W., PITTALUGA, S. & JAFFE, E. S. 2016. Multicentric Castleman disease: Where are we now? *Seminars in diagnostic pathology,* 33**,** 294-306.

WANG, H.-Y., WONG-SEFIDAN, I. & REID, E. 2014. Plasmablastic Lymphoma. *Cancers in People with HIV and Aids : Progress and Challenges.* New York, NY: Springer.

WILSON, J. B., MANET, E., GRUFFAT, H., BUSSON, P., BLONDEL, M. & FAHRAEUS, R. 2018. EBNA1: Oncogenic Activity, Immune Evasion and Biochemical Functions Provide

Targets for Novel Therapeutic Strategies against Epstein-Barr Virus- Associated Cancers. *Cancers,* 10**,** 109.

WU, T. C., MANN, R. B., CHARACHE, P., HAYWARD, S. D., STAAL, S., LAMBE, B. C. & AMBINDER, R. F. 1990. Detection of EBV gene expression in Reed-Sternberg cells of Hodgkin's disease. *Int J Cancer,* 46**,** 801-4.

XIAO, J., PALEFSKY, J. M., HERRERA, R., BERLINE, J. & TUGIZOV, S. M. 2008. The Epstein-Barr virus BMRF-2 protein facilitates virus attachment to oral epithelial cells. *Virology,* 370**,** 430-42.

YOUNG, L., YAP, L. & MURRAY, P. 2016. Epstein–Barr virus: more than 50 years old and still providing surprises. *Nature News - Cancer,* 16**,** 789-802.

YOUNG, L. S. & MURRAY, P. G. 2003. Epstein–Barr virus and oncogenesis: from latent genes to tumours. *Oncogene,* 22**,** 5108.

ZHANG, H., LI, Y., WANG, H. B., ZHANG, A., CHEN, M. L., FANG, Z. X., DONG, X. D., LI, S. B., DU, Y., XIONG, D., HE, J. Y., LI, M. Z., LIU, Y. M., ZHOU, A. J., ZHONG, Q., ZENG, Y. X., KIEFF, E., ZHANG, Z., GEWURZ, B. E., ZHAO, B. & ZENG, M. S. 2018. Ephrin receptor A2 is an epithelial cell receptor for Epstein-Barr virus entry. *Nat Microbiol,* 3**,** 1-8.

Appendix 1 – Reagents and buffers

A. Immunohistochemistry – manual method

Bluing solution

A 5ml volume of ammonia solution (Merck KGaA, Darmstadt, Germany) was added to 995ml deionised water. The solution was mixed well and stored at RT.

10mM Citric acid buffer solution pH 6

A 4.2g amount of citric acid (Merck KGaA, Darmstadt, Germany) was added to 1900ml of deionised H_2O. The solution was mixed well on a desktop mixer and the pH adjusted 6, using 10M sodium hydroxide. The mixture was then topped up to 2000ml with deionised water.

Tris/EDTA buffer solution (10 mM Tris Base, 1 mM EDTA) pH 9

A 2.42g amount of Trizma Base and 0.74g of EDTA (Merck KGaA, Darmstadt, Germany) was added to 1900ml deionised H_2O. The solution was mixed well on a desktop mixer and the pH of the solution was adjusted to 9, using 10M sodium hydroxide. The mixture was then topped up to 2000ml with deionised water.

3% Hydrogen Peroxide

A 3ml volume of hydrogen peroxide (Merck KGaA, Darmstadt, Germany) was added to 97ml deionised H_2O and mixed well.

Mayer's Haematoxylin

A 50g amount of aluminium sulphate (Alum), 1g of haematoxylin, 0.2g of sodium iodate, and 20ml of glacial acetic acid (Merck KGaA, Darmstadt, Germany) was added

to deionised H_2O and topped up to 1000ml. The solution was mixed well, boiled and allowed to cool. The solution was filtered if necessary once it was cooled down.

5% Normal Goat Serum

A 2.5ml volume of normal goat serum (NGS) (DAKO/Agilent, Santa Clara, CA, USA) was added to measuring cylinder and made up to 50ml with PBS. This solution was mixed well, aliquoted and stored at -20^{o}C for use later.

Phosphate buffered Saline (PBS)

Ten phosphate buffered saline (PBS) tablets (Oxoid, Hampshire, England) were dissolved in 1000ml of deionised H_2O. The solution was mixed well before use.

0.1% Phosphate buffered Saline Tween (PBS tween)

A 200µl volume of Tween 20 (Merck KGaA, Darmstadt, Germany) was added to 300ml of PBS.

3,3′- Diaminobenzidine (DAB)

Two drops of DAB was added to 2ml of substrate solution. Both solutions were included in the Liquid DAB + Substrate Chromogen System (DAKO/Agilent, Santa Clara, CA, USA) kit and was prepared in a 1:1 ratio.

B Immunohistochemistry – semi-automated method on Ventana XT auto-stainer reagents and buffers.

10X EZ Prep solution

EZ prep solution was used for paraffin removal in both IHC and ISH automated staining procedures. Two litres of EZ Prep reagent concentrate was made up to 20 litres using distilled water. This was stored on the shelf and decanted into the machine bulk container as required.

Reaction buffer concentrate

Reaction buffer is a Tris based buffer solution which was used to rinse between IHC and ISH staining procedures. Two litres of reaction buffer reagent concentrate was made up to 20 litres using distilled water.. This solution was stored on the shelf and decanted into the machine bulk container as required.

LCS

Also known as liquid coverslip, this solution was used “as is”, and was available in a 2L plastic bottle, prediluted. LCS is a high temperature coverslip solution which was used to prevent the aqueous solution from evaporating and the section drying out. This allowed for a stable IHC environment.

CC1

Also known as cell conditioning solution 1, was used “as is” and was available in a 2L plastic bottle. CC1 is a tris-based pre-treatment or antigen retrieval buffer.

OptiView DAB IHC Detection Kit

This kit was used for the semi-automated IHC staining. It contained propriety reagents in six 25ml dispensers, which were automatically applied by the analyser. These reagents were peroxidase, universal linker, HRP multimer, hydrogen peroxide (H_2O_2), 3,3′-Diaminobenzidine (DAB) and copper (copper sulphate).

C *In situ* hybridisation – automated method on Ventana XT auto-stainer reagents and buffers.

(With the exception of the DAB detection system mentioned above in the semi-automated IHC staining, certain of the bulk reagents for ISH *were the same. Below is additional bulk reagents and detection system specifically for* ISH*)*

EBER PROBE

The Ventana Inform EBER probe that was used was packaged in a 5ml automated dispenser. The concentration of the fluorescein labelled probe was 750ng/ml. The probe was used as is.

10X SSC

Sodium chloride sodium citrate buffer (SSC) was used for between step stringency wash during ISH. Two litres of 10xSSC reagent concentrate was made up to 10 litres using distilled water. The reagent was stored on the shelf and decanted into the machine bulk container as required.

CC2

Also known as cell conditioning solution 2, this solution was used “as is” and was available in a 2L plastic bottle. CC2 is a citric acid-based pre-treatment or antigen retrieval buffer.

ISH IVIEW BLUE DETECTION KIT

This kit was used for semi-automated ISH staining. It contained propriety reagents in six 25ml dispensers, which were automatically applied by the analyser. These reagents were anti-fluorescein mouse monoclonal antibody, purified goat anti mouse IgG, Streptavidin Alkaline Phosphatase, Enhancer (magnesium chloride solution), NBT (nitro blue tetrazolium) and BCIP (5-bromo-4-chloro-3-indolyl phosphate).

Red Counterstain II

This reagent was a propriety pre-packaged 10ml dispenser containing nuclear fast red solution. This reagent was used "as is" and dispensed automatically by the analyser.

ISH Protease 3

This reagent was a propriety pre-packaged 20ml dispenser containing a casein solution with a concentration 0.24 U/ml. This reagent was used "as is" and dispensed automatically by the analyser.

D Fluorescence *in situ* hybridisation (FISH) – manual method

1 M hydrochloric acid (HCl)

A 91.7ml volume of sterile H_20 was added to a graduated measuring cylinder. Using a graduated pipette, 8.3ml of concentrated HCl was added to the water.

0.2 N hydrochloric acid (HCl)

A 1ml volume of concentrated HCl was added to 49ml of sterile H_2O.

0.01 N hydrochloric acid (HCl)

A 3ml volume of 0.2N HCl was added to 57ml of sterile H_2O.

70% Ethanol

A 350ml volume of absolute ethanol was added to 150ml of sterile H_2O.

85% Ethanol

A 425ml volume of absolute ethanol was added to 75ml of sterile H_2O.

20X SSC (3 M sodium chloride; 0.3 M sodium citrate, pH 5.3)

A 66g amount of 20X SCC powder was added to 200ml of sterile H_2O. The solution was mixed well and the pH was adjusted to 5.3 with 1N HCl. The solution was then topped up with sterile water to a final volume of 250ml. This solution was stable at RT for 6 months.

2X SSC/0.3% IGEPAL CA-630

A 50ml volume of 20X SCC (pH 5.3) was added to 420ml of sterile H_2O. The solution was mixed thoroughly, and the pH adjusted to 7.25 with 1N NaOH. Thereafter 1.5ml of IGEPAL CA-630 was added to the solution and mixed well. The solution was then topped up to 500ml with sterile H_2O, filtered and was stable at RT for up to 6 months.

Pepsin (10% solution)

A 500mg amount of pepsin was added to 5ml of sterile H_2O. The solution was then aliquoted and stored at -20^{o}C for future use.

Pepsin working solution

A 75µl volume of 10% pepsin solution was added to 30ml of 0.01N HCl.

10M sodium hydroxide (NaOH)

A 40g amount of sodium hydroxide (Merck KGaA, Darmstadt, Germany) was added to a conical flask and topped up to the 100ml mark with deionised H_2O. The solution was placed on a desktop mixer and allowed to dissolve.

1M sodium thiocyanate

A 20.27g amount of NaSCN (Merck KGaA, Darmstadt, Germany) was added to 200ml of deionised H_2O. The solution was placed on a desktop mixer and mixed until all the dry ingredients were dissolved. The magnetic stirrer was removed, and the solution made up to 250ml with distilled H_2O.

Hybridisation probe preparation

Table 5.1: Hybridisation probe mix.

Number of sections	1x
Hybridisation buffer (µl)	3.5
Sterile H_2O (µl)	1.0
Probe (µl)	0.5
Total volume (µl)	5.0

APPENDIX 2 – Summary of patient results

Table 5.2: Summary of all case results in this project.

Study no.	Age	Gender	Site of biopsy	N/EN	HIV Status	EBV Status	EBNA1	EBNA2	LMP1	EBV Latency	*MYC* gene status
1	62	F	Mediastinum	EN	UNK	POS	NEG	NEG	NEG	0	TNS
2	30	F	Tonsil	EN	POS	POS	NEG	NEG	NEG	0	TNS
3	42	F	Oral Cavity	EN	POS	POS	NEG	NEG	NEG	0	Intact
4	46	M	Radius	EN	POS	POS	NEG	NEG	NEG	0	TNS
5	55	F	Leg	EN	POS	POS	NEG	NEG	NEG	0	TNS
6	38	M	Nasal	EN	POS	POS	NEG	NEG	NEG	0	TNS
7	35	F	Anal	EN	POS	POS	NEG	NEG	NEG	0	TNS
8	35	F	Oral Cavity	EN	POS	POS	NEG	NEG	NEG	0	TNS
9	38	M	Anal	EN	POS	POS	NEG	NEG	NEG	0	Translocated
10	32	M	Lymph Node	N	POS	POS	NEG	NEG	NEG	0	TNS
11	55	M	Lymph Node	N	NEG	NEG	-	-	-	None	TNS
12	31	F	Oral Cavity	EN	POS	POS	NEG	NEG	NEG	0	TNS
13	35	M	Oral Cavity	EN	POS	POS	NEG	NEG	NEG	0	Translocated
14	37	M	Thigh	EN	UNK	POS	NEG	NEG	NEG	0	TNS
15	37	M	Chest	EN	POS	POS	NEG	NEG	NEG	0	TNS
16	35	F	Breast	EN	POS	NEG	-	-	-	None	Translocated
17	26	M	Nasal	EN	POS	POS	NEG	NEG	NEG	0	Copy number variation, gain
18	49	F	Maxilla	EN	POS	POS	NEG	NEG	NEG	0	TNS
19	38	F	Lymph Node	N	POS	NEG	-	-	-	None	Copy number variation, gain
20	42	M	Lymph Node	N	POS	NEG	-	-	-	None	Copy number variation, gain
21	34	M	Small Bowel	EN	POS	POS	NEG	NEG	POS	2	Translocated
22	24	F	Maxilla	EN	POS	POS	NEG	NEG	NEG	0	TNS
23	41	F	Nasal	EN	POS	POS	POS	NEG	POS	2	Intact
24	24	M	Oral Cavity	EN	POS	POS	NEG	NEG	NEG	0	Intact
25	43	M	Oral Cavity	EN	POS	POS	POS	NEG	NEG	1	Copy number variation, gain
26	32	M	Neck	EN	POS	NEG	-	-	-	None	Copy number variation, gain
27	63	M	Testis	EN	POS	POS	NEG	NEG	NEG	0	Intact
28	30	F	Lymph Node	N	POS	POS	NEG	NEG	NEG	0	Intact
29	47	M	Lymph Node	N	POS	POS	NEG	NEG	NEG	0	Intact
30	35	M	Anal	EN	POS	NEG	-	-	-	None	Translocated
31	40	F	Tonsil	EN	POS	POS	POS	NEG	NEG	1	Copy number variation, gain
32	46	M	Lymph Node	N	POS	POS	POS	NEG	NEG	1	Copy number variation, gain

Study no.	Age	Gender	Site of biopsy	N/EN	HIV Status	EBV Status	EBNA1	EBNA2	LMP1	EBV Latency	*MYC* gene status
33	36	F	Nasal	EN	POS	POS	NEG	NEG	NEG	0	Copy number variation, gain
34	40	M	Nasal	EN	NEG	POS	POS	NEG	NEG	1	Intact
35	58	M	Lymph Node	N	POS	POS	POS	NEG	POS	2	TNS
36	48	M	Lymph Node	N	POS	NEG	-	-	-	None	Intact
37	42	F	Mandible	EN	POS	NEG	-	-	-	None	Copy number variation, gain
38	48	F	Lymph Node	N	POS	POS	NEG	NEG	NEG	0	TNS
39	32	M	Oral Cavity	EN	POS	POS	NEG	NEG	NEG	0	TNS
40	35	F	Pelvis	EN	POS	POS	NEG	NEG	NEG	0	Copy number variation, gain
41	40	M	Lymph Node	N	POS	POS	POS	NEG	POS	2	Translocated
42	40	M	Anal	EN	POS	POS	NEG	NEG	NEG	0	Intact
43	40	M	Oral Cavity	EN	POS	POS	NEG	NEG	NEG	0	Intact
44	64	M	Lymph Node	N	POS	POS	POS	NEG	NEG	1	Copy number variation, amplification
45	40	M	Maxilla	EN	NEG	POS	POS	NEG	NEG	1	Translocated
46	49	M	Subglottic mass	EN	POS	POS	POS	NEG	NEG	1	Intact
47	37	M	Gastric	EN	POS	POS	NEG	NEG	NEG	0	TNS
48	39	M	Oral Cavity	EN	POS	POS	NEG	NEG	NEG	0	TNS
49	38	F	Buttock	EN	POS	POS	POS	NEG	NEG	1	Translocated

Key: M=Male, F=Female, EN=Extranodal, N=Nodal, HIV=Human Immunodeficiency Virus, UNK=Unknown, POS=Positive, NEG=Negative, EBNA1=Epstein-Barr nuclear antigen 1, EBNA2=Epstein-Barr nuclear antigen 2, LMP1=Latent membrane protein 1, TNS=Tissue not suitable.